LUNDS UNIVERSITET
Lunds Tekniska Högskola

SVENSKA NATIONAL-
KOMMITTÉN FÖR MEKANIK

Svenska Mekanikdagar 2013
Lund 12 - 14 Juni

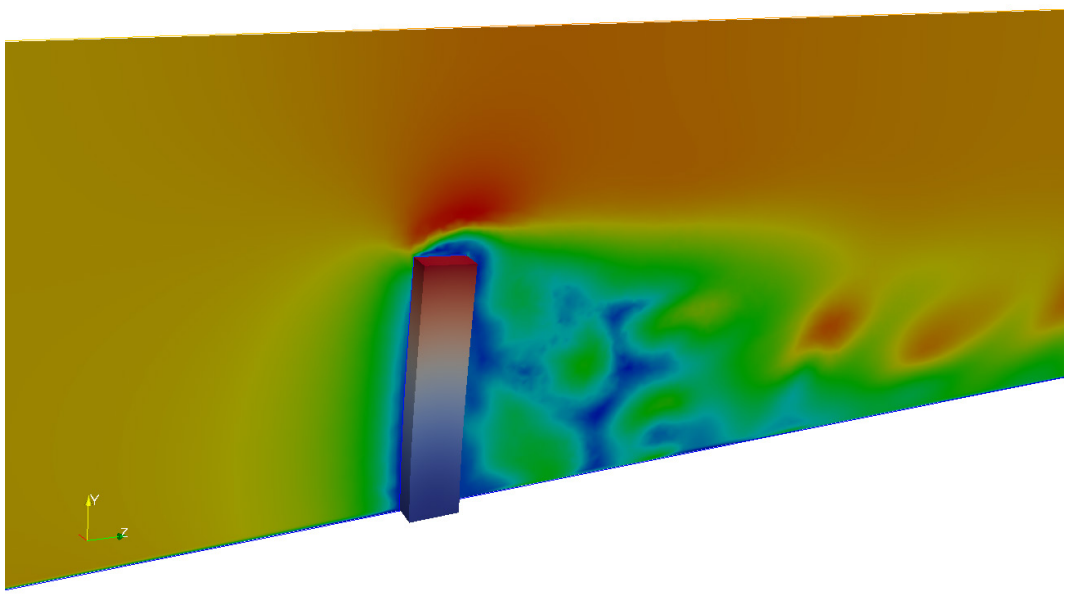

Förord

Svenska Mekanikdagar arrangerades för första gången 1974, och 2013 blir det 23:e arrangemanget. Konferensen organiseras av Nationalkommittén för Mekanik som är en underavdelning till Kungliga Vetenskapsakademien. Mötesserien har sedan starten utgjort en viktig plattform för utbyte av ideér mellan forskare inom mekanikområdet.

Årets upplaga av Svenska Mekanikdagar innehåller cirka 100 presentationer och föreläsningar. Hela landet är representerat och ämnesbredden är stor. Vi hoppas och tror att konferensen skall leda till nya insikter och till att nya kontakter knyts.

Välkomna till Lunds Tekniska Högskola,
Organisationskommitéen

Organisationskommitéen
Mathias Wallin, Hållfasthetslära
Solveig Melin, Mekanik
Johan Revstedt, Strömningslära
Johan Hektor, Hållfasthetslära
Dan Johansson, Mekanik
Henning Carlsson, Strömningslära

Sponsorer:

Studentlitteratur

LUNDS UNIVERSITET
Lunds Tekniska Högskola

Program

Tid	Program
	Onsdag 12/6
10:30	Registrering
11:40	Lunch
13:00	Öppnande
	Anders Axelsson, Rektor LTH
13:15	Odquistföreläsning
	Gradient based structural optimization and extensions
	Anders Klarbring
	Linköpings Universitet
14:05	Session 1
15:05	Kaffe
15:25	Session 2
17:00	Doktorand- och senioraktivitet
	Torsdag 13/6
08:45	*Tyre - Road Interaction*
	Wolfgang Kropp
	Chalmers
09:35	Session 3
10:35	Kaffe
10:55	Session 4
11:55	Lunch
13:00	*Jan Hult – Professor in Solid Mechanics*
	Lars Bråthe, Lennart Josefson
	Chalmers
13:15	*Fluid flow in industrial and natural processes*
	Staffan Lundsström
	Luleå Tekniska Universitet
14:05	Session 5
15:05	Kaffe
15:25-16:25	Session 6
17:30	Konferensmiddag
	Fredag 14/6
09:00	*Mekanisk provning och modellering i mikrometerskala: Röntgen-mikrotomografi och mekanisk provning av enskilda träceller*
	Kristofer Gamstedt
	Uppsala Universitet
09:50	Session 7
10:50	Kaffe
11:10	Session 8
12:10	Avslutning
12:20	Lunch

Plenarföreläsningar

Tid	Plenarföreläsningar M:A
	Onsdag 12/6
13:15-14:00	Odquistföreläsning *Gradient based structural optimization and extensions* Anders Klarbring Linköpings Universitet
	Torsdag 13/6
08:45-9:30	*Tyre - Road Interaction* Wolfgang Kropp Chalmers
13:00-13:15	*Jan Hult – Professor in Solid Mechanics* Lars Bråthe, Lennart Josefson Chalmers
13:15-14:00	*Fluid flow in industrial and natural processes* Staffan Lundsström Luleå Tekniska Universitet
	Fredag 14/6
09:00-09:45	*Mekanisk provning och modellering i mikrometerskala: Röntgen-mikrotomografi och mekanisk provning av enskilda träceller* Kristofer Gamstedt Uppsala Universitet

Session 1 (ons 12/6)

Tid	Konstitutiv modellering I M:A	Experimentella metoder I M:B	Värmeöverföring M:E	Mjuka vävnader M:D
14:05	*Anisotropy and crack propagation in pearlitic rail steel* N. Larijani Chalmers	*Determination of diffusion constant in bovine bone by means of Kalman filtering for experimental data* A. Shokry Lunds Universitet	*Experimental and Numerical Investigation of Electric Generator Cooling* H. Jamshidi Chalmers	*A theoretical approach towards smooth muscle modeling* B. Sharifimajd Linköpings Universitet
14:25	*The Effect of Lateral Pre-straining for the In-plane Mechanical Deformation Response pf Paperboard* T. Lindström Tetra Pak	*SAXS experiments of polycarbonate with in-situ loading* J. Engqvist Lunds Universitet	*Experimental Heat Transfer Study in an ITD with IR Thermography* B.M. Rojo Perez Chalmers	*Remodellering av glatt muskulatur vid ihållande kontraktion* J. Stålhand Linköpings Universitet
14:45	*The development of a constitutive model for paperboard* E. Borgqvist Lunds Universitet	*Effects of Electromagnetic Waves on Rock* B. Khodabandeloo Blekinge Tekniska högskola	*Grate aerodynamic – Study of gas flow in grate* P.E.C. Burström Luleå Tekniska Universitet	*Musculoskeletal Biomechanics for Paralympic Classification* L.J. Holmberg Linköpings Universitet

Session 2 (ons 12/6)

Tid	Numeriska metoder I M:A	Experimentella metoder II M:B	Strömning i gränsskikt M:E	Hårda vävnader M:D
15:25	*Using GPU accelerators for polycrystalline material simulations* Y. Mellbin Lunds Universitet	*Kärnbildning av gamma" partiklar i IN718* M. Fisk Malmö Högskola	*Rotating-disk boundary-layer flow* S. Imayama KTH	*Investigation of femoral strain patterns using digital image correlation* L. Grassi Lunds Universitet
15:45	*Phase stability of* $ZrH_{1.5}$ – a DFT study P.A.T. Olsson Malmö Högskola	*Effects of defects on the tensile strength of heterogeneous composite materials* T. Joffre Uppsala Universitet	*Modeling and validation of flow over a wall with large surface roughness* J. G. I. Hellström Luleå Tekniska Universitet	*Can widening of a stress fracture in a long bone decrease local strains sufficiently to enable healing?* H. Isaksson Lunds Universitet
16:05	*Nucleation of a second phase at a dislocation using a phase field approach* C. Bjerkén Malmö Högskola	*Residual stress and hydrogen effect on* $Ti{-}_6Al{-}_4V$ *alloys produced by Electron Beam Melting* T. Maimaitiyili Malmö Högskola	*Skin-friction drag reduction – Now with reinforced passive control* S. S. Sattarzadeh KTH	*Investigation of femoral fracture criteria in composite femur bone* M. Ahlgren Lunds Universitet
16:25	*Cracks and Fracture of Origami Patterns as Energy Absorbing Devices* R.R. Katangoori Blekinge Tekniska högskola	*PIV analysis of merging flow in a simplified model of a rotary kiln* S. Larsson Luleå Tekniska Universitet	*Flow control by means of plasma actuation – a study of the electric wind* J. Vernet KTH	

Session 3 (tor 13/6)

Tid	Industriella applikationer I M:A	Numeriska metoder II M:B	Strömningsmekanik I M:E	Biomekaniska transportfenomen M:D
09:35	*Acoustic particle separation in gaseous flows using ultrasound* R.I. Jajarmi KTH	*Utilising XFEM to model failure of thinwalled structures* M. Fagerström Chalmers	*Flow Visualization of Oil Flow inside a Gearbox Model* E.A. Hartono Chalmers	*Blood Flow in Large Bifurcating Arteries* S. van Wyk KTH
09:55	*Mechanical modeling and characterization of transformer pressboard* D. Tjahjanto KTH	*Material distribution optimization for acoustics: developments and challenges* M. Berggren Umeå Universitet	*Inlet Geometry Effects on the Flow in an Radial Turbine* J. Fjällman KTH	*Mechanical behaviour of transiently cross-linked actin networks – a chemo-mechanical constitutive model* B. Fallqvist KTH
10:15	*A framework for modelling the sealing process* H. Askfelt Lunds Universitet	*On a method for solving non-linear optimization problems with matrix inequality constraints* C.-J. Thore Linköpings Universitet	*Passive flow control for skin-friction drag reduction: AFRODITE* J.H.M. Fransson KTH	*Transport-based theory of Bone Remodeling involving Stress Driven Diffusion* I. Svensson Lunds Universitet

Session 4 (tor 13/6)

Tid	Konstitutiv modellering II M:A	Kollapsmekanismer M:B	Strömningsmekanik II M:E
10:55	*Model-based weldability charts for constructional steels* J.C. Ion Malmö Högskola	*Stress analysis around a through crack shaped void in a highly constrained copper strip using molecular dynamics* Dan Johansson Lunds Universitet	*Couette, Coriolis and Kelvin – is absolute vorticity conserved under rotation in shear flows* P.H. Alfredsson KTH
11:15	*Mikromekanisk analys av pulverpressning* E. Olsson KTH	*Longitudinellt kompressionsbrott i kolfiberförstärkt polymerkomposit* D. Svensson Högskolan i Skövde	*Grease flow modeling using micro particle image velocimetry* L.-G. Westerberg Luleå Tekniska Universitet
11:35	*Constitutive modelling of CGI on a microstructure level* L. Josefson Chalmers	*Spontant brott vid expanderande fasomvandling* P. Ståhle Lunds Universitet	*Large scale unsteady behaviour of turbulent pipe flow through* 90° *bends with varying degrees of curvature* C. Carlsson Lunds Universitet

Session 5 (tor 13/6)

Tid	Flerfasströmning I M:A	Industriella applikationer II M:B	Experimentella metoder III	Strömning i roterande maskiner I M:D
14:05	*Inverkan av biofibriller på hydrodynamisk stabilitet* M. Kvick KTH	*Parameterstudie över inverkan av järnvägshjuls löpbaneslitage på rullkontaktutmattning och nötning* K. Karttunen Chalmers	*Utvärdering av fiberfogstyrka hos massafibrer* M.S. Magnusson KTH	*The effect of atmospheric boundary layer depth on wind turbine power production* A. Al Sam Lunds Universitet
14:25	*Hydrodynamic alignment and assembly of nanocellulose* K. Håkansson KTH	*Investigation of surface initiated rolling contact fatigue with the asperity point load model* D. Hannes KTH	*Kohesiva lagar för lims temperaturberoende* Tomas Walander Högskolan i Skövde	*Experimental study of pressure fluctuations on a Kaplan turbine runner blade* K. Amiri Luleå Tekniska Universitet
14:45	*A particle-level fiber model, implemented in a general purpose CFD code* J. Andrić Chalmers	*Interaktionsmodeller för 2D FE-modellering på pekskärmar* D. Åkesson Lunds Universitet	*Experimentell studie av tröskelvärde för limutmattning med kohesiv lag.* A. Eklind Högskolan i Skövde	*Unsteady Turbulent Flow in Rotating Turbomachinery* A. Javadi Chalmers

Session 6 (tor 13/6)

Tid	Flerfasströmning II M:A	Dynamik I M:B	Konstitutiv modellering III M:E	Strömning i roterande maskiner II M:D
15:25	*Large eddy simulation of unsteady turbulent flow in semi-industrial size spray dryer* F. Innings Tetra Pak	*Dynamic higher order micropolar plate equations* H. Abadikhah Chalmers	*A remark on homogenization and virtual testing of micro-heterogeneous meterials* K. Runesson Chalmers	*LES Prediction of Near Surge condition in a Centrifugal Compressor* J. Kumar V. KTH
15:45	*Ice accretion modeling based on LES and LPT* R. Szasz Lunds Universitet	*Micropolar cloaking against Rayleigh waves* A. Khlopotin Chalmers	*Micromechanical model for back-calculation of stiffness contribution from cellulose nanoelements to the overall properties of composites* G. Josefsson Uppsala Universitet	*Numerical investigation of different gaps in Couette rheometer* N. Hamedi Lunds Universitet
16:05	*Simulering av en vätskestråles uppbrytning i stationär gas* A. Nygård KTH	*Experimental-Analytical Dynamic Substructuring* M. Gibanica Chalmers		*Fluid mechanics of rotor stator mixers* A. Lindahl Tetra Pak Processing System

Session 7 (fre 14/6)

Tid	Experimentella metoder IV M:A	Dynamik II M:B	Förbränning I M:E
9:50	*Experimental and Numerical fracture of cracks emanating from different types of flaws in thin polymer films* N. Mehmood Tetra Pak Packaging Solutions, Blekinge Tekniska högskola	*The granite rock fragmentation in percussive drilling* M. Saadati KTH, Atlas Copco	*Large eddy simulations and dynamic mode decomposition of flame/flow interaction in a lean premixed low swirl stabilized flame* H. Carlsson Lunds Universitet
10:10	*Thermally-activated delayed failure in heterogeneous solids: An experimental model system* S.B. Lindström Linköpings Universitet	*Comparison of contact dynamics in bladed Jeffcott rotors* F. Thierry Luleå Universitet	*Comprehensive study on combustion of single biomass particle* H. Fatehi Lunds Universitet
10:30	*Experimentell metod för stabila dragprov för tråd* A. Biel Högskolan i Skövde	*Wavelet transform of torsional vibrations of a Kaplan turbine* I. Jansson Luleå Universitet	*Flame Modelling with Finite Rate Chemistry and Implicit Large Eddy Simulations* E. Hodzic Lunds Universitet

Session 8 (fre 14/6)

Tid	Konstitutiv modellering IV M:A	Numeriska metoder III M:B	Förbränning II M:E
11:10	*On the modeling of grain size-dependent hardening in polycrystalline metals* M. Ekh Chalmers	*Numerical modeling and analysis of dynamic crack propagation in rubber* E. Elmukashfi KTH	*The Effect of Aluminium Particle Combustion on the Afterburning during a TNT Blast* E. Fedina Swedish Defence Research Agency – FOI
11:30	*Modeling of recrystallization* H. Hallberg Lunds Universitet	*Thermo-mechanical analysis of crack propagation in amorphous polymers* M. Kroon KTH	*On Auto-Ignition in Heavy Duty Diesel engines, a Large Eddy Simulation Study* R. Solsjö Lunds Universitet
11:50	*Unstable Formation of Hydride Precipitates* W. Reheman Lunds Universitet	*A non-affine microsphere formulation for electroactive polymers* S. Thylander Lunds Universitet	*Large Eddy Simulations of the flow in the exhaust port of a Dielsel engine* Y. Wang KTH

Plenarföreläsningar

Gradient based structural optimization and extensions

Anders Klarbring[1] and Bo Torstenfelt[2]
[1]Mechanics, Department of Management and Engineering, The Institute of Technology, Linköping University, Linköping, Sweden email: anders.klarbring@liu.se
[2]Solid Mechanics, Department of Management and Engineering, The Institute of Technology, Linköping University, Linköping, Sweden email: bo.torstenfelt@liu.se

The first part of the talk describes basic ideas and concepts of structural optimization - the scientific area dealing with computational design of load carrying mechanical structures. The sequential explicit convex approximation methods, dominating this area, are based on first order approximations of non-convex implicitly defined design optimization problems. An idea, which seems to be unique compared to other related fields, is a linearization in a so-called intermediate variable, which produces non-linear but convex approximations that are separable and easily solved by dual methods. The appearance and resolution of numerical instabilities such as mesh dependency and checkerboard patterns in the structural optimization subarea of topology optimization will also be discussed.

In the second part of the talk, the extensions of the methods of topology optimization to other physical domains, as well as to multi-physics problems, will be indicated. Modeling based on a dynamical systems approach to optimization will also be described. In particularly, its relation to bone remodeling will be indicated.

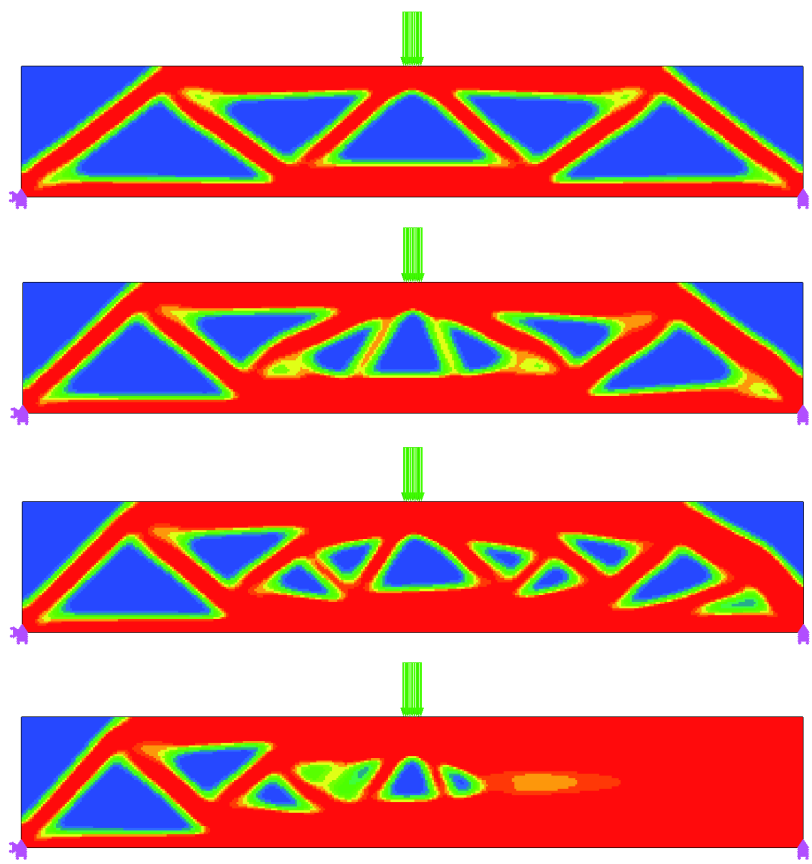

Figure 1: The top figure shows a standard solution of a topology optimization problem by a so-called SIMP method. The following three figures show how this solution is modified by the presence of growth stimulating nutrients.

Tyre - Road Interaction

Wolfgang Kropp[1]
[1]Applied Acoustic, Chalmers University of Technology, email: Wolfgang.Kropp@schalmers.se

When driving a car we are not always aware of the tremendous importance of the contact between the tyres and the road surface. However the interaction between tyre and road determines many of the main features of tyre performance such as braking, handling, wear, rolling resistance but also interior and exterior noise. The multitude of performance criteria makes the overall improvement of tyres often difficult. For instance improvement for noise might be in conflict to performance with respect to wear. At the same time tyre/road noise is the main source of road traffic noise over a wide range of driving speeds.

For understanding the interaction between tyre and road it is essential to be able to model the tyre-road interaction including the necessary degree of complexity. An introduction will be given to the analysis of tyre vibrations based on a so-called Wave Guide Finite Element model. Different waves as shown in Figure 1 (left) play different role in the transient rolling contact between tyre and road, but are also responsible for instance for sound generation or rolling resistance.

The main reason for tyre vibrations are the excitation due to the road roughness. The vibrations will lead for instance to sound radiation or to losses in the tyre structure which represent the rolling resistance. The main key for a successful simulation of the tyre-road interaction is to capture the important details of the transient rolling contact between the tyre tread and the rough road surface. An introduction is given to the different approaches which could be chosen for the modelling of the contact.

Finally the mechanisms behind tyre properties such as noise or rolling resistance are discussed and together with possible technical solutions. Figure 1 (right) show typical results for e.g. the modelling of sound radiation. Although the results are promising, it has shown that today it is not the modelling itself, which limits prediction accuracy but uncertainties in the input data (e.g. material data for the tyre).

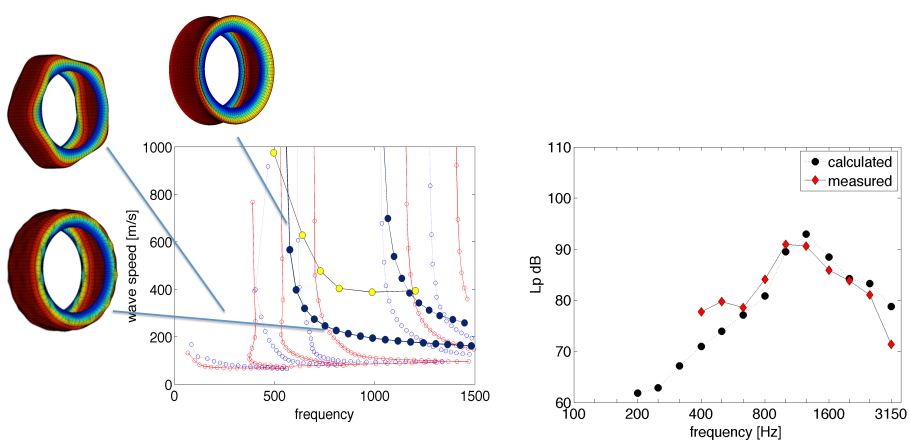

Figure 1: Dispersion diagram for waves on the tyre and some examples of the representative vibration patterns (left) and the corresponding *rms* of lift fluctuations (b) for two different mass ratios.

Jan Hult – Professor in Solid mechanics

Lars Bråthe[1], Lennart Josefson[2]
[1]email: Lars.Brathe@gmail.com
[2]Chalmers University of Technology, email: Lennart.Josefson@chalmers.se

Jan Hult, Professor Emeritus in Solid Mechanics at Chalmers, passed away earlier this year, aged 85 years. He was one of the first to study Engineering Physics at KTH. After his MSc, Professor Folke Odqvist at Solid Mechanics attracted him to a brilliant group of PhD-students, many of whom later became professors (e.g. Frithiof Niordson, Bertram Broberg and Janne Carlsson) in Solid Mechanics. Jan went to MIT to study with Professor Frank McClintock, again in a vibrant research environment. He derived the elasto-ideal plastic solution for the Mode III-case in Fracture Mechanics and earned a PhD in 1957. He then returned to KTH where he defended his PhD thesis on torsional fatigue in 1958.

Jan came to Chalmers in 1961 and became a Professor there in 1962, at the young age of 34 years. One part of his character was to take initiatives. During the years that followed he formalized the graduate education programme and created an open atmosphere at the department with much research discussions, industrial connections, frequent seminars and many international guests. His research focus was creep and damage mechanics, supervising several Licentiates and PhDs. With Odqvist he wrote the book “Kriechfestigkeit Metallischer Werkstoffe”. He was active in the international scientific community, in particular with IUTAM (International Union of Theoretical and Applied Mechanics) where he for some years was Secretary General.

Jan was also very interested in education and pedagogy. His courses often were pedagogic experiments in one direction or another. He modernized the courses in Solid Mechanics and wrote two new textbooks, “Hållfasthetslära” and later “Bära Brista”. He also wrote popular scientific books on this subject, “Laster och brott” and “Spänning och brott“ as well as a book on Cartesian tensors. These books, newpaper articles, radio talks and public lectures brought our subject to the general public.

In the late 1970ies Jan took up the History of Technology, a growing interest of his, and introduced and developed an elective course in the subject at Chalmers. This grew to be an established research subject with professorships at Chalmers as well as other universities. He supervised the first PhD in History of Technology at Chalmers.

Jan was a very enthusiastic and open-minded professor with a sharp intelligence. He was interested in and keenly supported students (undergraduate and graduate) and researchers. To many of us he is still a good example. He will be much missed.

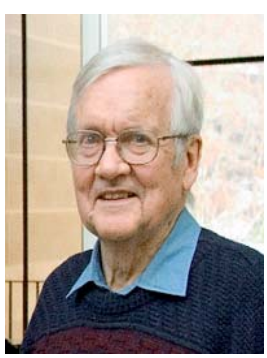

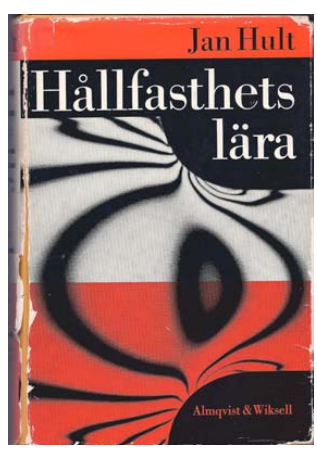

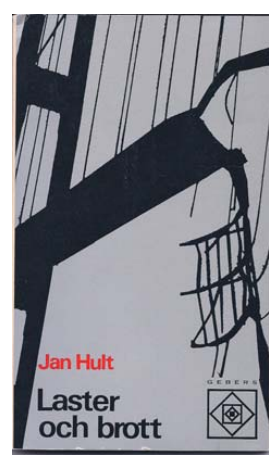

Fluid flow in industrial and natural processes

T. Staffan Lundström
[1]Division of Fluid and Experimental Mechanics, Luleå University of Technology, Luleå, Sweden
email: staffan.lundstrom@ltu.se

Fluid flow is complex even for cases that at a first glance may appear to be very simple such as flow through pipes, between parallel walls or around simple shaped obstacles. Adding to this the ambient conditions in most industrial and natural processes are far from perfect, the geometry faced by the fluid complex and the interaction with issues such as chemical processes, solid particles and solid structures can sometimes be strong. It is therefore not obvious how to study flow in real life with quality and trust.

In this talk the fluid flow in some industrial and natural processes are described, some strategies to model them are set-up and some results presented. To exemplify, during manufacturing of iron ore pellets fluid flow takes place on multiple scales ranging from the micro scale to scales of tenths of meters. In essence, iron ore is grained and refined, water and some chemicals are added and slurry is formed that is also refined to increase the mass fraction iron. The refined slurry is then dewatered and the formed mass is rolled into pellets with a diameter of about 1 cm and that has pores on the micrometre scale. The pellets are put on a belt and first dried and then sintered on the belt and/or within a rotary kiln (oven) that is approximately 70 m long. Naturally it is difficult to have one model capturing all phenomena of this process.

As a second application flow in-connection to hydro-power will be discussed in the context of spilling and fish migration. It is, for instance, well established that up-stream migrating fish may be steered to a fish-way leading around an obstacle like a dam with the use of attraction water. The optimal design of such attraction water is not known but from the efficiency aspect of a hydropower plant it is essential that the attraction water can be generated with as little energy loss as possible. In this context it is important to study how a noticeable water jet can be created with only usage of the water from the power plant. Likewise, it is essential that methods are developed that can safely guide downstream migrating fish like smolt passed hydropower plants without too much loss of the energy of the water.

A third application is liquid moulding of fibre reinforced polymer composites. During this process a monomer, a resin, is forced to impregnate a dry stack of fabrics with a rather intricate flow field as a result often involving the formation of bubbles and an uneven wetting flow front. The complex flow pattern can mainly be traced to dual-scale porosity and the situation becomes even more complex if particles, often with a function, are added to the resin.

Mekanisk provning och modellering i mikrometerskala: Röntgen-mikrotomografi och mekanisk provning av enskilda träceller

Kristofer Gamstedt
Uppsala universitet, Ångströmlaboratoriet, e-post: kristofer.gamstedt@angstrom.uu.se

Materialutveckling är än idag relativt empirisk, och ofta baserad på att blanda och testa. Förnyelsebara förpackningsmaterial är under stark framväxt, och där skulle materialmekaniken kunna spela en viktig roll för att rationalisera utvecklingen. Dessa material är i stor utsträckning baserade på vedfibrer från skogsråvara. I denna presentation kommer det visas ett par exempel på hur materialmekanik och nya experimentella metoder kan bidra till utveckling av nya material med bättre ingenjörsegenskaper, såsom styvhet, styrka, brottseghet och dimensionsstabilitet. Mikromekanik har under längre tid varit ett aktivt och nyttigt forskningsområde inom högpresterande fiberkompositer i flyg- och rymdtillämpningar, men har ännu inte bidragit på samma satt i utveckling av andra material som används i större volymer, som förpackningar och träfiberkompositer, där kemiska eller processtekniska metoder av tradition varit dominerande. Med ett experimentell mikromekaniskt tillvägagångssätt skulle man kunna identifiera vilka beståndsdelar och mikrostrukturella parametrar som bidrar mest till de önskvärda mekaniska egenskaperna, och på så sätt kunna styra tillverkningsprocessen och materialval för att förbättra prestandan hos materialen. De presenterade exemplen inskränker sig dock inte endast till denna materialklass, utan är tillämpbara i vidare mening.

Röntgen-mikrotomografi är en metod som utvecklats starkt under senare år, och med den kan man ta tredimensionella bilder av material. Vi har använt denna metod, både vid ESRF-synkrotronen i Grenoble och också en mindre bordsutrustning av märket Skyscan. Träfibrer är den lastbärande enheten i trä, papper, kartong och förnyelsebara kompositmaterial. Med in-situ provning med varierande relativ fuktighet och en liten dragprovare kan man mäta hur hela fibern deformeras under hygroskopisk eller mekanisk belastning. Cellväggens hygroexpansionskoefficient och styvhet kan således beräknas på ett sätt som inte var möjligt tidigare. Bildbehandling, CAD och FEM-modellering är nödvändiga verktyg för att identifiera dessa parametrar. Några bilder från denna process finns i figuren nedan. Experimentell validering av materialmekaniska modeller blir också möjligt. Nästa steg är att simulera effekter av olika mikrostrukturer och fibertyper i en strävan att skräddarsy materialen för optimala egenskaper.

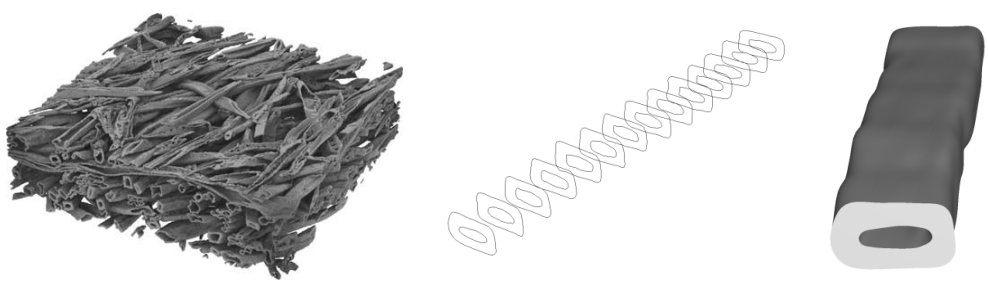

(a) (b) (c)

Figur 1: (a) 3D-bild av en träfiberkomposit. (b) Rekonstruktion av enskild träfiber. (c) Geometrisk modell av en träfiber, att användas i numeriska simuleringar.

Konstitutiv modellering I

onsdag 12/6 14:05-15:05

Anisotropy and crack propagation in pearlitic rail steel

Nasim Larijani[1], Magnus Ekh[2]
[1]Department of Applied Mechanics, Chalmers, email: nasim.larijani@chalmers.se
[2]Department of Applied Mechanics, Chalmers University of Technology

In a pearlitic structure, large deformations lead to a re-orientation and alignment of cementite lamellae on the microscopic level[1,2]. These changes in the microstructure of pearlitic steel under large plastic deformations induce substantial degrees of anisotropy in certain mechanical properties of the material like yield limit, fracture toughness and fatigue threshold values[3]. The alteration and induced directional dependence in these specific properties are equivalent to changes in resistance against initiation and growth of fatigue cracks and influence the fatigue life of the components.
In the present work the Rolling Contact Fatigue (RCF) cracks in rail samples from a full scale test rig were examined. Rolling contact fatigue cracks follow the weakest direction of the microstructure which in pearlitic railway rails is the aligned pearlite structure or singular weaknesses such as e.g. pro-eutectoid ferrites or slags (See Figure 1). Furthermore, the influence of the anisotropic layer on propagation of cracks in rail head is investigated. Based on the concept of material forces[4,5], a computational framework for simulation of propagation of planar cracks is formulated where the propagation rate is linked to a crack-driving force. An anisotropic fracture surface model is employed to capture the effect of changes in the resistance against crack propagation in different directions and depths in the surface layer. Results of simulations for cases with different characteristics in the surface layer show that the anisotropic layer has a substantial influence on the crack path.

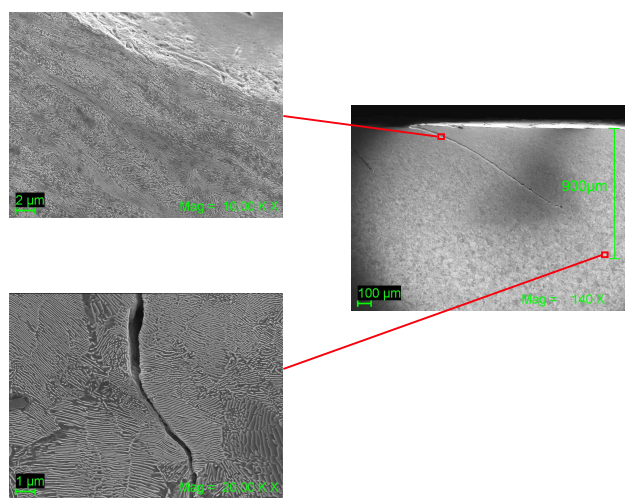

Figure 1: The fracture surface of a rolling contact fatigue crack at a point in the aligned surface layer and out of it.

[1]Toribio, *Mater. Sci. Engng. A* , **387–389**, 227–230 (2004)
[2]Wetscher, Stock and Pippan, *Mater. Sci. Engng. A* , **445–446**, 237–243 (2007)
[3]Hohenwarter, Taylor, Stock and Pippan, *Metall. Mater. Trans. A* , **42**, 1609–1618 (2011)
[4]Tillberg, Larsson and Runesson, *Int. J. Plasticity* , **26**, 992–1012,(2010)
[5]Brouzoulis, Larsson and Runesson, *Comput. Mech.*, **47**, 295–304, (2011)

The Effect of Lateral Pre-straining for the In-plane Mechanical Deformation Response of Paperboard

Tommy Lindström[1], Johan Tryding[2], Eric Borgqvist[3]
[1]Tetra Pak, email: tommy.lindstrom@tetrapak.com
[2]Tetra Pak, email: johan.tryding@tetrapak.com
[3]Lund University, email: eric.borgqvist@solid.lth.se

Paper and paperboard are widely and diversely used materials all over the world. Paperboard is commonly described as an anisotropic fibrous material and the modeling of paperboard has been, and still is, a large field of research. Originating from the manufactoring procedure, where the fibres tend to allign in the direction of movement in the machine, has the nomenclature Machine Direction (MD), Cross-machine Direction (CD) and Z Direction (ZD) been introduced for directions of the material.

The effect of lateral pre-straining in MD and CD is here investigated. The measurements in Figure 1 suggest that laterally pre-strained samples do not exhibit plastic hardening as predicted by previous elasto-plastic constitutive models for paperboard. To model the measured lateral mechanical deformation response an elasto-plastic model based on the Xia yield function[1] is devised and implemented in a finite element setting.

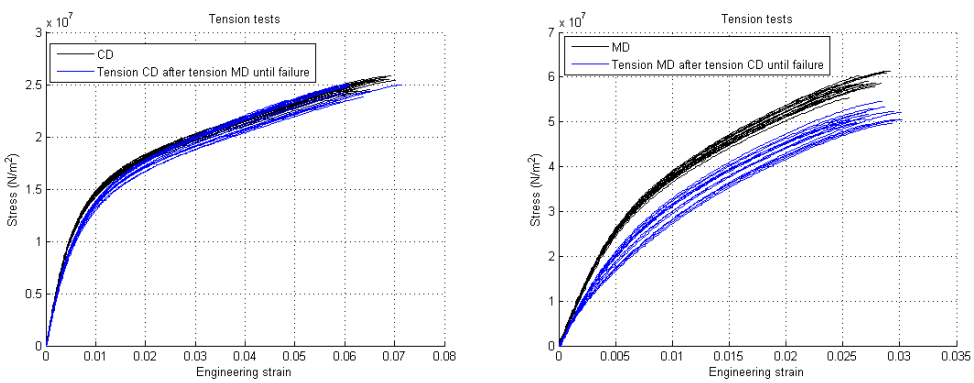

(a) Tension applied in MD followed by tension in CD

(b) Tension applied in CD followed by tension in MD

Figure 1: Comparison of unaffected and laterally pre-strained samples. The black lines (upper) denote measurements of unaffected samples and the gray lines (lower) denote the laterally pre-strained samples

[1] Xia et al., *Int. J. of Solids and Structures*, **39**, 4053-4071, (2002)

The development of a constituitve model for paperboard

Eric Borgqvist[1], Mathias Wallin, Matti Ristinmaa

[1]Avdelningen för Hållfastheslära, Lunds Tekniska Högskola, Lund, email: Eric.Borgqvist@solid.lth.se

Paperboard is made of several layers of wood-fibers and is used as the basis material within the packaging industry. A continuum model with orthotropic elasto-plastic properties coupled to a scalar damage variable at large strains is used for the modeling of paperboard. The effects of delamination between different pulps have not been considered. The in-plane and out-of-plane behavior is assumed to be decoupled, i.e. the Poisson's ratio is assumed to be zero both in the elastic as well as in the plastic regime. This allows for having one yield surface for the in-plane behavior and another damage surface for the plastic and damage behavior in the out-of-plane direction.

Paperboard is a highly frictional material, meaning that the failure stress in out-of plane shear is increased as the compression in the out-of-plane direction increases. New experimental equipment is currently under development for more accurately measuring this frictional behavior. The experimental method together with the modeling approach will be presented.

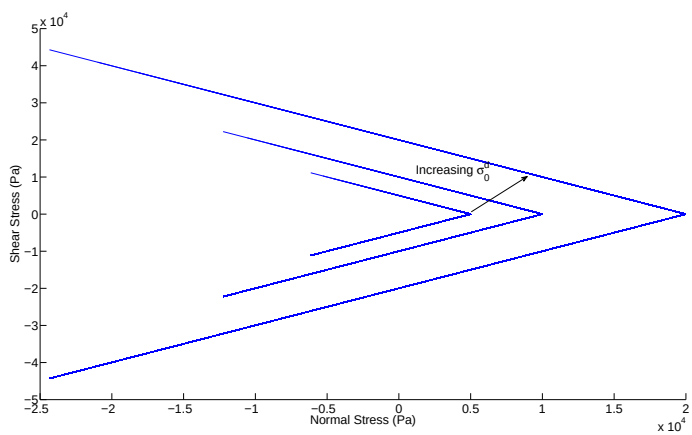

Figure 1: Illustration of the damage surface for the paperboard. The out-of-plane normal and shear stress is plotted for different values of the initial damage threshold. A higher shear stress is required for the damage to develop if normal compression is applied.

Experimentella metoder I

onsdag 12/6 14:05-15:05

Determination of diffusion constant in bovine bone by means of Kalman filtering for experimental data

Abdallah Shokry[1], Gustav Lindberg[2], Wureguli Reheman[3], Ingrid Svensson[4]

[1]Division of Solid Mechanics, Lund Technical Institute, email: abdallah.shokry@solid.lth.se
[2]Division of Solid Mechanics, Lund Technical Institute, email: gustav.lindberg@solid.lth.se
[3]Division of Solid Mechanics, Lund Technical Institute, email: wureguli.reheman@solid.lth.se
[4]Division of Solid Mechanics, Lund Technical Institute, email: ingrid.svensson@solid.lth.se

Measuring the diffusivity of various substances in compact bone in general is difficult. For instance, making use of micro computed tomography, micro CT, requires agents that should be separated from both bone, blood and other substances that exist in compact bone. In order to find a more easily accessible method, an experiment was set-up using the increased conductivity of a solution as a measurement of how many ions that have diffused into it. A series of compact bovine bone samples were put in a saturated solution of potassium chloride, KCl, for time period that was long enough to make the samples regarded as saturated. The samples were removed from the solution and molded in polyester leaving only the radial direction ends open. In a next step, the samples were put in distilled water where the ions that come from KCl in each bone sample diffuse into the water and change its conductivity. The conductivity was read over time using a conductivity meter equipment. It is directly proportional to the diffusion of KCl from the bovine bone sample. An analytical model fulfilling Fick's law was introduced and by means of Kalman filtering an estimation for the diffusion constant of potassium chloride in bovine bone is presented.

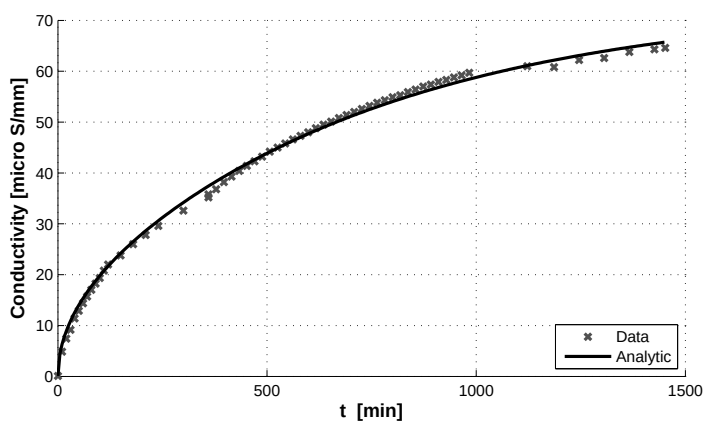

Figure 1: Analytical function using the parameters that obtained by means of Kalman filtering versus experimental data for bovine bone sample (Lateral Posterior 1).

SAXS experiments of polycarbonate with in-situ loading

Jonas Engqvist[1], Stephen Hall[2], Mathias Wallin[2], Matti Ristinmaa[2], Tomás Plivelic[3]
[1]Division of Solid Mechanics, Lund University, email: jonas.engqvist@solid.lth.se
[2]Division of Solid Mechanics, Lund University
[3]MAX IV Laboratory, Lund University

The anisotropy of amorphous glassy polymers evolves when the polymer is subjected to inhomogeneous deformation, e.g. uniaxial tension. This evolution can be modelled using a chain orientation distribution function (CODF). In order to establish a CODF small angle x-ray scattering (SAXS) experiments were performed at the I911-4 beamline of the MAX IV Synchrotron Laboratory at Lund University. The specimens studied were amorphous, initially isotropic glassy polycarbonate (PC). The SAXS experiments were done under in-situ uniaxial tensile loading of notched PC specimens. During the experiments the deformation of the specimen was measured using 3D-surface digital image correlation (DIC). For this purpose the specimen was painted with a black and white speckle pattern. The central part, where the x-ray beam hit the sample, was free of paint.

The in-situ loading was carried out using a custom built tensile test machine. To avoid relaxation of the polymer specimen the loading was continuous at a constant nominal displacement rate of 0.01 mm/min. SAXS measurements were made continuously during the loading at 20 points separated by 0.5 mm along a line down the center of the specimen. At the beginning of each SAXS measurement one pair of images was recorded for the DIC using two digital cameras. The use of two cameras allowed for measurement of the out-of-plane deformation. Figure 1 shows the strain field at three levels of deformation: before load, post localization (loaded) and unloaded. At each load level 2D SAXS patterns at three spacial locations are shown. The SAXS patterns shows alignment of the material at a microscopic level that are consistent with the macroscopic deformation shown by the DIC. The SAXS patterns from the specimen before load shows isotropic scattering. The images from the specimen under load shows some clear alignment of the scattering. After unloading some residual alignment of the scattering is shown.

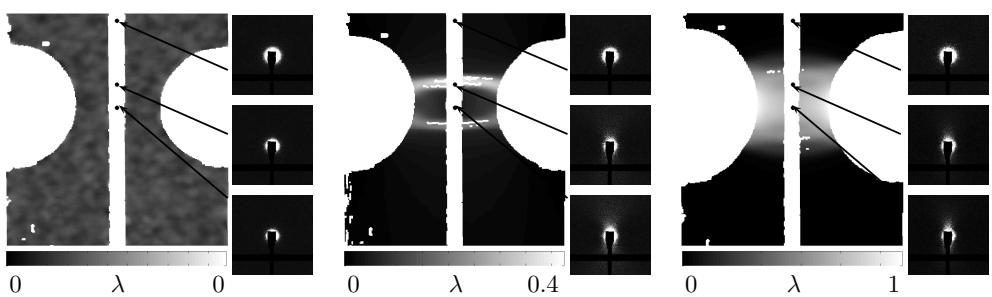

Figure 1: The large figures are showing the strain field at three levels of deformation. The small figures are showing the 2D SAXS pattern at three spacial locations at each deformation. The deformation levels are: (a) before loading, (b) loaded post localization, (c) unloaded after loading well past localization.

Acknowledgement

The financial support from the Crafoord foundation, grant no. 20110521 and 20120632, is greatly acknowledged. We are also grateful for the beamtime and support received from the MAX IV Laboratory and the I911-SAXS beamline, proposal 20120327.

Effects of Electromagnetic Waves on Rock

Babak Khodabandeloo[1], Mattias Eriksson, Ansel Berghuvund, Claes Hedberg

Blekinge Tekniska Högskola, Karlskrona
[1] *babak.khodabandeloo@bth.se*

It is known that the material state is affected when exposed to mechanical disturbances, heat, magnetic fields, and so on[1]. The observed effects are for instance change in expansion and decrease in Young's Module of Elasticity. In the ongoing project we experimentally investigate the effects of electromagnetic waves on a rock beam. The experimental setup is shown in Figure (1-a).

LEDs and Coil heaters are used for conditioning and a triangulating displacement laser is used for probing the deflection of the beam which is an indicator of the material state. LEDs are used as they produce less heat than other available light sources. The temperature of the rock is measured using four thermocouples at different positions on the rock. The test setup is placed in an isolated chamber to have more control on humidity and temperature. In Figure (1-b) the deflection and temperature variations for a sample conditioned by LED and Coil heater are shown respectively. As increase of temperature is an inevitable part of light radiation, we are making estimates on how much is a direct light effect, and how much is due to increase in temperature. Focusing on recovery curves is helpful as different models and equations govern cooling (effect of heat) and decay (quantum mechanics effects).

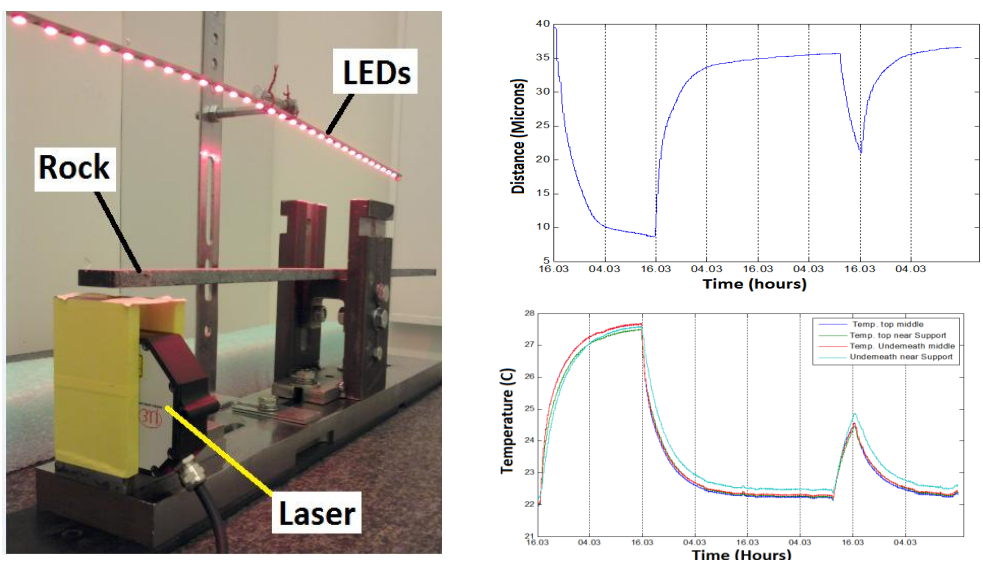

a) b)

Figure 1: Test setup used (left). Conditioning by Light or Heat; The resulting deflection vs. time (right-top) and the Temperature variations vs. time (right-below). (*Coil heaters and Thermocouples are not shown in this setup*)

1. Hedberg C.M., Andersson S.A, Haller K.C., Deflection dynamics of rock beam caused by ultrasound, *Mech. Time-Depend. Mater.*, (Jan) 2013

Värmeöverföring

onsdag 12/6 14:05-15:05

Experimental and Numerical Investigation of Electric Generator Cooling

Hamed Jamshidi[1], Håkan Nilsson[2], Valery Chernoray[3]
[1]Chalmers University of Technology, email: hamed.jamshidi@chalmers.se
[2] Chalmers University of Technology, email: hakan.nilsson@chalmers.se
[3] Chalmers University of Technology, email: valery.chernoray@chalmers.se

The importance of cooling in hydro-electric generators is high. This is because the main components of the generator, the cables and windings, are temperature-dependent. That is why the working temperature of the generator has to be controlled, in order to minimize hotspots that can cause material failure, and also to increase efficiency of the generator itself. In order to tackle the problem air is used as a cooling fluid, which circulates through the stator and rotor in the generator.

Air cooling of hydro power electric generators is going to be investigated experimentally and numerically. A predictive numerical approach was presented and validated[1]. The predicted flow field is independent of any experimental data at the inlet, and is determined completely by the solution. The numerical study has been performed using the OpenFOAM open source CFD software. A steady-state solver is used with the Frozen Rotor concept for the rotor-stator interaction. This means that there is no actual mesh movement in this study, but instead, the rotating regions in the domain are provided with source terms that account for rotation.

A laboratory model is designed and manufactured for experimental studies, Figure 1. The model is provided with static pressure holes and optical access for flow measurements using Particle Image Velocimetry (PIV). Inside the stator channels, 2D-2C PIV was used to measure velocity field. 2D-3C PIV was used to measure the other region, such as the region between the stator top lid and the top enclosure wall, and the region between the stator and the enclosure side wall.

The fully predictive numerical approach is shown to yield quantitatively similar results as the experimental flow measurements.

Both experiments and simulations show that there are large recirculation regions in the stator channels. One way to get rid of these recirculations is to have a modified fan designed based on turbomachinery theory which would build up the pressure better, yielding a higher flow rate that would fill up the channels better. A better fan design would also give a more smooth flow. A smoother flow makes both measurements and simulations easier. So a new centrifugal fan has been designed. This fan expected to deliver at least 20 percent more mass flow rate than the simple one.

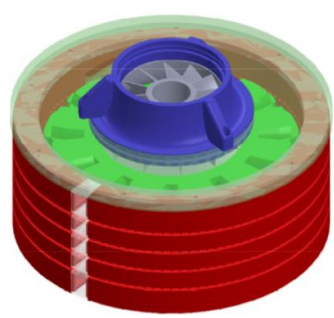

Figure 1: laboratory Generator model with modified fan; Stator (red), Rotor (green), New Fan (gray) and Fan Cover (Blue)

[1] Moradnia P., Chernoray V. and Nilsson H., HEFAT2011, 242-249, (2011)

Experimental Heat Transfer Study in an ITD with IR Thermography

Borja M. Rojo Perez[1], Valery Chernoray[2], Martin Johanson[3]

[1] Department of Applied Mechanics *Chalmers University of Technology 412 96 Göteborg, Sweden. email: borja.rojo@chlamers.se*

The intermediate turbine ducts (ITD) are used in modern jet engines to guide the flow from the high-pressure turbine (HPT) to the low-pressure turbine (LPT). The flow and heat transfer in a turbine duct is very complex. The flow has large secondary motions and is sensitive to flow separation, which is difficult to predict with numerical methods. Very limited information is available in open literature that can be used for validation of numerical methods. This experiment was done in a state-of-the-art aggressive intermediate turbine duct in a large-scale low-speed turbine facility at Chalmers. The duct configuration represents a modern counter rotating turbine design, with a flow turning structural vane, representative for a modern counter rotating engine system design. The facility has a turbine stage which provides realistic inlet conditions and operates at realistic flow Reynolds number[1]. The measurements were performed by using the Infrared Thermography.

A specially design vane is used in order to perform heat transfer measurements. The vane was made of a core with high thermal conductivity in order to have uniform temperature distribution in the volume and an insulating shell which creates large gradients of temperature. This method has allowed to measure the surface heat transfer coefficient by measuring the vane surface temperature. In order to achieve the highest accuracy of IR measurements the vane surface was covered with a special black velvet coating. The test section of the facility was instrumented with windows providing optical access for IR radiation. Phoenix MWIR Camera System was used for the measurements.

Experimentally obtained heat transfer coefficient map on two sides of the vane is shown in Fig. 1. The values of the heat transfer coefficient are typical for this component. The results clearly show the influence of the secondary flow and the tip leakage flow on the heat transfer. The counter-rotating vortices result in the areas of increased heat transfer due to the higher velocity induced next to the wall and higher local shear stress. Comparison of the experimental data with available CFD calculations demonstrated that prediction of the flow in the duct with loaded vane is challenging for CFD calculations. The suction side heat transfer distribution is predicted relatively well with certain discrepancies but the pressure side heat transfer coefficient distribution is not predicted correctly. Furthermore, it is found that the influence of the thermal radiation in the calculation of the convection heat transfer coefficient is important. Neglecting the radiation leads to additional error in determination of the heat transfer coeffcient which is 5 to 10 % in current case.

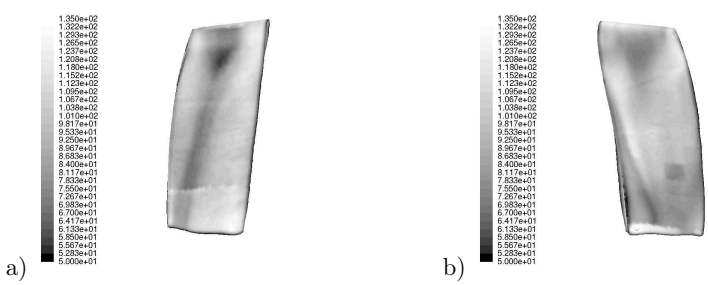

Figure 1: a) Film coefficient along pressure side. b) Film coefficient along suction side.

[1]C. Arroyo Osso, (2009) *Aerothermal Inestigation of an Intermediate Duct*, PhD Thesis, Chalmers University of Technology, Gothenburg, Sweden.

Grate aerodynamic

-Study of gas flow in grate

Per E. C. Burström[1*], A-L. Ljung[1], V. Frishfelds[2], T. S. Lundström[1] and B. Daniel Marjavaara[3]

[1]Division of Fluid and Experimental Mechanics, Luleå University of Technology, SE-971 87
[2]Liepaja University, Liela iela 14, LV-3401
[3]LKAB, SE-981 86 Kiruna

[*]E-mail: per.burstrom@ltu.se

Abstract

Iron ore pellets are a highly refined product supplied to the steel making industry for use in blast furnaces or direct reduction processes. The use of pellets offers many advantages such as customer adopted products, transportability and mechanical strength yet the production is time and energy consuming. Being such, there is a natural driving force to enhance the pelletization in order to optimize production and improve quality. The aim with this work is to study fluid dynamic phenomena in the induration furnace of a grate-kiln plant[1]. In specific how incoming process gas, leakage, and pellet bed influence the heat transfer through the bed. To achieve this numerical models are developed with which the heat transfer of an induration furnace can be examined and optimized. Heat transfer to a bed of iron ore pellets is therefore examined numerically on several scales. Two different modeling strategies to handle the porous bed are compared. The first is macro model that uses CFD and a porous media model to handle the bed of iron-ore. The second is a discrete micro-level model where the system of pellets is divided by modified Voronoi diagrams and the convective heat transfer of hot fluid flow through the system including dispersion due to random configuration of the pellets is modeled[2,3,4]. Results about drying of single pellets are applied there[5,6]. The two different strategies are compared and conclusions are drawn.

[1] Burström, P. E. C. , Lundström, T. S., Marjavaara, D., Töyrä, S., CFD-modelling of selective non-catalytic reduction of NOx in grate-kiln plants, Progress in Computational Fluid Dynamics, 10(5/6), 284-291 (2010)
[2] Ljung, A. L., Frishfelds, V., Lundström, T.S., Marjavaara, D., Modelling heat and mass transport in drying of a porous bed of iron ore pellets, Drying Technologies, 30(7), 760-773 (2012)
[3] Hellström, J.G.I., Frishfelds, V., Lundström, T.S., Mechanisms of flow-induced deformation of porous media, Journal of Fluid Mechanics, 664, 220-237 (2010)
[4] Jourak, A., Frishfelds, V., Hellström, J. G. I., Lundström, T.S., Derivation of Dispersion Coefficients Inside Three-dimensional Randomly Packed Beds of Spherical Particles, AIChE journal, in review (2013)
[5] Ljung, A-L. , Lundström, T. S. , Marjavaara, D., Tano, K., Convective drying of an individual iron ore pellet: Analysis with CFD, International Journal of Heat and Mass Transfer, 54(17-18), 3882-3890 (2011)
[6] Ljung, A-L. , Lundström, T. S. , Marjavaara, D., Tano, K., Influence of air humidity on drying of individual iron ore pellets, Drying Technology, 29(9) , 1101-1111 (2011)

Mjuka vävnader

onsdag 12/6 14:05-15:05

A theoretical approach towards smooth muscle modeling

Babak Sharifimajd[1], Jonas Sålhand[1]

[1]Division of Mechanics, IEI, Linköping University, email: babak.sharifimajd@liu.se

The physiological process of converting an external stimulus into a mechanical response in muscle cells are known as the excitation-contraction coupling. In smooth muscles, the external stimulus can be mechanical, electrical and/or chemical. Regardless of the type, they all lead to an increase in the intracellular calcium ion concentration which, in turn, triggers the contractile machinery. The smooth muscle cell membrane is the link between excitation and contraction processes by transporting ions in or out of the cell. The transporting of ions will change their concentration inside the cell which generates an electric field. This field can affect the smooth muscle cell in two ways: alternating the direction of a specific ion flux, and/or deforming the cell via the Maxwell stress[1].

In this work, we attempt to establish a model to predict the contractile behavior of smooth muscles by considering the effects of the cell membrane and the electric field. To this end, the smooth muscle cell is considered as a system consisting of dielectric material, perfect conductor, and free space. This system has the ability to contract, based on the kinematics introduced in Sharifimajd and Stålhand[2] and it occupies a volume V in the current configuration having the perimeter S which can include interfaces within the system as well. The external power exerted to this system is taken to be

$$\mathcal{P} = \int_V \mathbf{b}\cdot\mathbf{v}\ \mathrm{dV} + \int_S \mathbf{T}\cdot\mathbf{v}\ \mathrm{dS} + \int_V t_a u\ \mathrm{dV} - \int_S \hat{\mu}\mathbf{j}\cdot\mathbf{n}\ \mathrm{dS} + \int_V \hat{\pi} h\ \mathrm{dV} + \int_V \phi\dot{q}\ \mathrm{dV} + \int_S \phi\dot{\omega}\ \mathrm{dS} \tag{1}$$

where $\mathbf{b}$ and $\mathbf{T}$ are the mechanical and electrical body and surface forces, respectively, $t_a u$ is the energy expended for sliding the myosin and actin filaments[2], relatively, $\hat{\mu}$ and $\hat{\pi}$ are the electrochemical potentials of the ion transported by the ion flux $\mathbf{j}$ through the surface S with the outward normal vector $\mathbf{n}$ and the ion source h, respectively. Further, ϕ is the electrical potential, and ω and q are the surface and volume free charges existing in the system where the superscribed dot denotes the material time derivative. The form of the external power proposed is inspired by the external power exerted to a deformable dielectric material[1] along with the external power introduced to a system subjected to the diffusing species[3], and finally, the external power for muscle contraction[2].

By disregarding all thermal effects on the system and taking the Helmholtz free-energy function as follows,

$$\Psi = \psi_1(\mathbf{F}) + N(\varepsilon^a)\psi_2(\varepsilon^e, \boldsymbol{\alpha}) + \psi_3(\rho^{\mathrm{ion}}) + \psi_4(\mathbf{P}) + \psi_5(\boldsymbol{\alpha}), \tag{2}$$

and, applying the second law of thermodynamics, we can obtain the general form of constitutive relations required. In Eq. (2), $\mathbf{F}$ is the deformation gradient, $N \in [0,1]$ is a function which accounts for the effect of overlap between actin and myosin filaments in a macroscopic scale, and ε^a and ε^e are the active and elastic strains[2], respectively. Moreover, ρ^{ion} is the mass fraction of the ion transmitted into the system, $\mathbf{P}$ is the material polarization, and ψ_5 shows the dependency of the free energy on the cross-bridge formation and cycling with α_i to represent different states at which the myosin heads can be[4]. After defining the general form of constitutive relations, they are specialized for smooth muscle tissue and compared to experimental data to quantify the model.

[1]McMeeking and Landis, *T Am Soc Mech Eng J App Mech*, **72**, 581, (2005)
[2]Sharifimajd and Stålhand, *Biomech Model Mechanobiol*, 1, (2012)
[3]Gurtin et al., *The mechanics and thermodynamics of continua*. Cambridge University Press (2010)
[4]Hai and Murphy, *Am J Physiol*, **254**, C106, (1988)

Remodellering av glatt muskulatur vid ihållande kontraktion

Jonas Stålhand[1]
[1]Mekanik, Institutionen för ekonomisk och industriell utveckling, Linköpings tekniska högskola, Linköpings universitet, email: jonas.stalhand@liu.se

Glatta muskelceller återfinns i väggen på många håliga och rörformiga organ som artärer, hårsäckar, urinblåsa, luft- och matstrupe. Genom sin förmåga till aktiv kontraktion fyller dessa celler en fysiologisk funktion och möjliggör, till exempel, reglering av blodtrycket samt peristaltisk transport i matstrupen. Muskelns förmåga att generera kraft och kontrahera kan härledas till en cyklisk interaktion mellan två protein, de så kallade aktin- och myosinfilamenten. Dessa filament är arrangerade parvis i kontraktila element som spänner mellan ankringspunkter i cellens inre. När muskeln aktiveras binder myosinhuvuden till aktinet och translaterar filamenten relativt varandra. Denna translation fortplantar sig sedan i cellen via ankringpunkterna och det interna cellskelettet vilket leder till kontraktion. Tillsammans med kalciumjonkoncentrationen spelar filamentens överlapp en central roll för kontraktionskraften. Vid ett maximalt filamentöverlapp kan samtliga myosinhuvuden fästa till aktinet, men när filamenten förskjuts relativt varandra kommer änden på myosinfilementet att hamna utanför aktinfilamentet och dessa huvuden kan ej interagera, med följd att kraften sjunker.

Trots många likheter med skelett- och hjärtmuskulatur har glatt muskulatur ett antal unika egenskaper. En av dessa egenskaper är att den isometriska (maximala) kraften förblir konstant och oberoende av muskelns längd vid en ihållande kontraktion[1]. Denna anpassning sker inom loppet av minuter upp till timmar och är särskilt uttalad för glatta muskelceller i andningsvägarna och i urinblåsan, men förekommer även i artärsystemet. Experimentella resultat indikerar att anpassningsprocessen strävar efter att remodellera cellens inre struktur och att antalet kontraktila element ändras så ett maximalt överlapp mellan aktin- och myosinfilamenten återställs[2].

Sedan tidigare finns ett antal kontinuummodeller för muskelkontraktion baserade på grundläggande mekaniska och termodynamiska samband[3,4]. Dessa modeller är dock skräddarsydda för att studera själva kontraktionsförloppet som är betydligt snabbare än remodelleringen. I detta föredrag beskrivs hur en sådan modell[5] kan utökas för att även inkludera remodelleringen.

[1]Bossé et al., *Proc. Am. Thorac. Soc.*, **5**, 62–67, (2008)
[2]Kuo et al., *Am. J. Physiol. Cell Physiol.*, **285**, C384–390, (2003)
[3]Murtada et al., *J. Theor. Biol.*, **297**, 176–186
[4]Stalhand et al, *Prog. Biophys. Mol. Biol.*, **96**, 465–481, (2008)
[5]Sharifimajd och Stålhand, *Biomech. Modeling Mechanobiol.*, DOI 10.1007/s10237-012-0456-x

Musculoskeletal Biomechanics for Paralympic Classification

L Joakim Holmberg
Mechanics, Dept. of IEI, Inst. of Technology, Linköping University; joakim.holmberg@liu.se

The International Paralympic Committee (IPC) offers competitive sport opportunities for athletes with different impairments. To ensure competitions with equitable conditions, athletes with physical impairments are classified. The classification system aims to ensure that the success of an athlete is determined by endurance, fitness, mental focus, power, skill and tactical ability. Due to the difficulty to specify or even estimate how much an impairment impacts sports performance, there is a need for evidence-based research that can quantify the effect different impairments have on performance. Contemporary research in this area focuses on experimental methods. However, there are always psychological factors present and it is probably not possible to find two human beings with the same fitness, size, strength etc. Thus, using only experimental methods, it is hard to find the unbiased effect of an impairment on performance in a specific sport. Adding musculoskeletal biomechanics to classification, this problem may diminish.

The IPC define 8 types of physical impairments: impaired muscle power, impaired passive range of movement, loss of limb or limb deficiency, leg-length difference, short stature, hypertonia, ataxia and atheosis. Of these 8 impairment types, 4 (impaired muscle power, loss of limb or limb deficiency, leg-length difference, short stature) are readily implemented in contemporary available software for musculoskeletal biomechanics. Three impairment types (impaired passive range of movement, hypertonia, ataxia) may need some additional method development.

We have two examples from musculoskeletal simulations of cross-country skiing (double-poling). The first study[1] utilized two full-body simulation models that had the same kinematics and external kinetics, i.e. they performed the same task. The models also had the same anthropometric data except that one carried no muscles in the right lower leg and foot; thus mimicking a lower leg prosthesis and the 'loss of limb' impairment type. Results show that an able-bodied skier only has to produce about 80% metabolic muscle work compared to a disabled skier, see figure 1. In a follow-up study[2], we simulate the 'impaired muscle power' type. Raising the upper-body muscle strength with 20% yields a negligible difference in metabolic muscle work. Raising only the trunk muscle strength with 20% also yields a negligible difference. What happens in both cases is that metabolic muscle work is redistributed between body parts. This may indicate, that unless severe, the 'impaired muscle power' type can be handled by a skilled athlete, contrary to the 'loss of limb' impairment type. The two examples show that musculoskeletal biomechanics can strengthen classification with its quantitative data on the unbiased effect of different physical impairments.

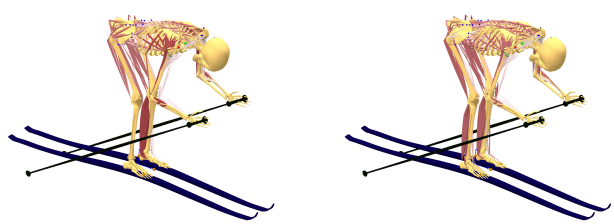

Figure 1: Visualization of disabled (left) and able-bodied (right) skiers during double-poling. Note that more bulging and darker muscles means higher muscular activity. Between models, compare e.g. the thigh muscles on the right leg or the muscles on the right shoulder.

[1] Holmberg et al., *Prosthet. Orthot. Int.*, **36**, 396, (2012)
[2] 'Work in progress', presented here for the first time.

Numeriska metoder I

onsdag 12/6 15:25-16:45

Using GPU accelerators for polycrystalline material simulations

Ylva Mellbin[1,2], Håkan Hallberg[1], Matti Ristinmaa[1]
[1]Division of Solid Mechanics, LTH, Lund
[2]email: Ylva.Mellbin@solid.lth.se

Crystal plasticity models are often used to model the deformation of polycrystalline materials. However, it is computationally very demanding. Adopting the common Taylor assumption it requires calculation of the deformation of several hundreds of crystalline grain to obtain the stress in a single integration point in the overlying FEM structure. Since there is no coupling between the grains, the calculations contains a large degree of parallelism.

One emerging technology for running massively parallell computations without using large computer clusters is porting the parallell parts of the calculations to the graphical processing unit (GPU). GPUs are designed to be able to perform the same floating point operations in parallell on a large number of threads. This ability has been taken advantage of in the implementation of the crystal plasticity model. A drawback with the GPU when used for scientific calculations is that it has a very limited amount of memory. This makes the implicit Eulers method usually used for solving the ODEs governing the deformation and hardening in each grain unsuitable for implementation on the GPU. Therefore another solution metod has been developed which requires less local memory but still manages to solve the stiff ODEs in question. This method is based on an operator split where the first part is calculated with a semi-implicit Eulers method while the other part is solved with a one step Newton iteration with a diagonalized Jacobian to avoid large matrix inversions.

Test results shows that the method gives a considerable speedup compared to the standard implementation. Even on an ordinary laptop the GPU implementation is more than an order of magnitude faster, and on a computer with a GPU suited for running computations the improvement is even larger.

Phase stability of $ZrH_{1.5}$ - a DFT study

Pär A. T. Olsson[1], Jakob Blomqvist[2], Christina Bjerken[3]
[1]Malmö University, email: Par.Olsson@mah.se
[2]Malmö University, email: Jakob.Blomqvist@mah.se
[3]Malmö University, email: Christina.Bjerken@mah.se

Due to its low thermal neutron capture cross section and good corrosion resistance, zirconium-based alloys are commonly employed as fuel cladding material in the core of nuclear power reactors. While in service, the fuel cladding material is in contact with water, which promotes the oxidation of Zr. This process releases free hydrogen, of which a portion enters the alloy and gives rise to the formation of brittle hydrides. This can have a detrimental effect on the integrity and the longevity of the material. Among the zirconium dihydrides (ZrH_x, $1.5 \leq x \leq 2$), the face centered tetragonal ϵ ($c < a$) and the cubic fluorite-type δ phases are known to exist. The $\delta \rightarrow \epsilon$ phase transition is known to depend on the hydrogen concentration, where ϵ is preferred at high hydrogen concentrations and δ occurs at lower hydrogen content. At which concentration and under what conditions the transition occurs is not well established and there is much discrepancy among the experimental observations.

The purpose of this work is to investigate the thermal influence on the phase stability of $ZrH_{1.5}$ using quantum mechanical density functional theory (DFT). The free energy is studied for different temperatures based on the quasi-harmonic approximation using the phonon density of states and the electron density of states. All DFT simulations are performed using the QUANTUM-ESPRESSO package, which is a plane wave based DFT package. For the electron-ion interaction we have used ultrasoft pseudopotentials of the Vanderbilt type. For Zr a pseudopotential that considers $4d^2 5s^2$ valence electrons and the $4s^2 4p^6$ semi-core states in the valence band was used while only the $1s^1$ electron is treated for H. The employed exchange correlation functional is that of Perdew, Burke and Ernzerhof (PBE) within the framework of the generalized gradient approximation.

We have evaluated the difference in free energy for the δ and ϵ phases for the temperature range 20-500 K in Fig. 1. The tetragonal structure has the lowest free energy for low temperatures. However, if the temperature is increased, at 229 K the δ phase becomes more stable. This implies that a phase transition occurs at that temperature and it explains why the cubic δ phase is observed experimentally at room temperature, despite the low formation energy of the tetragonal ϵ phase.

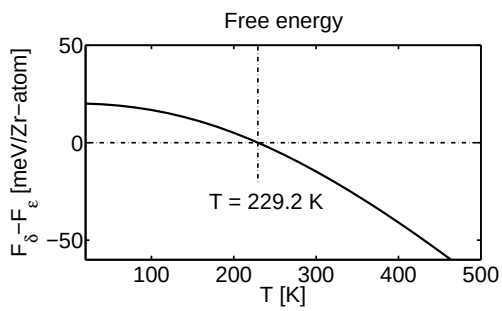

Figure 1: Difference in free energy for δ (cubic) and ϵ (tetragonal, $c < a$) hydrides for different temperatures. There is a phase transition at 229 K where the tetragonal phase transforms into cubic.

Nucleation of a second phase at a dislocation using a phase field approach

Christina Bjerkén[1]
[1]Faculty of Technology and Society, Malmö University, 205 06 Malmö, email: christina.bjerken@mah.se

Defects in a crystal, such as dislocations, give rise to internal strains, thus affecting the mechanical equilibrium condition. A phase field model is used to study the kinetics of second-phase transformation induced by an elastic defect, here an edge dislocation, in a crystalline elastic solid. A two-component structural order parameter $\bar{\eta} = (\eta_1, \eta_2)$, depending on space and time, defines the structure/orientation of the crystal and distinguishes the prevailing phases. The non-conserved order parameter $\bar{\eta}$ obeys the time-dependent Ginzburg-Landau equation[1], which is solved numerically using a finite volume method. Computations are made at a temperature above the transition temperature for an unordered matrix phase (I) for which $\bar{\eta} = (0, 0)$. The introduction of a dislocation may induce nucleation of two different ordered phases (II and III) defined by $\bar{\eta} = (0, \pm\eta)$ or $\bar{\eta} = (\pm\eta, 0)$, and $\bar{\eta} = (\pm\eta, \pm\eta)$, respectively. The phase transformation is followed until a steady state is reached. Figure 1 shows the distribution of phases at the vicinity of the dislocation at an early stage of the evolution, at an intermediate time, and at steady-state, respectively. It is seen that the presence of a dislocation first triggers the nucleation of one of the ordered phases, type III. This type of crystal structure then expands further into the material, while also phase II nucleates at the vicinity of the dislocation line. Phase II will eventually be the only ordered phase remaining. The model is applicable to systems where second-phase ordering occurs at stress raisers, i.e. the formation of different hydrides in titanium and zirconium alloys.

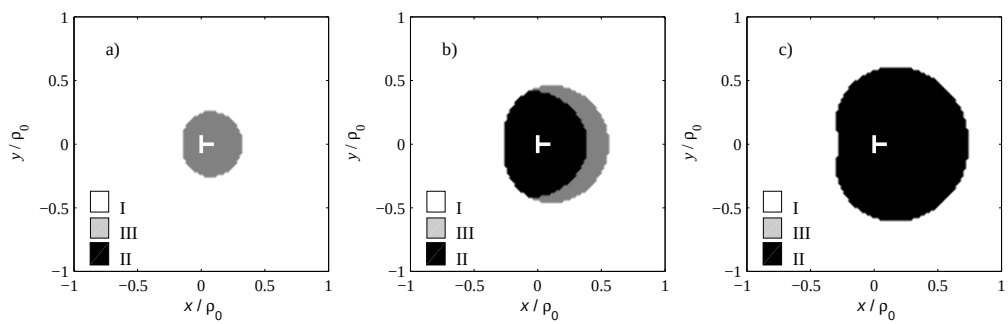

Figure 1: Evolution of two ordered phases (gray and black, resp.) from an unordered matrix phase (white) in the vicinity of a dislocation at a) an early stage, b) an intermediate stage, and c) steady state.

[1]Lifshitz and Pitaevskii, *Physical Kinetics*, Ch XII, Pergamon, Oxford, 1981

Cracks and Fracture of Origami Patterns as Energy Absorbing Devices

Rahul Reddy Katangoori[1], Sharon Kao-Walter, Mats Walter
Blekinge Tekniska Högskola, Karlskrona
[1]*rahul.reddy.katangoori@bth.se*

Thin walled tubes with origami patterns are popular design for the energy absorbing devices than the conventional tubes[1]. If the origami pattern is made by forming, there will be micro cracks. When they are subjected to these cracks, during the crushing process they will affect the deformation mode and collapse mode[2].

The main objective of this ongoing project we develop an accurate frame work for finite element analysis of fracturing in origami patterns. The numerical simulation of the collapse phenomenon has been undertaken using an implicit quasi-static non-linear finite element analysis in Abaqus with maximum number of cutbacks allowed for an increment. This allows to run the simulations in realistic time domain. Elasto-plastic material properties together damage initiation and damage evolution are used to define the failure in the material. For implementing a crack numerically we have used an effective and general technique of separating two parts by disconnecting the nodes. Also, what manufacturing process or arrangement we can have to alter the orientation of the crack to achieve better performance will be explored. The extended finite element method (XFEM) will be utilized thereby avoiding restrictions of the crack paths as in standard FEM.

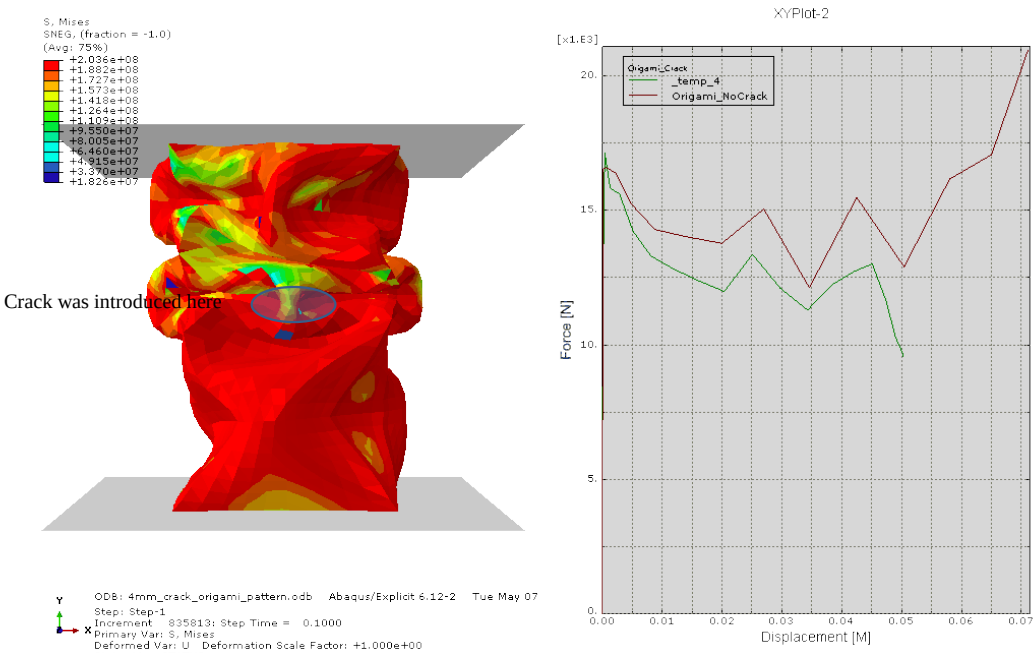

Figure 1: Origami tube with crack (a) after the crushing process (b) comparison of force-displacement of Origami tube without crack and with crack

[1] Jiayao Ma (2011). Thin walled Tube with Pre-folded Origami Patterns as Energy Absorption Devices, Department of Engineering Science, University of Oxford.

[2] Katangoori R. R., Kao-Walter. S., Zhong. Y., Conceptual study on an origami patterns of type I tapered square tube with and without a crack, 2013, Applied Mechanics and Materials, 275-277, 184.

Experimentella metoder II

onsdag 12/6 15:25-16:45

Kärnbilding av gamma´´ partiklar i IN718

Martin Fisk[1]
[1]Teknik och samhälle, Materialvetenskap, Malmö högskola, email: martin.fisk@mah.se

I familjen superlegeringar återfinns materialet Inconel 718; en krom-nickel-järnlegering som utvecklas på 1940-talet av en forskargrupp vid Wiggin alloys, England. Namnet Inconel är ett varumärke varför andra namn på legeringen är förekommande: IN718, Inco 718 eller Alloy 718 är de vanligaste. IN718 används vanligtvis i konstruktioners högtemperaturområden där krypbeständigheten på materialet måste vara god. Delar i flygplansmotorer, värmeväxlare, kärnkraft är några exempel. Materialet kan användas i temperaturer upp till ca 650°C utan att dess mekaniska egenskaper nämnvärt försämras.

IN718 får sin goda krypbeständighet på grund av utskilda γ''-partiklar som hindrar dislokationsrörelser i planet. De utskilda partiklarna bidrar även till att öka materialets sträckgräns i mycket stor utsträckning. För superlegeringen IN718 är γ''-partikelns kristallstruktur ett koherent (eller semikoherent, beroende på partikelns storlek) rymdcentrerad tetragonalt gitter, innehållande nickel och niob (Ni_3Nb). Vidare är pariklens form oblatformad med en excentricitet på ca 1/3 beroende på dess storlek (för mindre partiklar formas denna till att bli mer sfärisk). Volymandelen av partiklar och dess storlek beror på materialets åldringshistorik; dvs. åldringstemperatur och tid. För ett material som har genomgått en standardåldringsprocess – 760°C i 5 h – är volymandelen ca 13 vol.% och partiklarnas medeldiameter är ca 30 nm. Vid högre temperaturer löser partiklarna upp sig.

I dagsläget har väldigt få, eller inga, mätningar gjorts vid kärnbildning av γ''-partiklar i IN718. Vid denna presentation kommer resultat från ”Small angle x-ray scattering” (SAXS) körningar vid MAX-lab i Lund att presenteras. Resultatet har stor betydelse för att numeriskt kunna simulera kärnbildning och tillväxt av γ''-partiklar i IN718. Att numeriskt kunna simulera kärnbildning och tillväxt av γ''-partiklar medför att en materialmodell som kan prediktera partikelfördelning vid icke-isotermiska temperaturhistorier kan utvecklas. Detta är av stor betydelse för att man på ett säkert sätt skall kunna simulera partikelfördelningen i och intill en svets.

Effects of defects on the tensile strength of heterogeneous composite materials

Thomas Joffre[1], Arttu Miettinen[2], Erik L.G. Wernersson[3], Per Isaksson[1] and E. Kristofer Gamstedt[1]

[1]Uppsala University, Ångström Laboratory, Box 524 751 20, Uppsala, thomasjoffre@gmail.com
[2]University of Jyväskylä, Department of Physics, Box 35, FI-40014, Finland
[3]Swedish University of Agricultural Sciences, Centre for Image Analysis, Box 337, SE-751 05 Uppsala

Heterogeneous materials tend to fail at the weakest cross-section, where the presence microstructural heterogeneities or defects controls the tensile strength. Short-fibre composites is an example of a heterogenous material, where unwanted fibre agglomerates initiate tensile failure. In this study, the dimensions and orientation of fibre agglomerates have been analysed from three-dimensional images obtained by X-ray microtomography. The geometry of the specific agglomerate responsible for failure initiation has been identified and correlated with the strength. At the plane of fracture, a defect in the form of a large fibre agglomerate was almost inevitably found. These new experimental findings highlight a problem of some existing strength criteria[1,2], which are principally based on a rule of mixture of the strengths of constituent phases, and not on the weakest link. Only a weak correlation was found between stress concentration induced by the critical agglomerate and the strength. A strong correlation was however found between the stress intensity and the strength, which underlines the importance of the size of largest defects in formulation of improved failure criteria for short-fibre composites. The increased use of three-dimensional imaging will facilitate the quantification of dimensions of the critical flaws.

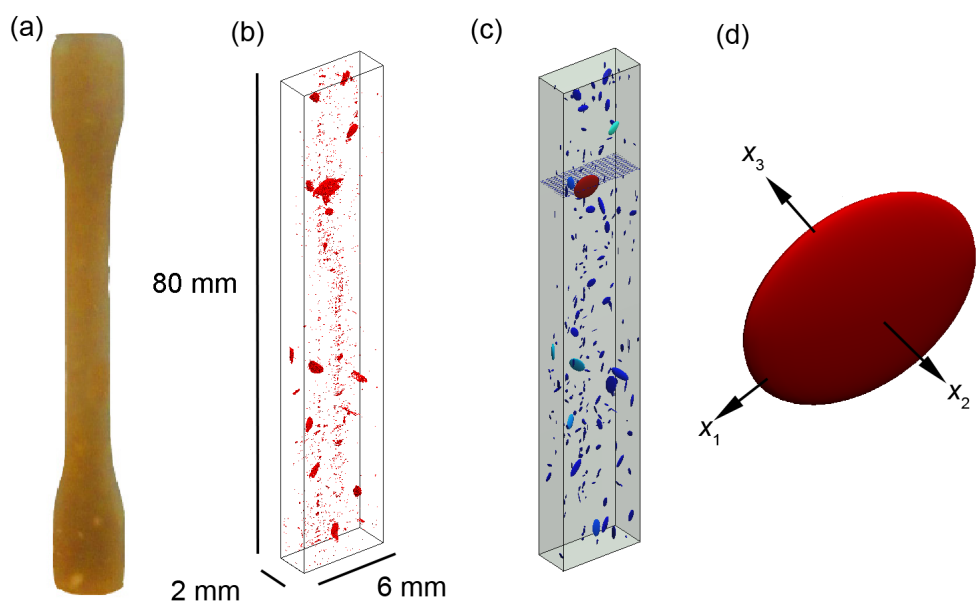

Figure 1: Identification of the critical agglomerate: (a) A composite dog bone sample. (b) Identification of the agglomerates with XμCT. (c) Modelling of the agglomerates using ellipsoids. The rupture plane is marked with small blue stripes. (d) Principal directions of the critical ellipsoid fitted to the critical agglomerate.

[1] Andersons and Joffe, *Composites Part A,* **42**, 129-135, (2011)
[2] Virk, Hall and Summerscales J, *Materials Science and Technology*, **ISSN: 02670836**, (2012)

Residual stress and hydrogen effect on Ti-6Al-4V alloys produced by Electron Beam Melting

T. Maimaitiyili[1], J. Blomqvist[1], A. Steuwer[2] ,M. Blackmur[3], C. Bjerkén[1], A. Safdar[1]
[1] Materials Science, Malmö University, email: tuerdi.maimaitiyili@mah.se
[2]Max IV Laboratory, Lund University
[3]School of Materials, Manchester University,

There is an internal, self-balanced stress known as residual stress (RS) that exists in all alloy systems without any external applied forces. Depending on the compressive or tensile nature and magnitude of the RS, it significantly affects the mechanical properties of the materials. Therefore, it is crucial to know the nature and magnitude of RS in material for safe and economical operation.

In this work, we used unique, multipurpose, high energy (50-150 KeV) beamline I12-JEEP (Joint Engineering, Environment and Processing) at Diamond Light Source in UK with Energy Dispersive X-Ray Diffraction (EDXRD) setup to map up the RS states in one of the most popular titanium alloys with a code name Ti6Al4V. This type of titanium alloy is widely used in biomedical and aerospace industry because of their excellent combination of a high strength/weight ratio and good corrosion resistance [1]. The Ti6Al4V which we were investigated are produced using electron beam melting (EBM) technique as a function of EBM processing parameters. In addition to relation between RS and processing parameters of EBM, the hydride formation versus processing parameters and as well as the effect of residual stress to the hydride precipitation in EBM built Ti6Al4V were investigated.

To find out the effect of EBM processing parameters to the residual stress development, various samples produced with different beam size, scanning speed and different building thickness were investigated. From each type of the sample four specimens were prepared and three of them loaded with hydrogen in different concentrations, i.e. the hydrogen concentration of the various samples are 262, 772, 951 and 1410 ppm. Other than these alloy samples we also measured clean and hydrided original powder samples which are used for make these solid samples in our studies. After data collection, the whole pattern fitting method Rietveld and Pawely were performed with structure analysis software package Topas-Academic [2] and GSAS [3].

[1]A. Safdar, , H.Z. He, L. Y. Wei, A. Snis and L.E.C. de Paz Rapid prototyping journal, (2011)
[2]A. A. Coelho (2004). TOPAS-Academic. http://www.topas-academic.net/
[3]A.C. Larson and R.B. Von Dreele, "General Structure Analysis System (GSAS)", Los Alamos National Laboratory Report LAUR 86-748 (1994)

PIV analysis of Merging Flow in a Simplified Model of a Rotary Kiln

Sofia Larsson[1], Reine Granström[1], Staffan Lundström[1], Daniel Marjavaara[2]
[1]Fluid Mechanics, Luleå University of Technology, email: sofia.larsson@ltu.se
[2]LKAB, Kiruna

Rotary kilns are used in a variety of industrial applications. The focus in this work is on characterizing the non-reacting, iso-thermal flow field in a rotary kiln used for iron ore pelletization. A downscaled, simplified model of the kiln is experimentally investigated using Particle Image Velocimetry. Five different momentum flux ratios of the two inlet ducts to the kiln are investigated in order to evaluate its effect on the flow field in general and the recirculation zone in particular. Time-averaged and phase-averaged analyses are reported, and it is found that the flow field resembles that of two parallel merging jets, with the same characteristic flow zones, as exemplified in Fig. 1. The back plate separating the inlet ducts acts as a bluff body to the flow and creates a region of reversed flow behind it. Due to the semi-circular cross-section of the jets, the wake is elongated along the walls. Conclusions are that the flow field shows a dependence on momentum flux ratio of the jets; as the momentum flux ratio approaches unity, there is an increasing presence of von Kármán-type coherent structures with a Strouhal number of between 0.16-0.18. These large-scale structures enhance the mixing of the jets and also affect the size of the recirculation zone. Due to the geometrical confinement the flow field in the kiln deviates from the flow field behind a bluff body in a free stream. The vortical structures converge towards the kiln walls, leading to a coupling between the wall shear layer and the vortex originating from the shear layer of opposite vorticity. This interaction results in a portion of the wall shear layer being ejected by the influence of the shed vortices.

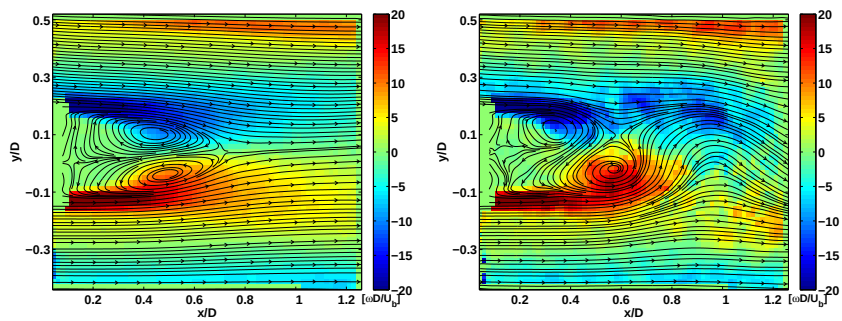

(a) Time-average (b) Phase-average

Figure 1: Time-averaged and phase-averaged results for matched momentum flux. The contours are coloured by vorticity and streamlines are added to highlight the flow patterns.

Strömning i gränsskikt

onsdag 12/6 15:25-16:45

Rotating-disk boundary-layer flow

Shintaro Imayama[1], P. Henrik Alfredsson[2], R. J. Lingwood[3]
Linné Flow Centre, KTH Mechanics.
[1]shintaro@mech.kth.se [2]phal@mech.kth.se [3]lingwood@mech.kth.se

Rotating-disk flow has been investigated not only as a simple model of cross-flow instability to compare with swept-wing flow but also for industrial flow applications with rotating configurations. About 28–32 stationary (in the rotating frame) convectively unstable cross-flow vortices are typically observed in the flow visualization[1], see as well as figure 1. However, the onset of transition is highly reproducible in various experimental facilities[2]. Lingwood[3] found local absolute instability for a certain travelling disturbance above $R = 507$ which may have main responsible for the transition process, where Reynolds number R is defined as $R = r^*\sqrt{\Omega^*/\nu^*}$, where r^* is a local radius, Ω^* is a rotational speed, ν^* is a kinematic viscosity and $*$ denotes dimensional value. A main objective of this experimental study is to investigate to what extent the absolute instability is involved into laminar-turbulent transition of rotating-disk flow.

Figure 1: Stationary-vortex distributions in the range of (black)$-0.12 < v < 0.12$(white), where v is ensemble-averaged azimuthal-fluctuation velocity normalized by local disk velocity measured by hot-wire anemometry at $z = 1.3$ where $z = z^*\sqrt{\Omega^*/\nu^*}$ is non-dimensional wall-normal height (polar coordinates and rotating anti-clockwise). Dotted lines indicates $R = 500$, 600, respectively moving outward. The edge of the contour is $R = 700$. Outer solid circle line indicates edge of the disk (i.e. $R = 731$).

[1]Kohama, Y., *Acta Mech*, **50**, 193-199, (1984)
[2]Imayama, S., Alfredsson, P. H., and Lingwood, R. J., *J. Fluid Mech.*, **716**, 638-657, (2013)
[3]Lingwood, R. J., *J. Fluid Mech.*, **299**, 17-33, (1995)

Modeling and validation of flow over a wall with large surface roughness

A. G. Andersson[1], T. M. Green[2], J. G. I. Hellström[3], P. Andreasson[4], T. S. Lundström[4]
[1]Division of Fluid and Experimental Mechanics, Luleå University of Technology
[2]Division of Fluid and Experimental Mechanics, Luleå University of Technology
[3] Division of Fluid and Experimental Mechanics, Luleå University of Technology, email: gunnar.hellstrom@ltu.se
[4] Division of Fluid and Experimental Mechanics, Luleå University of Technology and Vattenfall Research and Development
[4]Division of Fluid and Experimental Mechanics, Luleå University of Technology

Fluid flow over surfaces with large surface roughness is important in many applications such as hydropower tunnels and natural channels. When creating numerical models of such applications it is very impractical to include the wall roughness in the geometrical model both with regards to the geometric resolution required and the large computational cost of performing such simulations. Wall roughness is therefore typically estimated as a global parameter by some empirical relation and added mathematically into numerical simulations. It is here examined to what extent the surface roughness should be resolved in order to still capture the main flow features.

A high-resolution laser scanning of an excavated tunnel was used to create a geometry for Computational Fluid Dynamics (CFD) simulations and a scale model of the geometry (1:10) was constructed for experimental validation. A section of the side wall from the tunnel with dimensions 40x2.5 m was selected for the numerical and experimental models. The height of the roughness elements for this wall segment varied between 0-0.8 m. This rough wall was then deployed as a side wall in a rectangular channel where the other walls were considered smooth.

Simulations were performed with the commercial software CFX13 from Ansys Inc. A $k - \varepsilon$ turbulence model with standard wall functions was applied and the geometry of the rough surface was resolved to different degrees by numerical grids with varying element sizes. Particle Image Velocimetry (PIV) measurements were made on the scale model to validate the simulations, for the mesh resolution part. Double Averaging techniques have been utilized in order to capture both the time as well as the spatial variations along the central plane of the rough surface. The simulation shows a similar pattern as the measurement although the simulated velocities are lower and the location of maximum velocity occurs closer to the rough surface in the measurement. The double averages serve as a good evaluation technique for the flow regions close to the wall, when comparing the simulations and the measurements. An additional study has been performed on how well the geometrical resolution should be, i.e. how many points the surface is created from. In order to quantify how well resolved the rough surface should be both in laser scanning resolution as well as mesh resolution. For instance, there is a significant difference in the amount of vorticity created and also the alteration in pressure fluctuations when comparing the different surfaces hence the need to have a well resolved laser scanning is of the essence when performing simulations on flow problem with large scale surface roughness.

Skin-friction drag reduction - Now with reinforced passive control

Sohrab S. Sattarzadeh, Jens H. M. Fransson, Bengt E. G. Fallenius & Alessandro Talamelli
Linné Flow Centre, KTH Mechanics, email: jensf@mech.kth.se

It is well known that the skin-friction coefficient can increase by an order of magnitude in a turbulent boundary layer compared to a laminar one for high enough Reynolds numbers, therefore, delaying transition to turbulence plays an important role in reducing the skin-friction drag on any aerodynamically smooth body. Recent investigations have shown that well designed *roughness elements* mounted on the surface in the boundary layer can control the flow and delay the transition to turbulence by modulating the base flow in the spanwise direction.

Fransson et. al [1,2] were able to damp the growth of Tollmein-Schlichting (TS) waves and, consequently, delay the transition to turbulence by introducing finite amplitude streaks to the Blasius boundary layer on a flat plate, using circular surface roughnesses. In a more recent study Shahinfar et. al [3] have tested the passive control method by employing miniature vortex generators, MVGs, downstream of the disturbance source, in contrary to previous studies where the disturbances had been introduced in an already modulated boundary layer. Successful results for transition delay in the non-linear regime was also presented in their study where high forcing amplitudes of the TS waves were applied.

In the present study, by mounting a second set of MVGs downstream of the first array and reinforcing the streak amplitude, it is shown that the transition onset could successfully be pushed even further downstream. In figure 1, where streamwise fluctuating velocity distribution is depicted, it is observed that the onset of transition is pushed downstream from the case in the top figure to the middle one by adding one set of vortex generators. For the case where two sets of MVGs are mounted, as shown in the bottom figure, no onset of transition is captured within the measurement domain.

JHFM acknowledges the European Research Council for their financial support of the AFRODITE project through a Starting Independent Research Grant.

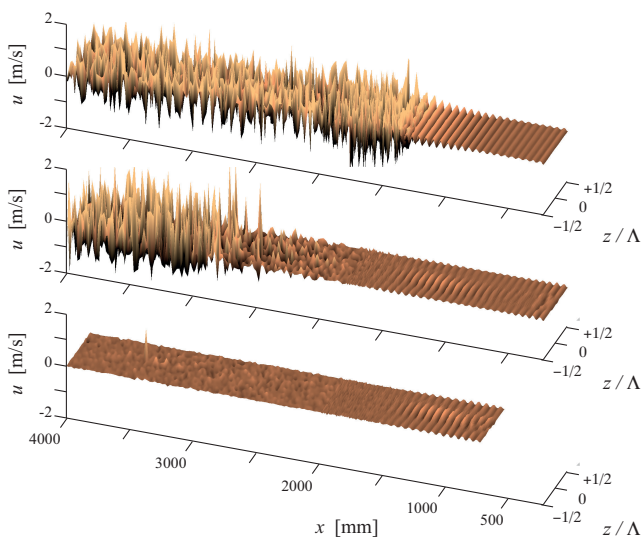

Figure 1: Streamwise fluctuating velocity distribution in a horizontal plane at $y/\delta_1 = 0.5$ above the plate for cases without MVGs (top), one array of MVGs (middle) and two arrays of MVGs (bottom). The freestream velocity is 6 m s^{-1}, and the first and second MVG arrays are mounted at $x = 222$ and 700 mm respectively. δ_1 is the displacement thickness and Λ the distance between MVG pairs.

[1]Fransson, J.H.M., Brandt, L., Talamelli, A. & Cossu, C., *Phys. Fluids*, **17**, 054110, (2005)
[2]Fransson, J.H.M., Talamelli, A., Brandt, L. & Cossu, C., *Phys. Rev. Lett.*, **96**, 064501, (2006)
[3]Shahinfar, S., Sattarzadeh, S.S., Fransson, J.H.M. & Talamelli, A., *Phys. Rev. Lett.*, **109**, 074501, (2012)

Flow control by means of plasma actuation - a study of the electric wind

Julie Vernet[1], Ramis Örlü[1], P. Henrik Alfredsson[1]
[1]Linné Flow Centre, KTH Mechanics, SE-10044 Stockholm, Sweden, email: julie@mech.kth.se

Reducing the aerodynamic drag on heavy vehicles is the mission of the **F**low **R**esearch on **A**dvanced and **N**ovel **C**ontrol **E**fficiency (FRANCE) project. The ability of Dielectric Barrier Discharge (DBD) plasma actuators to actively delay separation of the flow around the front corners of a truck cabin is under study. DBD plasma actuators are made of two electrodes asymmetrically placed on each side of a dielectric material, see Fig. 1(a). Plasma actuators present, among others, the advantage of not having any moving parts making them more robust than other types of actuators. By applying a high alternating voltage between the electrodes a plasma region is formed on the surface of the dielectric. This plasma is a consequence of accelerated electrons which ionize the surrounding medium: repulsion of positive ions during the ionization process induces momentum similar to a wall-jet, which here is called an electric wind. The present investigation focuses on the airflow induced by in-house made plasma actuators placed on a half-cylinder. The chosen geometry can be seen as a generic model of the flow around the corners of a truck cabin. Parameters such as driving voltage, frequency, dielectric thickness and their influence on the efficiency of the actuator are investigated by means of velocity measurements of the electric wind using Laser Doppler Velocimetry (LDV).

Mean velocity profiles show that the plasma actuators are able to produce wall jets with velocities of several meters per second. Increasing the driving voltage and frequency increases the jet velocities and its maximum moves closer to the wall, see Fig. 1(b). Because the actuator adopts the shape of the model, results show that the induced electric wind follows the surface of the cylinder, which is an advantage for future separation control. Close to the actuator the airflow becomes periodic in time due to the alternating driving current and the time variations of the electric wind were investigated through phase-averaged LDV measurements. The increase of induced velocities during both the forward and backward stroke of the high-voltage cycle shows agreement with the PUSH-push mechanism theory[1] of DBD plasma actuators.

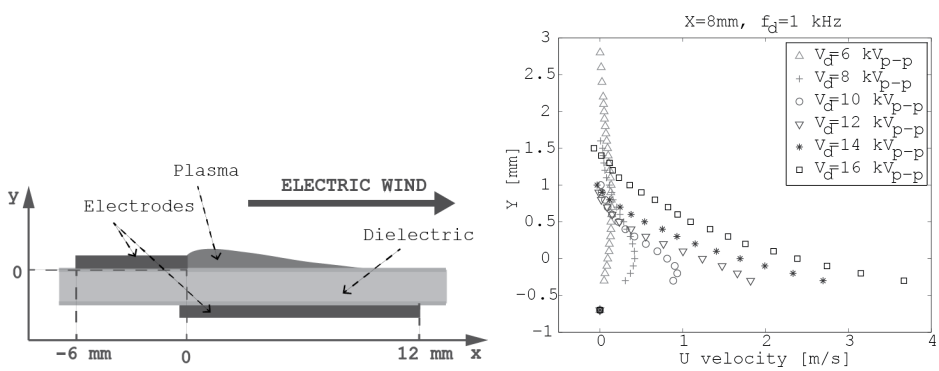

(a) (b)

Figure 1: (a) Sketch of the DBD plasma actuator used for this project. (b) Wall-normal profiles of the mean streamwise velocity component induced by the actuator plotted for different driving voltages (V_d) at the driving frequency f_d=1 kHz.

[1]Corke, Enloe and Wilkinson, *Annu. Rev. Fluids Mech.*, **42**, 505-529, (2010)

Hårda vävnader

onsdag 12/6 15:25-16:25

Investigation of femoral strain patterns using digital image correlation.

Lorenzo Grassi[1], Sami P. Väänänen[2], Saber Amin Yavari[3], Harrie Weinans[4], Jukka S. Jurvelin[2], Amir A. Zadpoor[3], Hanna Isaksson[1]
[1]Lund University, Sweden, email: lorenzo.grassi@solid.lth.se
[2]University of Eastern Finland, Finland
[3]Delft University of Technology, The Netherlands
[4]Erasmus Medical Center, The Netherlands

Introduction. In-vitro mechanical tests on proximal human femurs have been made with the aim of investigating the surface strain response[1] and to serve as a validation framework for numerical models[2]. Strain gauges (SG) are the current gold standard for surface strain measurement, but the number of measurements is limited, and data alteration due to their reinforcement effect may arise on thin cortex regions. The digital image correlation (DIC) technique is able to provide thousands of measurements using a non-contact method. The aim of the study was to investigate the strain response of cadaver human femurs at high strain rate, using a DIC system with high-speed cameras.

Methods. A fresh-frozen proximal cadaver femur was obtained (Ethical permission 5783/04/044/07). The specimen was prepared for DIC recording by painting a white background over the anterior surface, with a random black speckle pattern. The bone was loaded in a quasi-axial configuration at 15mm/s (Instron, Inc.). The DIC images were recorded at 3000 fps (two 1MPx cameras, Photron, Inc.). The images from the two cameras were correlated using Vic 3D 2010 (Correlated Solutions, Inc.). Simulated extensometers and SGs were identified (Fig. 1b).

Results. DIC provided about 50000 uniquely traceable points. The maximum recorded load was 7856 N. Both the simulated extensometer data (Fig 1b) and the actuator displacement showed a significant correlation with the force recorded by the load cell (R^2=0.99, 1000N<force<7856 N). The principal strains recorded by the simulated strain gauges were also correlated with the applied force (R^2>0.94, Fig 1c).

Discussion. A femur was loaded until fracture at a rate of 15 mm/s, which can be considered to be close to physiological conditions. The mechanical behaviour of the bone was overall linear up to fracture, in accordance with previous experiments[1]. This was confirmed by the low amount of residual strains recorded in the specimen immediately after fracture (average von Mises strain 0.44±0.46%), with the highest residual strains localized near the fracture rim. Qualitative investigation of the high-speed movies showed that the fracture began along the superior aspect of the femoral neck, which was mainly solicited in tension. Fracture occurred as a very quick event (less than 0.3 ms), and no clear stress or strain concentration areas were identifiable in that region before the fracture (Fig 1a).

The main limitation of the present work is that only one cadaver femur has been investigated. Two more specimens were tested, and their analysis is currently ongoing. Further data analysis is also required in order to better understand the mechanisms leading to the fracture onset. Based on the current results, the set-up may provide extensive information about the strain evolution under fast loads, including strains in the fracture region. This may contribute to a better explanation of the failure mechanisms of bones, and provide a solid benchmark for the validation of numerical models.

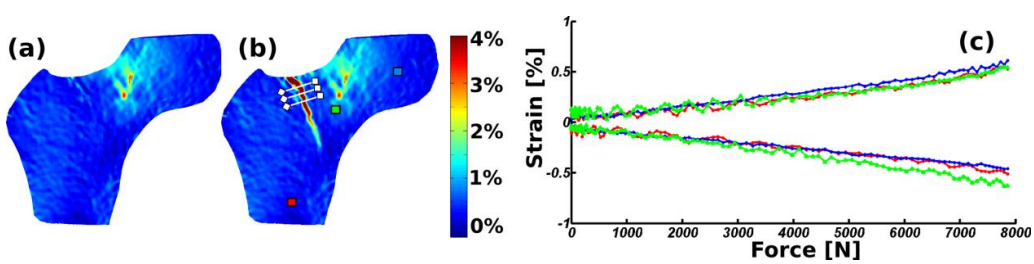

Figure 1: (a) 1st principal strains before, and (b) after fracture: the simulated SGs and extensometers are evidenced; (c) principal strains (SG on the head in blue, on the neck in green, and on the diaphysis in red) as a function of the applied force.

[1] Juszczyk et al., *Jbiomech*, **44**, (2011)
[2] Viceconti et al., *Clin Biomech*, **20**, (2005)

Can widening of a stress fracture in a long bone decrease local strains sufficiently to enable healing?

Emil Fågelberg[1], Lorenzo Grassi [1], Per Aspenberg [2], Hanna Isaksson [1]
[1]Div of Solid Mechanics, Lund University, email: hanna.isaksson@solid.lth.se
[2] Department of Orthopedics, Linköping University

Introduction: Stress fractures at the anterior border of the tibial mid-diaphysis are often problematic to heal, possibly because strains in the fracture gap are too large. Therefore, surgical intervention may be inevitable. Today, the surgical methods focus on achieving complete stability of the crack gap. In this study, a potential method that is less invasive is hypothesized and evaluated from a biomechanical point of view. The concept is to widen the fracture gap by drilling a hole with a large diameter from the anterior border, through the crack and into the medullary cavity. The aim of the present study was to evaluate the differences in the mechanical response of the intact, fractured and drilled tibia, using a finite element (FE) model.

Methods: The geometry of the tibia was acquired from clinical CT images via semi-automatic segmentation. FE models were established for an intact tibia and a tibia with a stress fracture before and after drilling. Poroelastic orthotropic material properties were used for the cortical bone, whereas in the trabecular bone isotropic material properties were mapped over each element based on CT density [1]. Soft granulation tissue was modeled in the fracture gap and drilled hole. The stiffness of the intact tibia was validated against *in vitro* experimental data [2]. The load magnitude was set equal to the highest tibio-femoral contact force during gait and stair climbing [3]. The force was applied at the tibial condyles of the FE models, while the distal end was fixed to prevent rigid body motion.

Results: The stiffness of the intact tibia model was within the range of the experimental data. However, some differences were noted for bending in the sagittal plane (16 %). In the crack region, high max principal strains (> 15 %) were predicted in a large portion of the soft tissue both during gait (Fig 1) and stair climbing. The fluid flow was predicted to be 1-6 µm/s at the external border of the soft tissue. After drilling, the magnitude decreased significantly: strains < 1 %, fluid flow less than 0.5µm/s in the soft tissue. When investigating the overall tibia stiffness, the drilling was found to have a minor effect. The largest differences were observed for bending in the sagittal plane, in which the drilled tibia were 9.9 % less stiff than the intact tibia, whereas the tibia with a stress fracture was 2.6 % less stiff than the intact tibia.

Discussion: The high strains and fluid flows predicted in the stress fracture before drilling, together with existing tissue differentiation theories may explain the low healing capacity of the stress fracture. The dramatic decrease of the predicted strains in the drilled tibia suggests that the healing capacity may increase. This is also supported by the favorable outcome of a similar surgical procedure [4]. Only a small decrease of the tibia stiffness is predicted after drilling. Therefore, drilling is not believed to affect the mechanical function of the tibia significantly.

Acknowledgements: Swedish National Centre for Research in Sports.

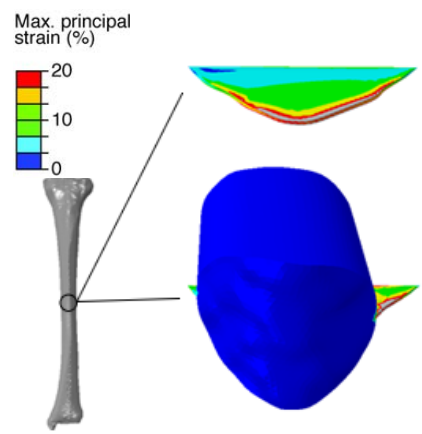

Figure 1: Tibia model (left) with max principal strain in the soft tissue in the crack before and after drilling (right) during gait.

[1] Linde et al., J Biomech, 1992.
[2] Cristofolini et al., J Biomech 2010.
[3] Taylor et al., J Orthop Res 2005.
[4] Miyamoto et al, Am J Sports Med, 2009.

Investigation of femoral fracture criteria in composite femur bone

Malin Ahlgren[1], Lorenzo Grassi[2], Hanna Isaksson[3]

[1] Div. of Solid Mechanics, Lund University, Sweden, email: malin.ahlgren.lth@gmail.com

Introduction. Patient-specific finite element (FE) models have been proposed as a tool to improve bone strength and the accuracy of fracture risk prediction in individuals. However, there is no consensus in the literature about the fracture mechanisms occurring in human femora, and only a few studies compared the different criteria and definition of bone fracture. Therefore the aim of this study was to investigate different fracture criteria on a FE model of composite femur bone and validate the fracture prediction results against experimental data.

Methods. A FE model of a composite femur bone (Sawbones, Inc.) was generated according to a previously proposed procedure[1] and four different fracture criteria were implemented into an ABAQUS (v6.9, Dassault Systemes) subroutine. The chosen criteria were based on maximum principal stress, maximum principal strain, Hoffman and Mohr-Coulomb theories. The ultimate strength was set to 106 MPa in tension and 156 MPa in compression (values provided by the manufacturer, www.sawbones.com), and the strain limits[2] were set to 0.78% in tension and 1.1% in compression. An element was considered as damaged when the fracture threshold value was reached in at least one integration point, and its corresponding Young's modulus was set to 5% of its original value. When all the integration points of the same element were above the fracture threshold, the element was considered as failed. The bone was assumed to be fractured when at least five connected elements were failed. Model validation was performed against experimental strain data collected using digital image correlation[3].

Results. The predicted fracture line (Fig 1a) was in qualitative agreement with the experimentally achieved fracture line (Fig 1b) for all the criteria tested. The fracture load predicted by the FE model was 4861 N when implementing the maximum principal stress criterion (-11% of the experimentally measured fracture load), and 5131 N when using Hoffman, Mohr-Coulomb, and maximum principal strain criteria (-5%). The accuracy of the FE models when predicting the strain distribution at fracture is reported in table 1.

Discussion. The FE predicted fracture load and location were investigated using four different fracture criteria. The fracture location was predicted consistently for all the four criteria, whereas the maximum principal stress criterion showed a higher error in fracture load prediction. The maximum principal strain criterion showed a high accuracy when predicting fracture load (-5%), while predicting strains at fracture with a good accuracy (both slope and $R^2 = 0.9$, RMSE = 10%). These results suggest that the fracture is a strain-driven phenomenon, in accordance with previous studies[4]. The main limitation of the present work is that only one composite bone has been investigated. However, five more composite femora were tested and their numerical analysis is pending. The proposed procedure will be directly extended to human femora FE models as future work.

Criteria	R^2	slope	RMSE
Maximum principal stress	0.90	0.86	10%
Maximum principal strain	0.90	0.89	10%
Hoffman	0.91	0.86	10%
Mohr-Coulomb	0.78	1.02	17%

Table 1: Linear correlation of the predicted strains against the experimentally measured values.

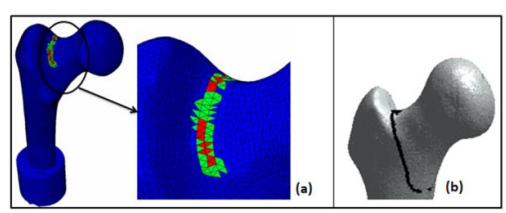

Figure 1: (a) Bone fracture with the maximum principal strain criterion. Failed element in red, damaged in green; (b) Experimental fracture line.

[1]Grassi et al., *J Mech Behav Biomed Mater* 2013
[2]Oden et al., *J Orthop Res*. 1999
[3]Väänänen et al., *Proc. of the 18th ESB Congress* 2012
[4]Schileo et al., *J Biomech* 2008

Industriella applikationer I

torsdag 13/6 09:35-10:35

Acoustic particle separation in gaseous flows using ultrasound

Ramin Imani Jajarmi[1], Markus Steibel[2], Klas Engvall[3], Etienne Robert[3]
[1]Ph.D student, ramin@mech.kth.se
[2]M.Sc, steibel@es.mw.tum.de
[3]Professor, kengvall@kth.se
[4]Researcher, etienne@mech.kth.se

The separation of particles by size (fractionation) or other physical properties such as density has numerous applications in different technologies. The particle separation techniques are used in material processing, polymer recycling, food processing, fuel industry, and even in biotechnology to separate cells, bacteria or yeast[1]. The commonly used separation techniques can vary based on the particles and the carrier flow characteristics. Screens, sieves and filters are the simple methods that fractionate particles, while they suffer from various difficulties, such as clogging, fouling and in case of fractioning the smaller sized particles, inducing a large pressure drop along the flow stream. Centrifuges, hydrocyclone, clarifiers and precoat filters are typically used when aim is to separate fine particles at low concentration[2], Nevertheless, in case of the shear sensitive particles even the centrifuges, hydrocyclone and clarifiers are incapacitated. However, other separation techniques, which utilize electric or magnetic fields can be envisaged for particle range of 0.01-10 um[3]. In these methods, particles have to be charged naturally or induced. And, this requires high power consumption and generation of undesired ozone[4]. The incapacity of the all mentioned techniques in dealing with small particles has lead to development of new techniques. The acoustic particle separation is one of these methods that has drawn a lot of attention from past two decades. Although, it was in 1874 that Knudt and Lehman reported the segregation of particles in ultrasonic standing waves, it was not until recently that the practical applications were identified. In this method, suspended particles experience a force from the resonant acoustic field, if there is a non-zero acoustic contrast between the particles and their suspending fluid. The magnitude of impart forces to particle from the acoustic field depends on the size of the particles as well as the density and compressibility of both solids and the suspending fluids. As the associated forces to the acoustic field can be many orders of magnitude greater than the weight of particles, rapid separations are possible [5]. Over the past two decades, most of the studies were mainly focused into the separation of suspended particles in aqueous medium, and not many studies have investigated the separation of suspended particles in gaseous medium. The former technique currently is a mature field and its applications are extensively used in biological and biomedical applications, where particles can be separated, manipulated and sorted according to size and density [6]. Although, there is no recognized fundamental limitation averting the development of separation of suspended particles in gaseous medium, but studies on this topic is still limited and applications rare. The generation and propagation of high amplitude and high frequency acoustic field in gases are some of the associated challenges to this work. In addition, the used technique in the current state-of-art particle separation in aqueous medium cannot easily be applied into gaseous applications as the different suspending medium come along with different phenomenon that have to be taken into account. In this study two different methods have been used to measure the particle separation efficiency. The laser light scattering method provides us the whole-field information, while the Scanning Mobility Particle Sizer (SMPS) system gives us information about the redistribution of particles inside the channel. On top of these, the sound intensity measurment using microphone can inform about the sound intensity magnitude along the channel height at different frequencies and transducer excitation veoltage. As we expected, particles will experience higher acoustic force at certain frequencies range and higher excitation voltage of the transducer.

[1]N. Aboobaker, J. N. Meegoda, D. Blackmore, *ASCE J. Environmental Engineering*, **129(5)**, 427-434, (2003)
[2]R. J. Wakeman, A. J. L. Bailey, *Trans IChemE J. Environmental Engineering*, **78, Part A**, 651-661, (2000)
[3]Dwayne A. Johnson, Donlad L. Feke, *J. Separations Technology*, **5**, 251-258, (1995)
[4]Dwayne A. Johnson, Donlad L. Feke, *J. Separations Technology*, **5**, 251-258, (1995)
[5]Zenon I. Mandralis, Donald L. Feke, *J. Chemical Engineerfng Science*, **43(23)**, 3897-3905, (1993)
[6]Adams, J. D., Soh, H. T. , *J. Applied physics letters*, **, 97(6)**, (2010)

Mechanical modeling and characterization of transformer pressboard

Denny Tjahjanto[1], Sören Östlund[2], Orlando Girlanda[3]
[1]KTH Royal Institute of Technology, Department of Solid Mechanics, email: dennyt@kth.se
[2] KTH Royal Institute of Technology, Department of Solid Mechanics, email:soren@kth.se
[3]ABB Corporate Research, email: orlando.girlanda@se.abb.com

Cellulose-based components constitute the bulk of the current insulation for transformers. Cellulose is a living material which combines excellent electrical properties and good mechanical performance. As polymeric materials, cellulose is very sensitive to moisture and temperature. These factors can influence the electrical and mechanical performance of a transformer throughout its lifetime. In order to ensure the quality of the product during transformer manufacturing, as well as during transformer life-time services, adequate models for predicting the physical properties of its constituents are in needed.

The present investigation tackles the mechanical description of pressboard. For this purpose, three-dimensional, continuum-based constitutive models are developed for in-plane and out-of-plane behavior of the pressboard material. The models are based on an anisotropic viscoelastic–viscoplastic constitutive law, which includes features that are particular for cellulose-based materials, e.g. peculiar double nature of fiber-network-based and porous material. In first place the material is orthotropic by nature, i.e. the in-plane mechanical properties markedly differ from the out-of-plane ones. Particular regard is taken when considering the effect of out-of-plane stresses which both cause viscous deformation and permanent compacting or densification. The validation of the model is performed by comparing the experimental data on pressboard and the results of finite element simulations.

A framework for modelling the sealing process

Henrik Askfelt[1], Matti Ristinmaa[1], N.S. Ottosen[1]
[1]Solid Mechanics, Lund University, Box 118 SE-22100 Lund, email: henrik.askfelt@solid.lth.se

The aim of this work is to get a better understanding of the material behaviour of paperboard and to construct a constitutive model for paperboard that is able to capture the response of paperboard during sealing. During the sealing process, which is a very rapid procedure, the paperboard is exposed to very large plastic deformations and large temperature variations. One of the obstacles to deal with when modelling paperboard is the complex micro structure. In the present work use is being made of mixture theory which by introducing volume fractions allows for each phase in a material to be handled separately. Starting from the fundamentals of mixture theory balance laws are set up for each constituent. Summing up the constituents constraints and balance laws are derived for each phase as well as for the entire mixture , cf. Hassanizadeh and Gray[1,2], Bennethum and Cushman[3,4] and Ristinmaa et al.[5]. First and second law of thermodynamics are used to derive the energy balance and dissipation inequality. All constitutive relations are derived in agreement with the dissipation inequality and fitted against available experimental data of paperboard. The time interval for the sealing process is of the magnitude 0.5s which motivates including dynamic affects into the modelling. Simulations are performed in a finite strain setting, using a multiplicative split to separate elastic and inelastic deformation gradients.

[1] Hassanizadeh, M., and Gray, W. G., *Advances in Water Resources*,**2**, 131-144, (1979).
[2] Hassanizadeh, M., and Gray, W. G., *Advances in Water Resources*,**2**, 191-203, (1979).
[3] Bennethum, L. S. and Cushman, J, H., *Int. J. Engrg. Sci*,**34**, 125-145, (1996).
[4] Bennethum, L. S. and Cushman, J, H., *Int. J. Engrg. Sci*, **34**, 147-169, (1996).
[5] Ristinmaa, M., Ottosen, N. S. and Johannesson, B., *Int. J. Engrg. Sci* , **49**, 1185-1203, (2011).

Numeriska metoder II

torsdag 13/6 09:35-10:35

Utilising XFEM to model failure of thinwalled structures

Martin Fagerström[1], Salar Mostofizadeh[2], Jim Brouzoulis[3]
[1]Dept. Applied Mechanics, Chalmers Univ. Tech., email: martin.fagerstrom@chalmers.se
[2]M2i - Materials innovation institute, Delft, The Netherlands
[3]Dept. Applied Mechanics, Chalmers Univ. Tech.

The eXtended Finite Element Method (XFEM), exploring the partition of unity concept in terms of an enriched FE-space in order to represent strong (*e.g.* discontinuity in the field itself) and/or weak (*e.g.* discontinuity in the spatial derivative) discontinuities, has been extensively used in the literature ever since it was presented by Belytschko and co-workers in 1999[1,2]. Interesting applications are mesh independent representation of cracks and crack propagation, holes, inclusions, evolving grain and phase boundaries etc.

The current contribution will aim at giving an overview of XFEM and the developments thereof with the application to modelling of crack propagation and failure, focusing on the work performed at the Department of Applied Mechanics at Chalmers. Starting from the basics of XFEM, specifics related to robustness and efficiency, extensions of the XFEM concept and applications to industrial relevant loading conditions and materials will be discussed.

Currently, the developments are made within two parallel projects on XFEM representation of crack propagation, from which numerical results will be presented. The first project focuses on ductile failure of thin and large metal structures addressing issues related both to the modelling of the ductile failure process as to robustness and computational efficiency of the structural representation. As an example, the result from a validation simulation of the proposed approach can be seen in Figure 1a, where we successfully have managed to reproduce the progressive failure response observed in the experiment conducted by Muscat-Fenech and Atkins[3].

The second project is devoted to crashworthiness of structural composites with the aim of developing a shell element formulation that can simultaneously handle multiple delaminations (within one shell element) and through-thickness cracking (splitting), both being important mechanisms in the modelling of composite crushing. As a first step, a shell element formulation has been established that is able to represent multiple delaminations, cf. Figure 1b. The basic features of this formulation and some preliminary results will be presented.

Acknowledgements

Parts of this research were carried out under project number M41.2.10378 in the framework of the Research Program of the Materials innovation institute M2i (www.m2i.nl). This work also receives funding from the European Community's Seventh Framework Programme (FP7/2007-2013) under grant agreement no. 314182 (the MATISSE project). This publication solely reflects the authors' views. The European Community and M2i are not liable for any use that may be made of the information contained herein.

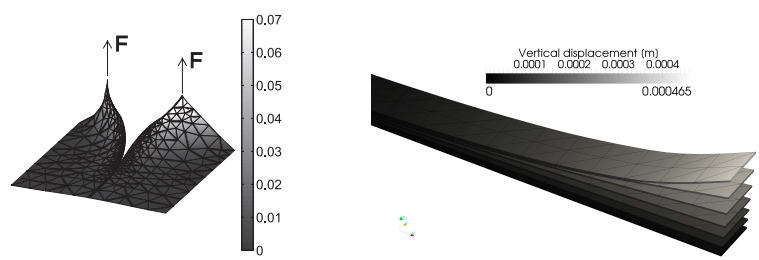

a) b)

Figure 1: Recent XFEM results: a) Ductile crack propagation in a clamped steel plate subjected to out-of-plane forces; b) multiple delamination composite shell element for crash analysis.

[1]T. Belytschko and T. Black, *Int. J. Numer. Meth. Eng.*, **45**, 601, (1999)
[2]N. Moës, J. Dolbow and T. Belytschko, *Int. J. Numer. Meth. Eng.*, **46**, 131, (1999)
[3]C.M. Muscat-Fenechand A.G. Atkins, *Int. J Fracture*, **84**, 297, (1997).

Material distribution optimization for acoustics: developments and challenges

Martin Berggren[1], Esubalewe Yedeg, Eddie Wadbro

Department of Computing Science, [1]email: martin.berggren@cs.umu.se

The material distribution approach to topology optimization is a well-established technique for design optimization of static load-bearing elastic structures.[1] In this approach, an optimization algorithm determines whether each finite element in the design region should represent solid material or void. During the last ten years, it has been demonstrated that the method also carries over to the optimization of sound-hard material interacting with acoustic waves. Many of the standard techniques developed for elastic problems, such as the combination of design filters and penalty, can directly be used also for acoustics problems. However, there are particularities with acoustics problems that call for the development of new approaches.

The minimization of *compliance* utilizes a structure of the elasticity equations that is not natural for acoustics problems. It is more natural for many wave propagation problems to optimize the *wave energy flux* over surfaces, in order to control the transmission and distribution of acoustic energy. Another particularity for acoustics problems concerns the constitution of effective shapes. The left figure below depicts a cross section of a cylindrically-symmetric reactive muffler. The internal layout of the expansion chamber has been optimized for minimal transmission of acoustic power, and the final design has at least 10 dB transmission loss in the frequency range 227–1425 Hz. We note that the optimized layout comprises two (sub)expansion chambers and one Helmholtz resonator. (Note the very narrow opening to the middle chamber!) An important advantage with using material distribution optimization for this kind of design problems is that such a layout structure does not have to be specified in advance, but is the result of the optimization. In order for the optimization procedure to allow the creation of such structures—particularly the narrow openings to the Helmholtz resonators—we needed to apply special techniques such as an *anisotropic* design filter, elongated in the radial direction.

Propagating waves interact strongly with interfaces, boundary surfaces, corners, slits, and holes through diffraction and reflection in a way that does not really have a counterpart for non-wave problems such as static elasticity. An example[2] that reveals the kind of shapes that tend to appear in acoustic material distribution optimization is the acoustic horn–lens combination depicted to the right in the figure. Material-distribution optimization is used to place sound-hard material in a region in front of an acoustic horn in order to create a constant 100° beam width over the frequency band 250–1000 Hz. The structures act as an acoustic lens that diffracts higher frequencies more than lower, counteracting the beamwidth narrowing typical for acoustic horns. In this case, the appearance of thin, sub-wavelength structures necessitated the use of a very fine mesh, and a design filter could not be used without preventing the narrow structures to appear.

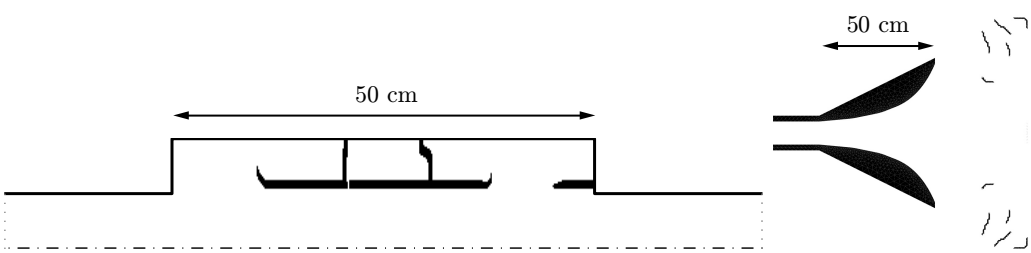

The optimization of a muffler for minimal transmission produces expansion chambers and Helmholtz resonators (left). The optimization of an acoustic horn–lens combination for constant beam width produces thin structures that diffracts the waves (right).[2]

[1]M. P. Bendsøe, O. Sigmund. *Topology Optimization. Theory, Methods, and Applications. Springer, 2003.*

[2]Taken from Wadbro et al. *J. Comput. Appl. Math.*, **234**:1781–1787, 2010.

On a method for solving non-linear optimization problems with matrix inequality constraints

Carl-Johan Thore[1]
[1]Division of Mechanics, Linköping University, email: carl-johan.thore@liu.se

A matrix $\boldsymbol{A} \in \mathbb{R}^{n\times n}$ is said to be positive semi-definite if $\boldsymbol{x}^T\boldsymbol{A}\boldsymbol{x} \geq 0$ for all $\boldsymbol{x} \in \mathbb{R}^n$; we write this using the notation "$\boldsymbol{A} \succeq \boldsymbol{0}$". A non-linear optimization problem (NLP) with matrix inequality constraints is a problem of the form

$$\begin{aligned} &\underset{\boldsymbol{x}\in\mathbb{R}^n}{\text{minimize}} \quad f(\boldsymbol{x}) \\ &\text{subject to} \quad \begin{cases} \boldsymbol{l} \leq \boldsymbol{g}(\boldsymbol{x}) \leq \boldsymbol{u} \\ \boldsymbol{A}(\boldsymbol{x}) \succeq \boldsymbol{0}, \end{cases} \end{aligned} \tag{1}$$

where $\boldsymbol{l}$ and $\boldsymbol{u}$ are fixed vectors, and $\boldsymbol{A}$ is a matrix-valued function from $\mathbb{R}^n$ to the space of symmetric $m \times m$ matrices with real entries. The functions f, $\boldsymbol{g}$ and $\boldsymbol{A}$ are at least twice continuously differentiable and may be both both non-linear and non-convex.

Certain special cases of problem (1) where $\boldsymbol{A}$ is a linear or bilinear function (and f and $\boldsymbol{g}$ also have some special structure) have been studied extensively[1,2]. These efforts have resulted in many efficient solvers[3], which are nowadays frequently employed in control theoretic applications, and to some extent in structural optimization. For the general case, however, when f, $\boldsymbol{g}$ and $\boldsymbol{A}$ may be both non-linear and non-convex, the state of matters is less satisfactory — in fact, to the author's knowledge, the only publicly available solver for such problems is `PENNON`[4].

This presentation concerns a numerical method for solving problems of the type (1). The method is based on a reformulation of this problem into a standard NLP which can be tackled by currently available NLP-solvers. The talk will provide theoretical background and include results from benchmarks using the author's code `fminsdp`. Specifically, numerical treatment of a number of interesting problems from truss topology optimization will be considered. An example of such a problem is the minimization of the weight of a truss subject to compliance and global stability constraints[5]:

$$\begin{aligned} &\underset{\boldsymbol{x}\in\mathbb{R}^m}{\text{minimize}} \quad \sum_{i=1}^{m} x_i \\ &\text{subject to} \quad \begin{cases} \boldsymbol{f}^T\boldsymbol{u}(\boldsymbol{x}) \leq c \\ \boldsymbol{x} \geq \boldsymbol{0} \\ \boldsymbol{K}(\boldsymbol{x}) + \boldsymbol{G}(\boldsymbol{u}(\boldsymbol{x}), \boldsymbol{x}) \succeq \boldsymbol{0} \end{cases} \end{aligned} \tag{2}$$

Here, $\boldsymbol{x}$ contains the volumes of the m bars in the truss, $\boldsymbol{f}$ is the applied load, $\boldsymbol{u}(\boldsymbol{x})$ is a displacement vector satisfying $\boldsymbol{K}(\boldsymbol{x})\boldsymbol{u} = \boldsymbol{f}$, $\boldsymbol{K}(\boldsymbol{x})$ being the stiffness matrix, c is an upper bound on the compliance, and $\boldsymbol{G}(\boldsymbol{u}(\boldsymbol{x}), \boldsymbol{x})$ is the geometric stiffness matrix. The most interesting thing here is the global stability constraint, which is expressed as a non-linear, non-convex matrix inequality. It can be shown[5] that a solution to problem (2) corresponds to a truss that will not exhibit global (linear) buckling for loads of the form $\tau\boldsymbol{f}$, with $\tau \in [0, 1)$.

[1]Boyd et. al, *Linear Matrix Inequalities in System and Control Theory*, 1994
[2]Antwerp & Braatz, A tutorial on linear and bilinear matrix inequalities, Journal of Process Control, 2000
[3]The code YALMIP by J. Löfgren (http://users.isy.liu.se/johanl/yalmip/) provides a convenient interface to many of these.
[4]Kočvara & Stingl, PENNON – a code for convex nonlinear and semidefinite programming, Optimization Methods and Software, 2003
[5]Kočvara, On the modeling and solving of the truss design problem with global stability constraints, Structural and Multidisciplinary Optimization, 2002

Strömningsmekanik I

torsdag 13/6 09:35-10:35

Flow Visualization of Oil Flow inside a Gearbox Model

Erwin Adi Hartono, Valery Chernoray
Fluid Dynamics, Applied Mechanics, Chalmers University of Technology, 412 96 Gothenburg
email: erwin-adi.hartono@chalmers.se

Gearbox is an essential element in power transmission. Efficient gearbox means efficient power transmission. Hence lower energy consumption. Losses in the gearbox can be sorted into two; load-dependent and load-independent losses. Load-dependent are related to friction, and load-independent losses are mainly related to lubricant. Load-independent losses are the focus of this paper.

An experimental rig (Chalmers gearbox rig) based on the FZG gear test rig was built. The test gears have a slight gap in between the mate teeth and are driven by slave belt and in order to eliminate contact (friction). The idea is to get pure load-independent losses.

Flow visualization study was chosen as a first method to study oil flow inside a gearbox. A set of external flash and a camera were used to capture instantaneous splashes in different pitch line velocity and different oil level. Hydrotreated process oil was used due to its transparency. The temperature of the oil was maintained at 40°C to match the viscosity of Castrol Syntrans 75W-85 at 90°C. Understanding the splash behavior are essential in order to understand the flow phenomena and to be able to study the flow further with more advance method, such as computational fluid dynamics (CFD) or particle image velocimetry (PIV).

Figure 1(a) shows the Chalmers gearbox rig and figure 1(b) shows the experimental setup. The camera is located in front of the test section and a flash is located on top of the test section. Three reflectors were used to make the lighting uniform. Two reflectors (see white box in figure 2b) located at the sides and one reflector under the test section.

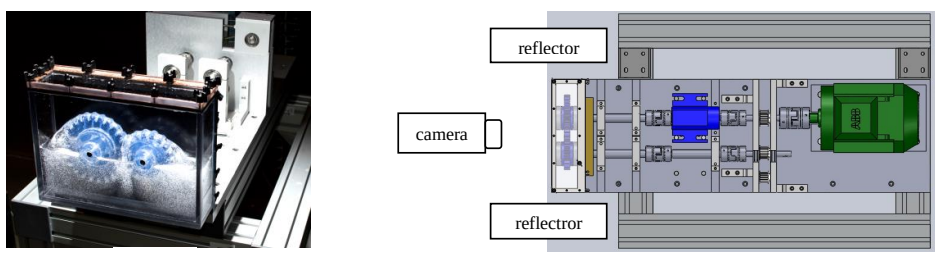

(a) (b)

Figure 1: The experimental rig (a) The Chalmers gearbox rig (b) The experimental setup

The flow phenomena of oil flow inside a gearbox are quite complex, as seen in figure 2. There are free-surface flow, splash, drops, bubble formation, etc. In higher level of oil the bubbles form faster compare to the lower level. The advantages or disadvantages of presence of bubbles are not yet known, and need to be studied furthermore. The amount of oil that was dragged by the gear is increasing in the higher level oil, hence higher losses are generated.

(a) (b) (c)

Figure 2: Instantaneous splash with 0.06 m/s pitch line velocity and oil level at ;(a) Centerline (b) 1 tooth height small gear (c) 1 tooth height big gear

[1] Michaelis, Höhn and Hinterstoißer, *Industrial Lubrication and Tribology*, **63/1**, 46-55, (2011)
[2] Stavytskyy, Nosko, Fil, Karpov, and Velychko, *OL PAN*, **10B**, 205-213, (2009)
[3] Changenet and Velex, *J. Mech. Design.*, **129**, 128-133, (2007)

Inlet Geometry Effects on the Flow in an Radial Turbine

Johan Fjällman[1], Mihai Mihaescu[2], Laszlo Fuchs[3]
[1]CCGEx, Kungliga Tekniska Högskolan, email: johanf@mech.kth.se
[2]CCGEx, Kungliga Tekniska Högskolan,
[3]CCGEx, Kungliga Tekniska Högskolan,

In this study the unsteady flow through an exhaust manifold and the radial turbine of an automotive turbocharger is analyzed. With the new European emission legislation coming into effect in 2014 the need for more efficient engines is increasing. The current trends in the industry is to use downsizing together with a well matched turbocharger system to achieve higher efficiencies and lower emissions. Since more and more of the development work is being performed by simulations there is an increasing need for more accurate methods. Currently in the automotive industry the simulations are being performed by the RANS/URANS methods. This has the advantage of being robust and fast but there are issues with the methods that makes them unsuitable for these kinds of flows. The flow in the exhaust manifold and turbine produces unsteadiness, caused by the geometry, that overlaps the natural turbulent spectra. This cannot be handled by the RANS methods and as such they cannot predict the specific flow. This makes the Large Eddy Simulation the method of choice for these kinds of flows.

The simulations in this study have been performed using both the URANS and LES methods on geometries with and without the exhaust manifold. Comparisons are made between both simulation methods and with gas-stand experiments. The comparisons are made in order to assess the differences between the methods and how the inflow geometry affects the flow in the volute and experimentally measured quantities. The instantaneous velocity field through the volute and wheel region can be seen in figure 1, case with exhaust manifold.

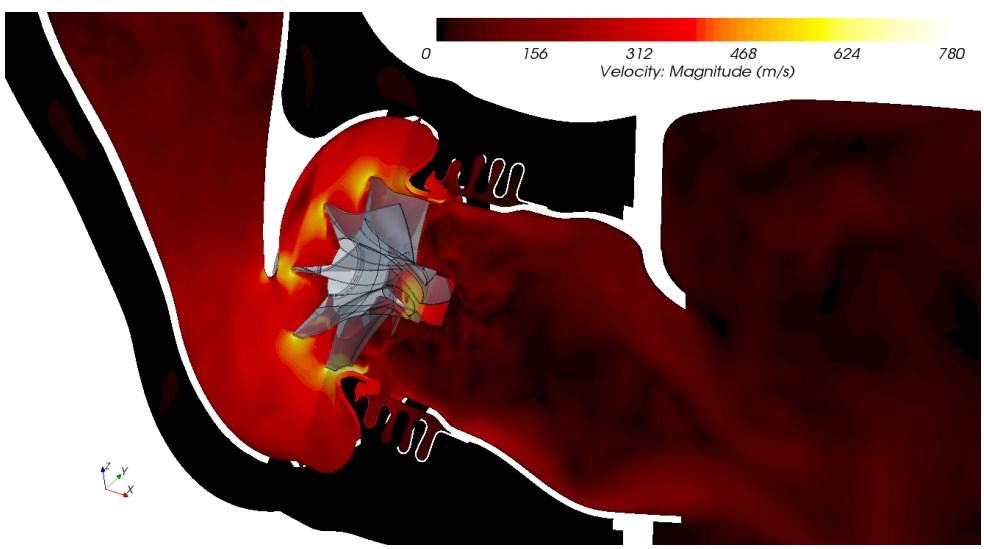

Figure 1: Instantaneous velocity field through the volute, wheel and the exit region.

Passive flow control for skin-friction drag reduction: AFRODITE

Shahab Shahinfar, Jens H. M. Fransson, Sohrab S. Sattarsadeh, Alessandro Talamelli
Linné Flow Centre, KTH Mechanics, email: jensf@mech.kth.se

Classical vortex generators, known for their efficiency in delaying or even inhibiting boundary layer separation, are here shown to be coveted devices for transition to turbulence delay. The present devices are miniature with respect to classical vortex generators but are tremendously powerful in modulating the laminar boundary layer in the direction orthogonal to the base flow and parallel to the surface. The modulation generates an additional term in the perturbation energy equation, which counteracts the wall-normal production term, and hence stabilizes the flow. Our experimental results show that these devices are really effective in delaying transition but we also reveal their Achilles' heel[1].

The physical mechanism of the stabilizing effect is known[2] and has previously been shown to be strong enough to delay transition to turbulence in wind tunnel experiments[3], where the base flow was modulated by means of cylindrical roughness elements. Later this result has been confirmed numerically in[4]. The experimental design (as well as the numerical simulation) was, however, fairly laboured, since the artificial disturbance was introduced downstream of the cylindrical roughness array avoiding any potential non-linear interaction of the incoming disturbance with the roughness array. In a recent study the flow configuration and experimental setup has challenged the passive flow control method by generating controlled disturbances upstream of the boundary layer modulators and showed promising results in being capable of delaying transition to turbulence[1].

In this experimental investigation we show that miniature vortex generators (MVGs) really are suitable devices in accomplishing transition delay and plausible to work in real flow applications. MVGs are clearly superior to circular roughness elements, since the flow is allowed to pass right through them, possibly reducing the absolute instability region behind the devices and allowing for twice as high amplitude streaks to be generated, but still with some margin to the threshold amplitude beyond which the streaky base flow becomes unstable. This makes the streaky base flow much more robust for external perturbations, a prerequisite for real flow applications. Furthermore, in the present setup the TS waves are being generated upstream of the MVG array, leaving the full and nasty receptivity process of the incoming wave by the MVG array, which really challenges the present passive flow control method. Despite this, transition delay is convincingly accomplished (see figure 1).

This work is financially supported by the European Research Council and is performed within the AFRODITE research programme, which stands for Advanced Fluid Research On Drag reduction In Turbulence Experiments.

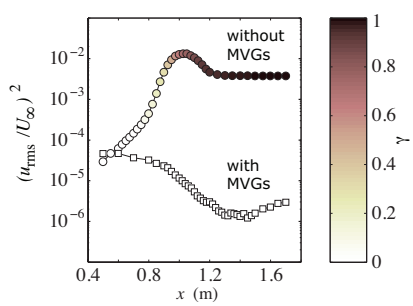

Figure 1: Boundary layer energy evolution in the downstream direction with and without MVGs plotted with (□)- and (○)-symbols, respectively, at $U_\infty = 7.7$ m s^{-1}. The streak amplitude with the MVGs amounts to 21% of U_∞. The color bar applied on the symbols corresponds to the intermittency (γ) of the velocity signal.

[1] Shahinfar, S., Sattarzadeh, S.S., Fransson, J.H.M. & Talamelli, A. (2012). *Phys. Rev. Lett.* **109**, 074501.
[2] Cossu, C. & Brandt, L. (2004). *Eur. J. Mech./B Fluids* **23**, 815–833.
[3] Fransson, J.H.M., Talamelli, A., Brandt, L. & Cossu, C. (2006). *Phys. Rev. Lett.* **96**, 064501.
[4] Schlatter, P., Deusebio, E., de Lange, R. & Brandt, L. (2010). *Int. J. Flow Contr.* **2**, 259–288.

Biomekaniska transportfenomen

torsdag 13/6 09:35-10:35

Blood Flow in Large Bifurcating Arteries

Stevin van Wyk[1], Lisa Prahl Wittberg[1], Laszlo Fuchs[1]
[1]Linné FLOW Centre, Royal Institute of Technology (KTH), Stockholm, Sweden
email: stevin@mech.kth.se

Blood flow, driven by the pulsations of the heart, is characterized by complex fluid mechanical and biochemical process interactions. The induced flow is necessary to facilitate the transport of oxygen bearing Red Blood Cells (RBC) (∼45% bulk volume fraction) and other organic matter to the body. This mixture results in the highly non-Newtonian nature of the blood though still often assumed to behave as a homogeneous fluid in the larger arteries. The distribution of the RBCs varies in regions of curvature or bifurcation due to secondary flow structures and leads to viscous non-inhomogeneities. The variations in viscosity have a large impact on the flow and fluid mechanical factors such as the Wall Shear Stress (WSS) and WSS gradients believed to play an important role in an arterial disease such as atherosclerosis.

In our investigations of the flow in idealized as well as patient specific geometries, the blood is considered to be a non-Newtonian, non-homogeneous fluid mixture. A two-phase finite volume solver is employed to solve a mixture model formulation, where three non-Newtonian empirical models valid for different RBC loading and shear rate are implemented. Pulsatile inflow conditions are chosen to represent physiological flow conditions in the aorta and its larger branches.

Our studies provide further indications that the effects of fluid mechanical aspects can be correlated with the diseased regions of the larger arteries. Figure 1 shows an example of the large variations in RBC distribution that can be observed due to the arterial branching and curvature of the aorta [1]. This results in local RBC dilution due to the secondary flow structures, consequently determining the bulk RBC loading on each of the branches of the arterial network. The local variation in RBC concentration also determines the magnitudes of the WSS and WSS gradients, important for identifying regions susceptible to atherosclerosis.

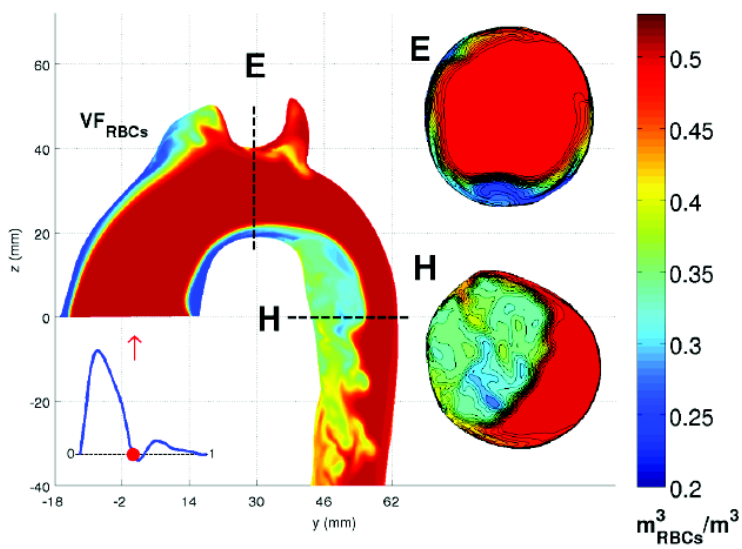

Figure 1: RBC distribution in the aorta during the deceleration phase of the cardiac cycle, for a given inlet distribution and bulk concentration of ∼45%.

[1]Prahl Wittberg, L.; van Wyk, S.; Fuchs, L.; Gutmark, E.; Backeljauw, P.; Gutmark−Little, I. **The Impact of Aortic Arch Geometry on Flow Characteristics.** *51st AIAA Aerospace Sciences Meeting including the New Horizons Forum and Aerospace Exposition, Dallas, United States of America, 2013*

Mechanical behaviour of transiently cross-linked actin networks – a chemo-mechanical constitutive model

Björn Fallqvist[1], Martin Kroon[2]
[1]Kungliga Tekniska Högskolan, bfa@kth.se
[21]Kungliga Tekniska Högskolan, mkroon@kth.se

Ett mycket viktigt protein i den biologiska cellen är aktin, som i form av nätverk i cytoskelettet ger den mycket av dess styvhet. Flera typer av aktin finns i cellen, av vilka den mest grundläggande är G-aktin (Globular), som kan polymeriseras till s.k. F-actin filament. Dessa filament kan sedan anta ett flertal olika former; s.k. ”stress fibers” som förankrar cellen till den yttre matrisen men även olika typer av filamentnätverk som skapas genom att proteiner såsom filamin och α-actinin skapar bindningar mellan enskilda filament. Om nätverket utsätts för mekaniska laster kan dessa bindningar brytas, och nätverket förändras på en tidsskala som beror på typen av bindning. Detta orsakar ett visokelastiskt beteende, med spänningsrelaxation vid konstant töjning.

Genom att använda en existerande kemisk modell för α-actinin som binds och släpper, har vi utvecklat en konstitutiv modell för det tidsberoende beteendet hos isotropa aktinnätverk. Deformationen delas upp i en viskös och en elastisk del, och en töjningsenergifuntion för nätverket formuleras. Töjningsenergifunktionen beror på den elastiska deformationen, som i sin tur p.g.a. viskösa effekter också är tidsberoende (enligt en termodynamiskt konsistent evolutionslag).

Den existerande kemiska modellen modifierades med en exponentiell faktor beroende på töjningsenergin i bindningarna. Under deformation släpper därmed bindningarna med en hastighet som beror exponentiellt på töjningsenergin.

För att verifiera den konstitutiva modellen användes resultat från viskoelastiska relaxationstest av aktinnätverk. Det visade sig att för vissa modellparametrar kan den initiella hastiga spänningsrelaxationen och även den viskösa responsen på längre tidsskalor predikteras av den kemisk-mekaniska modellen.

Transport-based theory of Bone Remodeling involving Stress Driven Diffusion

Ingrid Svensson[1], Gustav Lindberg[1], Per Ståhle[1] and Leslie Banks-Sills[1,2]

[1]Division of Solid Mechanics, Lund University, Sweden
[2]Dreszer Fracture Mechanics Laboratory, Tel Aviv University, Israel

Mechanical stresses occur in skeletal bones due to physiological activity. There is much evidence in the literature demonstrating that mechanical oscillating loading stimulates bone remodeling and that the remodeling process is most active close to the periosteum, i.e. the outer surface of the long bones. However, neither the transport process from the macroscopic level down to the cell-level is not yet fully understood nor the adaptation processes of cells to variations in the loading environment. The hypothesis is that substances that promote bone growth are transported by stress driven diffusion from the medullar cavity to the outer surface of long skeletal bone and there promote bone growth.

In order to investigate the role of transport processes on remodeling in skeletal bones a computational model is established and equations for the flux of nutrients, e.g. nitric oxide synthase (NOS) or messenger molecules, such as prostaglandin E_2 (PGE_2), are written for the cross-section of a long bone. Both one and two-dimensional models will be considered. Using the one-dimensional model, an analytic solution is obtained for the concentration at the periosteum of the matter of interest. The obtained partial differential equation is linearized and solved analytically. The effect of loading frequency, number of cycles and strain level is examined for several experiments that were found in the literature. It is seen that the concentration is greatest on the tensile side of the bone; this location coincides with the greatest amount of bone modeling from experimental findings. Next, a two-dimensional model of the cross-section of a long bone is considered. Calculations of stress driven diffusion are performed under steady state conditions. A sinusoidal time dependence is assumed for the concentration of nutrients. In this way, it was possible to reformulate the problem to determine an analogy with the bending of a plate in the shape of the bone cross-section on an elastic foundation. This problem was solved by means of the finite element method. The concentration of nutrients in the cambium layer of the periosteum was obtained for different choices of load frequencies. The results are compared to experimental findings suggesting increased bone growth occurs in the neighborhood of relatively high nutrient concentration.

This understanding has implications for fracture healing, medical treatment of disorders such as osteoporosis as well as bone adaptation leading to loosening of orthopedic or dental implants.

Konstitutiv modellering II

torsdag 13/6 10:55-11:55

Model-based weldability charts for constructional steels

John C. Ion[1], Michael F. Ashby[2]
[1]Materials Science, Malmö högskola, 205 06 Malmö, Sweden, email: john.ion@mah.se
[2]Dept of Engineering, Cambridge University, Cambridge CB2 1PZ, UK, email: mfa2@cam.ac.uk

Despite extensive research, a numerical measure of weldability remains elusive. Here we define the weldability of constructional steels in terms of two quantities that characterise: i) the material being welded (a *material* index) and ii) the welding process (a *process* index). The material index describes both the hardenability of the steel, in terms of solid-state phase transformations that occur in the weld heat affected zone (HAZ), and the hardness of transformation products. The material index is based on steel composition through the use of a simple carbon equivalent formula. The process index characterises the property of the welding process most relevant to weldability - its energy input - which defines the thermal cycles experienced in the weld.

The indices are used in analytical models of thermal cycles induced in the HAZ adjacent to the fusion line (where hardness reaches a maximum) and in empirical descriptions of the subsequent phase transformations. The analytical models used are based on conventional theories of heat flow and phase transformations. They are constructed such that they can be calibrated using both experimental data and theoretical data generated using more detailed numerical modelling methods - the analytical models capture the essential features of more complex methods.

Model-based relationships between the indices are generated, and used to construct features on *weldability charts*. Thus a model-based contour representing the volume fraction of martensite formed in a weld HAZ can be constructed as a function of weld energy input and carbon equivalent (the *x* and *y* axes of the chart, respectively), Fig. 1a). Similarly, a contour representing a given value of maximum weld HAZ hardness can be constructed, Fig. 1b).

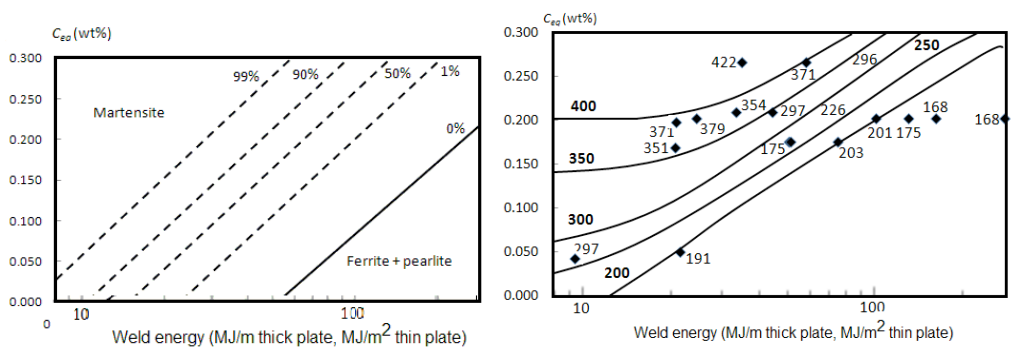

a) b)

Figure 1: Weldability charts for process parameter selection (a) based on an acceptable volume fraction of martensite in the weld HAZ (broken lines), (b) based on an acceptable weld HAZ hardness (contours represent model-based hardness predictions and points represent experimental measurements).

The charts enable steel composition and welding parameters to be selected for a given acceptance criterion: combinations of carbon equivalent and weld energy that lie to the right of the criterion (a given martensite volume fraction or hardness in a) and b), respectively) can be selected for experimental verification, thus expediting the development of a welding procedure.

Mikromekanisk analys av pulverpressning

Erik Olsson[1], Per-Lennart Larsson[2]
[1]Instutionen för Hållfasthetslära, KTH, Stockholm, email: erolsson@kth.se
[2]Instutionen för Hållfasthetslära, KTH, Stockholm, email: pelle@hallf.kth.se

Pressning av spraytorkade pulvergranuler med efterföljande sintring är ett vanligt sätt att tillverka hårdmetallkomponenter såsom borrar och skärstål. Under pressningen och under hantering av den pressade kroppen före sintring kan defekter uppstå som kan finnas kvar i den färdiga sintrade komponenten. För att förutsäga dessa defekter och få en bättre förståelse för det mekaniska beteendet har pulverpressning analyserats numeriskt med hjälp av diskreta elementmetoden (DEM).

I DEM modelleras rörelsen hos de enskilda partiklarna och de lokala kontaktkrafterna mellan partiklarna bestämmer det makroskopiska beteendet. För att få tillförlitliga resultat är det därför av vikt att ha en så noggrann beskrivning som möjligt av kontakten mellan två pulverpartiklar. I det fallet att partiklarna har ett känt materialbeteende finns (semi)-analytiska lösningar för två sfärer i kontakt[1][2] men för partiklar med okänt materialbeteende, till exempel spraytorkade granuler, behövs en experimentell karakterisering.

Här presenteras två typer av mikromekaniska experiment för att bestämma beteendet hos spraytorkade granuler; kompressionsprov på enskilda granuler och nanoindentering av granulerna. Dessa experiment används för att bestämma materialbeteendet hos pulvergranulerna som sedan används i en FEM-simulering av två granuler i kontakt. Kontaktegenskaperna exporteras sedan till ett DEM-program där enaxlig kompaktering simuleras. Simuleringarna jämförs med egna pressningsexperiment och jämförelsen visar en mycket god överensstämmelse mellan simuleringar och experiment.

Vidare så simuleras avlastning av den pressade kroppen för att kunna beskriva återfjädringen vilket också jämförs med experiment. Resultaten visar att bindning mellan partiklarna spelar en viktig roll för att noggrant kunna förutsäga den avlastade kroppens dimensioner.

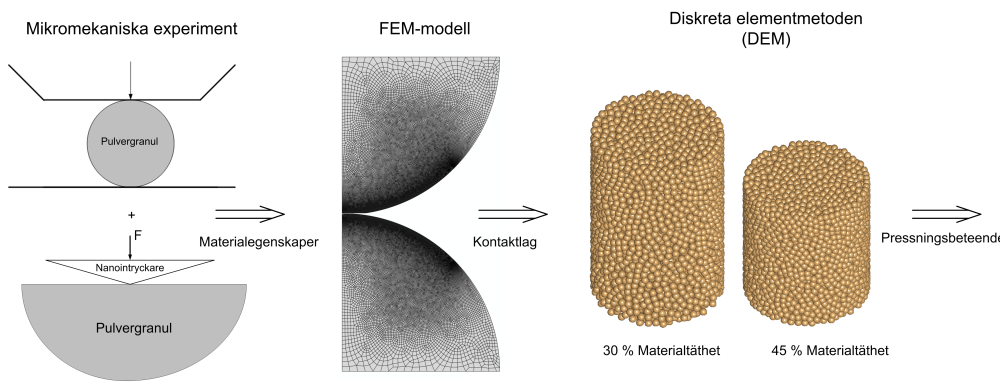

Figure 1: Skiss av analysmetoden från mikromekaniska experiment via kontaktmodell i FEM till makroskopiska egenskaper från DEM-simuleringar.

[1]Storåkers et. al, *Int. J. Solid. Struct.*, **34**, 24, (1997)
[2]Olsson and Larsson, *J. Mech. Phys. Solids*, **61**, 5, (2013)

Constitutive modelling of CGI on a microstructure level

Peter Hellström[1], Kim Olander[1], Torsten Sjögren[2], Martin Fagerström[3], Lennart Josefson[3]

[1]Semcon Caran AB, email: peter.hellstrom@semcon.com
[1]Semcon Caran AB, email: kim.olander@semcon.com
[2]SP Technical Research Institute of Sweden, email: torsten.sjogren@sp.se
[3]Chalmers university of Technology, email:martin.fagerstrom@chalmers.se
[3]Chalmers university of Technology, email: lennart.josefson@chalmers.se

This paper deals with finding parameters for the Johnson-Cook (JC) constitutive model[1] and fracture model[2] in order to obtain a realistic representation of the deformation and fracture response of Compacted Graphite Iron (CGI). The parameters are needed when simulating e.g. machining processes of CGI in order to optimize and receive a better knowledge of the process and the influence of the micro structure. Two cases are considered: In the first case CGI is treated as a homogenous material, not taking into account the two entering constituents, pearlite and graphite. In the second case, the actual heterogeneity of CGI is considered, taking the morphology of the two constituents into account by explicitly including them in the finite element (FE) analyses.

To find the material parameters, tensile tests have been conducted on flat test specimens with four different notch geometries. The strains are recorded using a Digital Image Correlation (DIC) system. In addition to this, FE-analyses are conducted on the same geometries, from which the stress triaxiality in the fracture zone is computed and used as input to the fracture parameter calibration. Data from the tensile tests and the FE-analyses are imported into Matlab where optimization scripts utilizing the non-linear least square method are used to find the parameters in the JC-material models.

In the constitutive model only the isotropic hardening part is studied, and in the fracture model only the tri-axial part is considered. Thus, for both models, the temperature and strain rate parts could not be covered in the experiments.

Results for both models agree well (experiments and FE-analysis) though for the heterogenous model it is difficult to find representative areas in highly strained parts, see figure below.

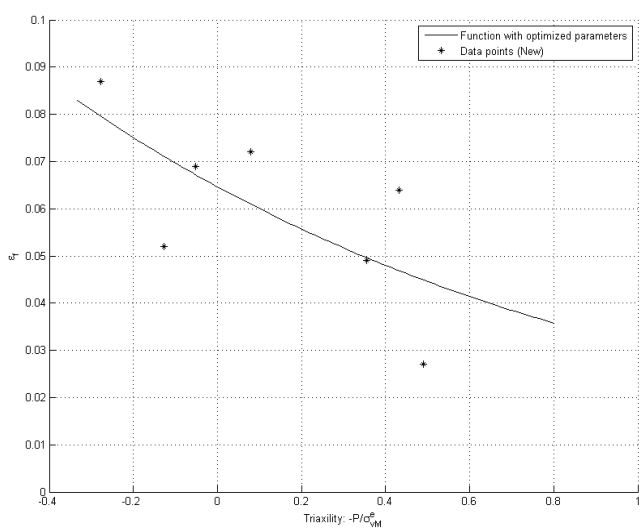

Figure 1: Fracture strain ε_f for different values of tri-axiality –P, where $P = \sigma_{kk}/3$, as non-dimensionalised by the von Mises effective stress

[1] Johnson and Cook, *Proc. 7th Int. Sym. Ballistics*, pp 541–547, (1983).
[2] Johnson and Cook, *Eng. Fract. Mech.*, **21**, 31, (1985).

Kollapsmekanismer

torsdag 13/6 10:55-11:55

Stress analysis around a through crack shaped void in a highly constrained copper strip using molecular dynamics

Dan Johansson[1], Per Hansson[2], Solveig Melin[3]
[1]PhD Student, email: dan.johansson@mek.lth.se
[2]Associate Professor, email: per.hansson@mek.lth.se
[3]Professor, email: solveig.melin@mek.lth.se

In experiments it has been shown that materials behave differently on the nanoscale as compared to the macroscale. For example Cuenot et al. [1] showed through atomic force microscopy that the elastic modulii for small metallic nanowires and polymer nanotubes differ significantly from bulk values. This is due to factors such as the increasing number of surface atoms in relation to number of bulk atoms with decreasing size, and to the relatively lower dislocation density as compared to macroscopic structures. Also geometrical factors, such as crystal orientation, strongly influence the material properties; cf. e.g. [2].

Considering thin metallic layers, one difficulty lies in finding proper dimensioning rules that are scientifically based and commonly accepted among designers. One challenge lies in the prediction of sudden failure of the layer induced by mechanical loading. One critical failure mode is cracking. Even if the crack is small, of the length of a few nanometers only, it might jeopardize the functionality of the coating and, eventually, extend to cause complete collapse of the component. Such unexpected events are, of course, necessary to understand and be able to predict

In this paper a small rectangular strip of fcc Cu, containing a through crack on the nanoscale and subjected to loading under displacement control, is simulated using molecular dynamics (MD). The geometry is highly constrained and chosen to mimic that of a thin strip between two stiff layers. The Lennard-Jones pair potential is used for the inter-atomic forces. The centrally placed crack shaped void is created by removing a few atoms inside the specimen. The crack is loaded perpendicular to the crack plane and the tensile stress is studied as it varies over the depth 2*d* of the strip. Comparisons with finite element (FE) analyses are made and the results show better agreement between FE and MD for strips of large dimensions and strips under high strain.

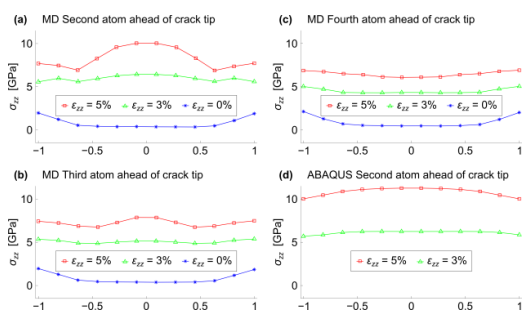

Figure 1: Tensile stress variation over the strip depth for a strip with a depth of 6unit cells.

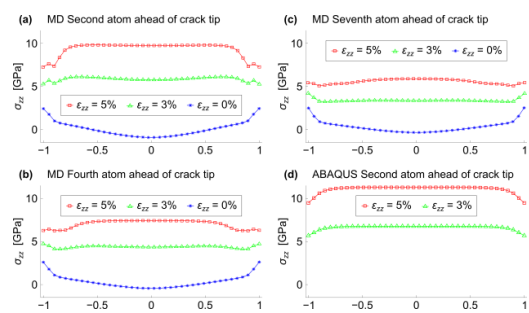

Figure 2: Tensile stress variation over the strip depth for a strip with a depth of 20unit cells.

[1] Cuenot S et al., *Phys. Rev. B*, 69, 165410 (2004)
[2] P. Olsson, S. Melin and C. Persson, *Phys. Rev. B*, 76, 224112 (2007)

Longitudinellt kompressionsbrott i kolfiberförstärkt polymerkomposit

D. Svensson[1], K.S. Alfredsson[1], U. Stigh[1], N.E. Jansson[2]
[1]Materialmekanik, Högskolan i Skövde, email: daniel.svensson@his.se
[2]GKN Aerospace Engine Systems Sweden, Trollhättan

Polymerkompositer är generellt spröda material och istället för plasticitet uppkommer en progressiv skadetillväxt vid spänningskoncentrationer som relaxerar spänningarna. Elastiska analyser med uppmätta materialegenskaper från kupongtest underskattar därför hållfastheten och istället måste hållfastheten provas fram på laminatnivå. Dessa värden varierar med material, laminatupplägg, tjocklek o.s.v. och blir därför mycket dyra att bestämma experimentellt för varje möjlig kombination. För att drastiskt reducera antalet prover har på senare tid allt större fokus lagts på att utveckla modeller och metoder att simulera progressiv skadetillväxt. Dessa modeller börjar även implementeras i kommersiella Finita Element (FE) program, t.ex. Abaqus och LS-Dyna. För att kunna modellera skadeutveckling krävs att brottenergin för den aktuella brottmoden är känd. Standardtester har utvecklats för att mäta brottenergin associerad med vissa skademoder men hittills har ingen provmetod för longitudinellt kompressionsbrott standardiserats. Longitudinellt kompressionsbrott sker vanligen genom att fibrerna knäcks lokalt och bildar en zon av knäckta, roterade fibrer, ett s.k. kinkband bildas, se Fig 1a.

Vanligen studeras kompressionsbrott i multiriktade laminat. Detta kräver borträkning av energidissipation p.g.a. intralaminära sprickor. Vidare försummas inverkan av eventuella interageringseffekter. I detta arbete har en testuppställning för mätning av brottenergin associerad med longitudinellt kompressionsbrott utformats, se Fig 1b. Skada lokaliseras i ett område där fibrer är orienterade parallellt med lastriktningen och därför kan brottmoden studeras i isolerad form. Vidare är utvärderingsmetoden baserad på J-integralen[1] som generaliserats till det tredimensionella fallet. Bidragen till J-integralen bestäms genom att mäta töjningsfältet med ett digital image correlation system. FE-simuleringar används som ett verktyg att utvärdera det lokala beteendet i skadezonen. Det huvudsakliga beteendet är återskapat genom att modellera skadezonen som en kohesiv zon och övrig geometri med linjära plan spänningselement. Den kohesiva lagen består av en linjärelastisk del, följd av ett område med svagt ökande spänning innan spänningen abrupt sjunker till noll i samband med instabilitet.

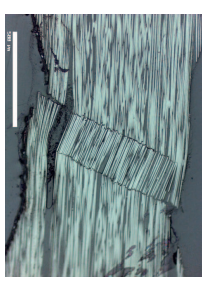

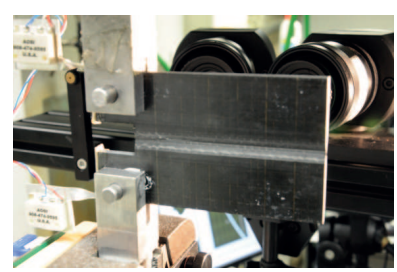

Figur 1: (a) Mikroskopibild av fiberbrott i form av kinkbandsformation. Längdskalan indikerar 500 μm. (b) Experimentell uppställning.

[1]J.R. Rice. A path independent integral and the approximative analysis of strain concentration by notches and holes. *Journal of applied mechanics.*, **88**, 379-386, (1968)

Spontant brott vid expanderande fasomvandling

Per Ståhle

Hållfasthetslära, email: pers@solid.lth.se

Fasomvandling som ger materialet en större volym, är föremålet för denna studie. Fasen som bildas utfälls som en inklusion i en matris av det ursprungliga fasen. Inklusionerna växer genom att mer och mer av det omgivande matrismaterialet införlivas. Fasomvandlingen behandlas som en enkel homogen svällning. Materialen antas var elastiskt idealplastiskt. Hills klassiska lösning för expanderande inneslutningar behandlar processen i ett steg och utgångspunkten är att hela inneslutning sväller simultant. Resultatet förutspår att spänningen i inklusionen blir en homogen hydrostatisk kompression. De analytiska lösningarna för cylindriska och sfäriska utfällningar ger plastisk deformation i områden som omger inkulsionen. I den genomförda studien beaktas inklusionens tillväxt såatt den pågående fasomvandlingen sker i sfärens eller cylinderns periferi. Resultatet predikterar spänningar i inklusionen som kan delas upp i tre fält med en tangentiell spänning som är kompressiv, och dragspänning närmare inklusionens mitt. Den radiella respektive den tangentiella spänningen går från tryck till drag i ett område med en radie som är cirka en tredjedel resp. en femtedel av inklusionens radie. Nära inklusionens mitt råder ett hydrostatiskt spänningstillstånd som är singulärt ($\sigma_h \ -\ln r$).

I ljuset av studien kan typisk krackelering och sprickor i exempelvis zirkoniumhydrid förklaras.

Mikroskopbilden visar en zirkoniumhydrid, som bildats i närheten av en nedkyld punkt. materialet är Zr-2.5 wt% Nb från en tryckledning. Den negativa temperaturgradienten drar väte från omgivningen till den kalla kontakten. Inledningsvis är vätet löst i det kristallina zirkoniumet. Vid en kritisk koncentration bildas zirkoniumhydrid. En spricka ses korsa hydriden.

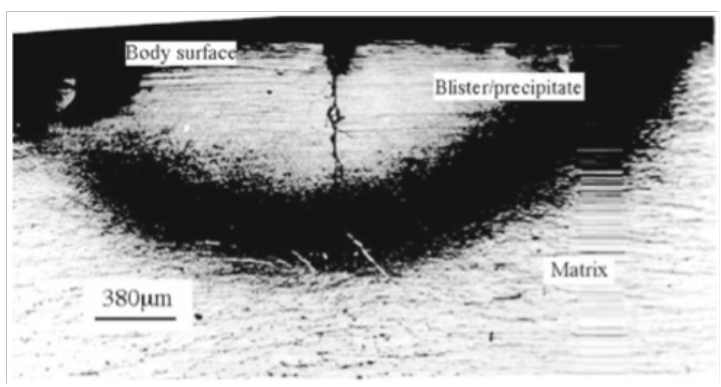

Figure 1: Zirkoniumhydrid med typisk krackelering

Strömningsmekanik II

torsdag 13/6 10:55-11:55

Couette, Coriolis and Kelvin - is absolute vorticity conserved under rotation in shear flows ?

Alexandre Suryadi[1], Antonio Segalini[2], P. Henrik Alfredsson[3]
Linné FLOW Centre, KTH Mechanics
[1]alexandre@mech.kth.se, [2]segalini@mech.kth.se, [3]hal@mech.kth.se

Fluids undergoing system rotation are affected by Coriolis forces that may dramatically change the flow behaviour even under rather slow rotation. The Coriolis force per unit mass can be written as

$$\mathbf{f} = -2\boldsymbol{\Omega} \times \mathbf{u}$$

where $\boldsymbol{\Omega}$ is the system rotation vector and $\mathbf{u}$ the fluid velocity vector. Examples of such flows are spanwise rotating channel flows, such as pressure driven Poiseuille flow and rotating plane Couette flow (RPCF) (see figure 1a). This gives rise to a Coriolis force that is directed normal to the walls. In Poiseuille flow one half of the channel becomes unstably stratified in terms of the Coriolis force and the other stably stratified, whereas for RPCF the whole channel becomes either stably or unstably stratified depending on the direction of rotation (cyclonic or anti-cyclonic rotation, respectively). These flows are governed by two flow parameters, the Reynolds number $\mathrm{Re} = U_w h/\nu$ and a rotation number $\Omega = \boldsymbol{\Omega} \cdot \mathbf{e_z} h^2/\nu$, where U_w is the wall velocity, h half the channel width and ν the kinematic viscosity. For RPCF the linear stability boundary is given by $\mathrm{Re} = \Omega + 107\Omega^{-1}$ and the instability first show up as streamwise oriented roll cells.

If a two-dimensional turbulent channel flow is influenced by sufficiently large anti-cyclonic system rotation, i.e. the rotation is oriented in opposite direction to the mean flow vorticity, it has been observed that the absolute vorticity, i.e. the sum of the averaged spanwise flow vorticity and system rotation, tends to zero in the central region, and this phenomenon has so far eluded a theoretical explanation. Here we show, through a unique experiment at low Reynolds number in RPCF undergoing anti-cyclonic rotation that also such a flow, albeit not homogeneous in the spanwise direction due to the instability developing from the Coriolis force, still shows the same effect, namely that the absolute vorticity tends to zero (figure 1b).

We offer an explanation to this based on a formulation of the Kelvin's circulation theorem derived from the Reynolds averaged Euler equation in the rotating reference frame,

$$\frac{\overline{\mathrm{D}}\Gamma_a}{\mathrm{D}t} = \frac{\overline{\mathrm{D}}}{\mathrm{D}t} \int_{S_\gamma} (\langle \boldsymbol{\omega} \rangle + 2\boldsymbol{\Omega}_z) \cdot \boldsymbol{n} \, \mathrm{d}S = 0 \tag{1}$$

where $\boldsymbol{\omega} = \nabla \times \boldsymbol{u}$ is the instantaneous vorticity vector, stating that the mean flow circulation for a given material path will be approximately preserved in the central region of the RPCF.

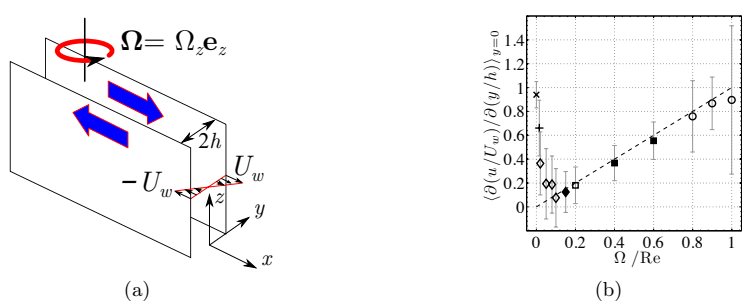

(a) (b)

Figure 1: (a) Geometry of plane rotating Couette flow (b) Scaled velocity gradient at the centre plane of the channel obtained through PIV measurements. Chain-dotted line indicates zero absolute vorticity.

Grease flow modeling using micro particle image velocimetry

Lars G. Westerberg[1], T. Staffan Lundström[1], Torbjörn Green[1], Erik Höglund[2], Jinxia Li[2], Piet M. Lugt[3], Pieter Baart[3]
[1]Division of Fluid and Experimental Mechanics, Luleå University of Technology, SE-971 87 Luleå, email: lars-goran.westerberg@ltu.se
[2]Division of Machine Elements, Luleå University of Technology, SE-971 87 Luleå
[3]SKF Engineering and Research Centre, Nieuwegein, The Netherlands.

The flow dynamics of a lubrication mechanism is very complex, much due to the complex rheology and composition of the grease. In order to obtain an optimal lubrication, both the initial amount of grease and the position of the grease are highly important as too much grease will contribute to an increased friction, and grease in the wrong place will negatively affect the replenishment through oil bleeding. To understand the flow dynamics of grease hence is highly important for the understanding of the lubrication mechanism. Using micro Particle Image Velocimetry (μPIV) we have in a series of studies investigated the dynamics of grease flow in 2D straight channels with- and without restrictions, and in a full 3D configuration comprising a double restriction seal geometry. Velocity profiles for greases of different thickness have been measured, showing the influence of the grease rheology on the grease flow behavior.

Large scale unsteady behaviour of turbulent pipe flow through 90° bends with varying degrees of curvature

Christian Carlsson[1], Laszlo Fuchs[1]
[1]Division of Fluid Mechanics, Lund University, email: christian.carlsson@energy.lth.se

The practice of transporting fluids in pipes is ubiquitous, and the associated need to bend pipes is of course clear. The temporal behaviour of the flow in these circumstances is important, where, e.g., flow induced oscillations can cause significant fatigue.
While laminar flow through curved pipes has been studied extensively (see review article [1]), showing the steady characteristic *Dean motion*, turbulent flow through 90° bends can be subject to large scale unsteady behaviour, a phenomenon known in the literature as "swirl switching". Even though several studies have been aimed at elucidating its nature [2] [3] [4] [5], the underlying mechanism is still unknown. Through *large eddy simulations* (LES), together with the utilization of *proper orthogonal decomposition* (POD) and the more recent *dynamic mode decomposition* (DMD) [6], an attempt has been made to determine the origin of the phenomenon. Flows in pipes with four different curvature ratios r_o/R_b, where r_o is the radius of the pipe and R_b the radius of the bend, have been analyzed.

[1] Berger, Talbot, and Yao, *Ann. Rev. Fluid Mech.*, **15**, 461-512, (1983)
[2] Tunstall and Harvey, *J. Fluid. Mech.*, **34**, 595-608, (1968)
[3] Rütten, Schröder, and Meinke, *Phys. Fluids*, **17**, (2005)
[4] Hellström, Zlatinov, Smits, and Cao, *Seventh inter. symp. on turb. and shear flow phenomenon*, (2011)
[5] Kalpakli and Örlü, *Int. J. Heat Fluid Flow*, (2013)
[6] Schmid, *J. Fluid Mech.*, **656**, 5-28, (2010)

Flerfasströmning I

torsdag 13/6 14:05-15:05

Inverkan av bio-fibriller på hydrodynamisk stabilitet

Mathias Kvick[1], Fredrik Lundell[2], Lisa Prahl Wittberg[3], L. Daniel Söderberg[4]
[1]Wallenberg Wood Science Center, KTH Mekanik, email: kvick@mech.kth.se
[2]Wallenberg Wood Science Center, KTH Mekanik, email: fredrik@mech.kth.se
[3]Linné FLOW Centre, KTH Mekanik email: prahl@mech.kth.se
[4]Innventia AB, Stockholm, email: daniel.soderberg@innventia.com

Experiment och en linjär stabilitetsanalys är utförda för flödet i en kurvig, roterande, rektangulär kanal. Arbetet är utfört för att få en förståelse för hur den hydrodynamiska stabiliteten påverkas när Nano-Fibrillerad Cellulosa (NFC) är tillsatt i ett flöde. I experimentet visualiseras strukturerna i flödet och bilder av dessa strukturer insamlas. I den linjära stabilitetsanalysen modelleras fibrillerna som en orienteringsberoende spänningstensor. I både experiment och teori ses en klar stabilisering av flödet när NFC är tillsatt. Denna stabilisering är mindre än förväntat baserat på den uppmätta och beräknade effektiva viskositeten. Vidare ses en stor inverkan av fibrillerna på den transienta tillväxten, medan vågtalet i spännviddsled knappt påverkas. I figuren nedan ses en avbildning av experimentet, flödet kommer in i den högra kammaren strömmar genom den kurviga kanalen till utloppet i den vänstra kammaren. Den andra figuren är en typisk bild tagen under ett experiment som visar den första instabiliteten som uppstår, nämligen virvlar i strömningsled.

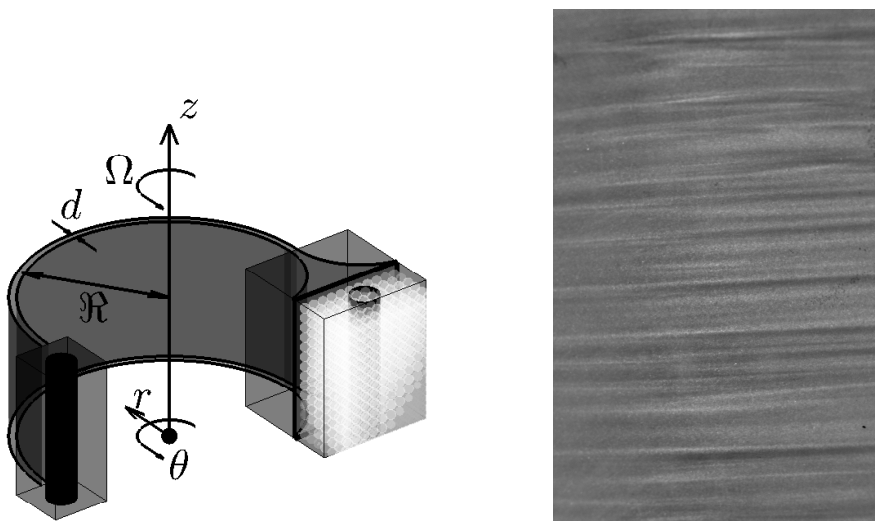

Figure 1: Vänster: Sketch av den experimentiella uppställningen. Höger: Exempelbild av den primära instabiliteten, dvs virvlar i strömningsled, från experiment med vatten.

Hydrodynamic alignment and assembly of nano-cellulose

Karl Håkansson[1,2,5], Fredrik Lundell[1,2], Andreas Fall[1,3], Lisa Prahl Wittberg[1,2], Lars Wågberg[1,3] and L. Daniel Söderberg[1,2,4]

[1]Wallenberg Wood Science Center, Royal Institute of Technology, SE-100 44 Stockholm
[2]Linné Flow Centre, Dept. of Mechanics, Royal Institute of Technology, SE-100 44 Stockholm
[3]Fibre and Polymer Technology, Royal Institute of Technology, SE-100 44 Stockholm
[4]Innventia AB, BOX 5604, SE-114 86 Stockholm, Sweden
[5]email: karlh@mech.kth.se

The strength of a wood fibre is attributed the long stiff cellulose chains, located in the cell wall. These cellulose chains are packed into bundles, named nano-fibrils, consisting of approximately 16 chains. In different parts of a tree, the properties of the wood fibres are different in order to cope with the forces acting locally on a specific part of the tree. The tree designs the properties of each fibre by varying the orientation of the nano-fibrils in the fibre; the fibre becomes strong and stiff if all nano-fibrils are oriented in the direction of the fibre and vice versa. The strongest wood fibres are as strong as glass fibre and almost as stiff as Kevlar.[1] It is hence desirable to create a process in which it is possible to manufacture man made filaments mimicking the properties of the wood fibre. Such process is under development, with the underlying idea to align freely moving cellulose nano-fibrils by hydrodynamical forces, whereafter a phase change from liquid to gel is started, creating a fibril-network.

Figure 1 (left) depicts the channel used to align the fibrils, two outer water flows are focusing the core flow containing the fibrils. Due to the elongated shape of the fibrils, they are aligned in the flow direction as the core flow is focused and accelerated. The orientation of a single fibril is not trivial to determine since the fibril is smaller than the wavelength of light, with a diameter of $\sim$ 40nm and a length of $\sim 2\mu$m. The degree of alignment in the focusing has been studied experimentally by polarized light, and numerically with a flow simulation in COMSOL and a computation of the 1D Smoluchowski equation. The fibrils are seen to align in the acceleration as hypothesized and the alignment is seen to increase as the acceleration is increased.

By introducing surface charges on the fibrils (carboxyl groups) the fibrils are able to repel one another, making it possible to have a high concentration of fibrils without aggregation.[2] However, by letting ions diffuse into the dispersion, it is possible to screen the surface charges, which will lead to a fast aggregation and hence a phase change from dispersion into gel. In this setup, ions are seeded into the fibril dispersion from the outer flows, allowing the fibrils to first align due to the acceleration. Figure 1 (right) shows a nano-cellulose filament made from the hydrodynamical spinning apparatus.

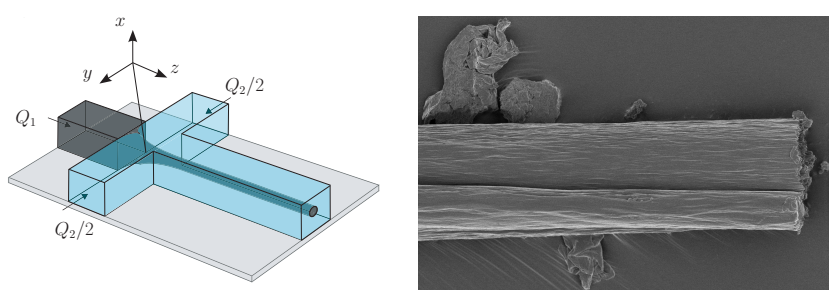

Figure 1: **Left**, schematic of the flow focusing setup. **Right**, scanning electron microscope image of a nano-cellulose filament.

[1]Page and Hosseiny, *J. Pulp. Paper. Sci.*, 99, (1983)
[2]Fall *et al.*, *Langmuir*, **27**, 11332, (2011)

A particle-level fiber model, implemented in a general purpose CFD code

Jelena Andrić[1], Stefan B. Lindström[2], Srdjan Sasic[1], Håkan Nilsson[1]

[1]Division of Fluid Dynamics, Chalmers University of Technology, email: jelena.andric@chalmers.se
[2]Mechanics, IEI, Linköping University, email: stefan.lindstroem@gmail.com

The dynamics of particles suspended in flowing fluid are of great importance in papermaking and composites processing. One example is the making of pulp mats for use in hygiene products. The fiber dynamics of the sheet forming process are one of the crucial factors that influence the microstructures, and thus the characteristics, of the product[1,2].

A particle-level fiber model has been implemented in a general purpose, open-source computational fluid dynamics code. The fibers are modeled as chains of cylindrical segments. The segments are tracked individually and their equations of motion account for the hydrodynamic forces and torques from the interaction with the fluid, and the connectivity forces and moments that ensure the fiber integrity. In the flexible version of this model, the elastic bending and twisting torques are included. The segment inertia is taken into account and a one-way coupling with the fluid phase is considered.

The flexible fiber model is applied to the rotational motion of *an isolated cylindrical fiber* in a low segment Reynolds number simple shear flow[3]. In the case of a stiff, straight fiber, the computed period of rotation is in good agreement with the one computed using Jeffery's equation for an equivalent spheroid aspect ratio[4]. A qualitative comparison is made with experimental data for flexible fibers. These results show that the implemented model can reproduce the experimentally observed dynamics of rigid and flexible fibers successfully. The behavior of *50 fully flexible fibers* (chains of cylindrical segments connected with ball and socket joints) is studied in DNS of channel flow[5]. The initially vertical fibers follow the turbulent structures, and tend to align with the flow, see Fig.1. The dependence of the fiber motion on initial position and density is analyzed for *50 fully rigid fibers* in a RANS simulation of the ERCOFTAC Conical Diffuser[6].

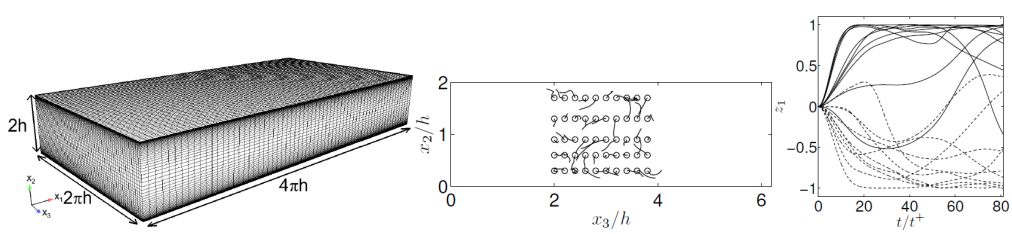

Figure 1: DNS of channel flow. Left: Computational domain and (coarse) mesh. Center: Fiber trajectories. Right: Fiber re-orientation (0 is non-aligned, and ±1 is aligned, with the x_1 direction).

[1] Ross, R. F. and Klingenberg, D. J., "Dynamic simulation of flexible fibers composed of linked rigid bodies", *J. Chem. Phys*., 106:2949–2960, 1997.

[2] Matsuoka, T. and Yamamoto, S., "Dynamic simulation of fiber suspensions in shear flow", *J. Chem. Phys.*, 102:2254–2260, 1995.

[3] Andrić, J., Lindström, B. S., Sasic, S., Nilsson, H., "Description and validation of a flexible fiber model, implemented in a general-purpose CFD code", *8th International Conference on Multiphase Flow ICMF 2013*, Jeju, Korea, May 26 - 31, 2013.

[4] Jeffery, G.B., "The motion of ellipsoidal particles immersed in a viscous fluid.", *Proc. Roy. Soc. London Ser.A*, 102:161–179, 1922

[5] Andrić, J., Fredriksson, S., Lindström, B. S., Sasic, S., Nilsson, H., "A study of a flexible fiber model and its behavior in DNS of turbulent channel flow". Accepted for publication in *ACTA Mechanica*, 2013.

[6] Andrić, J., Lindström, B. S., Sasic, S., Nilsson, H., "A particle-level rigid fiber model for high-Reynolds number flow, implemented in a general-purpose CFD code", *8th International Conference on Multiphase Flow ICMF 2013*, Jeju, Korea, May 26 - 31, 2013.

Industriella applikationer II

torsdag 13/6 14:05-15:05

Parameterstudie över inverkan av järnvägshjuls löpbaneslitage på rullkontaktutmattning och nötning

Kalle Karttunen[1], Elena Kabo[2], Anders Ekberg[3]
[1]Tillämpad mekanik, Chalmers Tekniska Högskola, email: kalle.karttunen@chalmers.se
[2] även Qamcom Research & Technology AB, email: elena.kabo@chalmers.se
[3] Tillämpad mekanik, Chalmers Tekniska Högskola, email: anders.ekberg@chalmers.se

Järnvägshjuls transversella profil påverkar både vagnars gångdynamik och den resulterande nedbrytningen av både räl och hjul. Tidigare studier har visat att underhållsgränsen för löpbaneslitage (eng. *hollow wear*) har en dålig korrelation gentemot vilka hjul som löper stor risk att drabbas av rullkontaktutmattning[1]. För att undersöka vilka geometriparametrar hos ett nött hjul som ger störst inverkan på utmattning och ytterligare nötning har en numerisk parameterstudie genomförts. Denna innefattar hjulprofiler med idealiserat löpbaneslitage (se Figur 1) approximerat som elliptiska kurvor och cirkulära övergångar mellan dessa ellipser och den nominella hjulprofilen. Fordonsdynamiska simuleringar utförs med det kommersiella programpaketet GENSYS[2]. Fordonsmodellen innefattar en godsvagn (med de slitna hjulprofilerna) vilken körs på ett spår med olika kurvradier. Spårets sidolägesfel är medtagna i simuleringarna. Med hjälp av hjul/räl krafter och värden på kontaktarean framtagna i simuleringarna kan olika skademått utvärderas.

Två olika skademått används vid jämförelsen av de olika hjulprofilerna. Det första skademåttet, FI_{surf}, är ett mått relaterad till ytinitierad rullkontaktutmattning[3], vilken postuleras uppkomma då $FI_{\text{surf}} > 0$. Det andra skademåttet, $T\gamma$, är ett mått på energin som har tagits upp i kontaktareorna för hjulet och rälen. $T\gamma$ antas här relatera till nötning[4]. Ytinitierad rullkontakt utmattning och nötning anses vara konkurrerande skademekanismer då utmattningssprickornas djup reduceras vid nötning.

Resultaten visar att även om löpbaneslitagets djup är ungefär konstant mellan de olika slitna hjulprofilerna så kan skademåtten variera mycket. Detta visar att nuvarande underhållsgränser (vilka baseras på djupet av löpbaneslitaget) sannolikt är för rudimentära. Ett exempel på hur en parameter påverkar skademåtten kan ses i Figur 1b där lutningen hos ellipsen i Figur 1a, θ, varieras mellan 1.4 och 2.9° (lutningen på rälen är 1.9°). För en kurva med radien 500 m ser man (Figur 1b) hur FI_{surf} ökar med minskande lutning på ellipserna. När lutningen på ellipsen är större än lutningen på rälen (dvs. lutning 2.4 och 2.9° för ellipsen) så är 75:e percentilen av FI_{surf} negativ, vilket innebär att risken för rullkontaktutmattning är relativt liten. Övriga parametrar som är med i studien är ellipsens konvexitet (främst genom parametern b i Figur 1a), positionen för ellipsens centrum, samt radien på den cirkulära övergången mellan ellipsen och nominella hjulprofilen vid flänsen på hjulet (R_2).

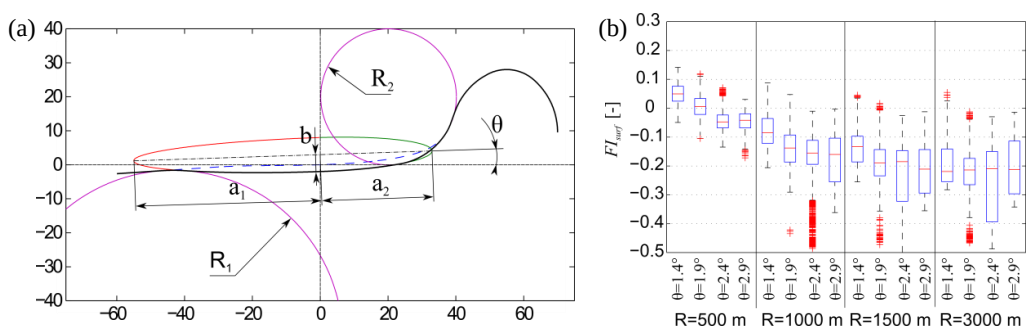

Figur 1: Geometriparametrar vid generering av en hjulprofil med löpbaneslitage (a) och inverkan av slitna hjulprofiler på risken för ytinitierad rullkontaktutmattning (presenterat i en s.k. boxplot) för första axelns inre hjul då vagnen körs i cirkulära kurvor med radier 500, 1000, 1500, och 3000 m (b).

[1] Fröhling, Spangenberg och Hettasch, *Vehicle System Dynamics*, **50** (supp 1), 319-334, (2012)
[2] GENSYS, www.gensys.se
[3] Ekberg, Kabo och Andersson, *Fatigue & Fracture of Engineering Materials & Structures*, **25**, 899-909, (2002)
[4] Pearce och Sherratt, *Wear*, **144**, 343-351, (1991)

Investigation of surface initiated rolling contact fatigue with the asperity point load model

D. Hannes*, B. Alfredsson†
Department of Solid Mechanics, KTH Royal Institute of Technology, Stockholm,
*daveh@kth.se, †alfred@kth.se

Many machine elements contain highly loaded surfaces with repeated rolling contact. Typical examples are gears, bearings, cams or wheel-rail contacts. The loaded contact surfaces of these applications may eventually suffer from rolling contact fatigue (RCF) or spalling. The damage consisting of cracks and craters or spalls in the contact surfaces, may result in dysfunctionality or even final failure of the machine element. Surface initiated spalling is related to asperities on the contact surfaces, as they induce three-dimensional contact loads and act as local stress raisers [1]. The asperity point load mechanism illustrated in Figure 1, provides the tensile surface stresses which can explain both initiation [2] and propagation [3,4] of surface initiated RCF damage.

A parametric investigation was performed to study the contribution of surface roughness, friction and a constant residual surface stress to the RCF damage process. The effects on initiation, crack path and fatigue life at both early and developed damage were examined for a gear application. Both a one-parameter-at-a-time approach and a 2-level full factorial design were carried out with the asperity point load model [5].

Surface roughness and local friction properties were found to control crack initiation, whereas the simulated crack path was primarily affected by the residual surface stress, especially for developed damage. Reduced surface roughness, improved lubrication and a compressive residual surface stress all contributed to increase the simulated fatigue life. The asperity point load model could predict effects on RCF that are observed with experiments. The results further support the asperity point load mechanism as the source behind surface initiated RCF.

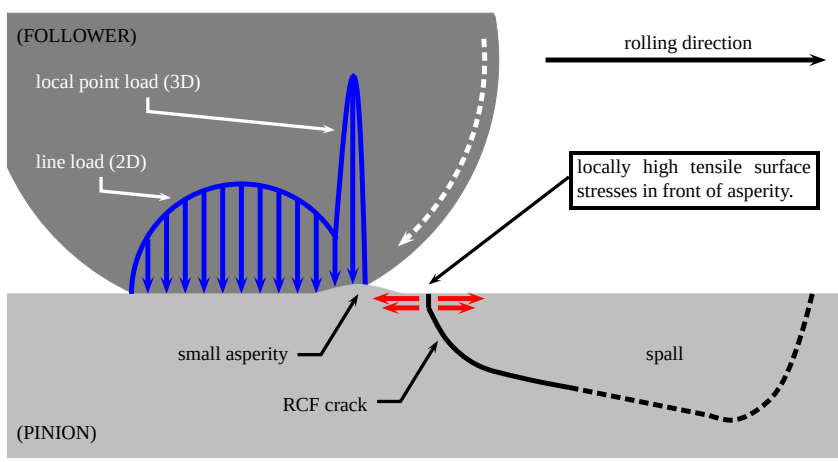

Figure 1: The asperity point load mechanism illustrated with an equivalent gear geometry.

[1] Olsson, in: *Engineering Against Fatigue*, A.A. Balkema, The Netherlands, (1999)
[2] Dahlberg and Alfredsson, *Int. J. Fatigue*, **30**, 1606, (2008)
[3] Hannes and Alfredsson, *Engng Fract. Mech.*, **78**, 2848, (2011)
[4] Hannes and Alfredsson, *Engng Fract. Mech.*, **83**, 62, (2012)
[5] Hannes and Alfredsson, *Wear*, **294-295**, 457, (2012)

Interaktionsmodeller för 2D FE-modellering på pekskärmar

D. Åkesson[1], J. Lindemann[2]
[1]Division of structural mechanics, PO Box 118, 221 00 Lund, daniel.akesson@construction.lth.se
[2]Division of structural mechanics, PO Box 118, 221 00 Lund, jonas.lindemann@byggmek.lth.se

Med lanseringen av smarta telefoner och pekplattor har användandet av multi-touch gränssnitt fort blivit populärt. Med detta gränssnitt förloras en del av precisionen som uppnås med en muspekare och ersätts med en känsla direkt manipulation. Det gör gränssnittet intressant för strukturmekaniska applikationer, genom att ge användaren en känsla av att direkt kunna manipulera en modell. Gränssnittet lämpar sig också väl för det tidiga designskedet samt i utbildningssyfte, då fokus inte ligger på precisionen utan på att ge användaren en förståelse för hur modellen fungerar.

För att undersöka hur multi-touch gränssnittet kan användas för strukturmekaniska applikationer utvecklades en koncept applikation under namnet Sketch-a-Frame [1]. Sketch-a-Frame är en enkel finita element applikation för iPad som använder balkelement för att studera ram- och fackverksmodeller. Applikationen bygger på samt utvecklar koncept från programmet pointSketch [2].

Användargränssnitten för många av dagens FE-program har länge följt samma modell, de består generellt av ett antal delmoment uppritning, definering av randvilkor, laster, beräkning för att komma till det slutgiltiga steget där resultatet visualiseras. Under utvecklingen av Sketch-a-Frame insågs att ett traditionellt gränssnitt för muspekare inte fungerar lika bra på ett touchgränssnitt. Istället för de olika delstegen visualiseras resultatet då modellen är stabil, om det är en mekanism så visualiseras denna med en animation. Utvecklingen av ritvektygen var en iterativ process vilket har medfört att de fungerar som användarna förväntar sig att de ska fungera, vilket gör applikationen intuitiv att använda. Verktyg finns för att visualisera förskjutningar, normalkrafter, moment, spänningar samt normaliserad redundans [3].

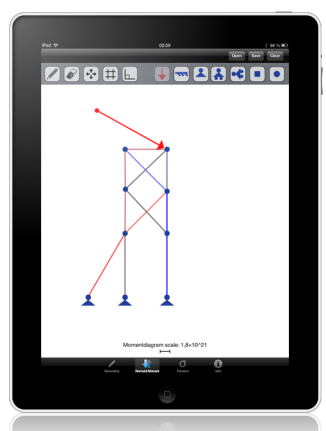

Figure 1: iPad med applikationen Sketch a Frame

[1]D. Åkesson, Interaction models for 2D finite element modeling on touch devices *Master's dissertation, Department of Construction Sciences, LTH, Lund* ISSN 0281-6679 (2013)

[2]P. Olsson, Conceptual studies in structural design : pointSketch a based approach for use in the early stages of the achitectural process, *Doktorsavhandlingar vid Chalmers tekniska högskola.* Ny serie , ISSN 0346-718X; nr 2435 (2006)

[3]G. Tibert, L. M. Achi, Static redundancy factors in conceptual design, *Proceedings of NSCM25* (2012)

Experimentella metoder III

torsdag 13/6 14:05-15:05

Utvärdering av fiberfogsstyrka hos massafibrer

Mikael S. Magnusson[1,2], Sören Östlund[1]
[1]BiMaC Innovation, Institutionen för Hållfasthetslära, KTH, Stockholm
[2]email: mima@kth.se

Hållfasthetsegenskaperna hos fiberfogar är nyckeln till uppbyggnaden av styrka hos fibrösa material såsom papper och kartong. För att effektivt skräddarsy sådana materials mekaniska egenskaper genom kemisk eller mekanisk behandling och för att förstå hur sådana modifieringar påverkar egenskaperna på mikroskopisk nivå är provning av individuella fiber–fiber–kors en allmänt använd metod. Belastningen i en fiberfog vid provning av individuella fiber–fiber kors är dock generellt mycket komplicerad och ytterligare kunskap om hur fiberfogars mekaniska egenskaper skall utvärderas är önskvärd.

En metod för tillverkning, provning, samt utvärdering av den komplicerade belastningen vid provning av fiber–fiberkors (Figur 1) har tagits fram. Metoden har tillämpats för att studera de resulterande krafter och moment som uppstår i fiberfogen vid brott då fiber–fiber–kors provats med varierande geometri och vid skjuvande-, öppnande-, rivande belastning, samt ett biaxiellt lastfall där fibrerna sträcktes med en förlast innan fiberfogen belastades till brott i en skjuvande typ av belastning.

Resultaten visar att styrkan hos individuellt framställda fiber–fiberkors följer en approximativt exponentiell fördelning och är oberoende av det nominella trycket under torkningen i intervallet [0.7–15] kPa.

Det konventionella antagandet att den lokala brottlasten är rent skjuvande vid global skjuvning av fiber–fiber kors skattar för vissa prov upp till 23 % fel. Vidare har en övre gräns för styrkan hos fiberfogar uppskattats för prover belastade i fyra principiellt olika lastmoder. Belastningsmoden uppskattades i skalade snittstorheter i termer av normal och skjuvspänning, beräknade med finit element analys (Figur 1) av samtliga prover, där snittkraften normalt mot fiber–fiber gränsskiktet, i skjuvled samt det öppnande och vridande momenten kring gränsskiktets centroid beaktats.

Pappersmekanik är en flerskalig disciplin där mikromekanisk provning kan tillföra nya resultat av stor betydelse för förståelsen av brottbeteendet hos fiberfogar. Dessa resultat kan användas på såväl makroskopisk nivå såsom nätverksmodellering samt vid skattning av olika kemiska modifieringar av fibrer.

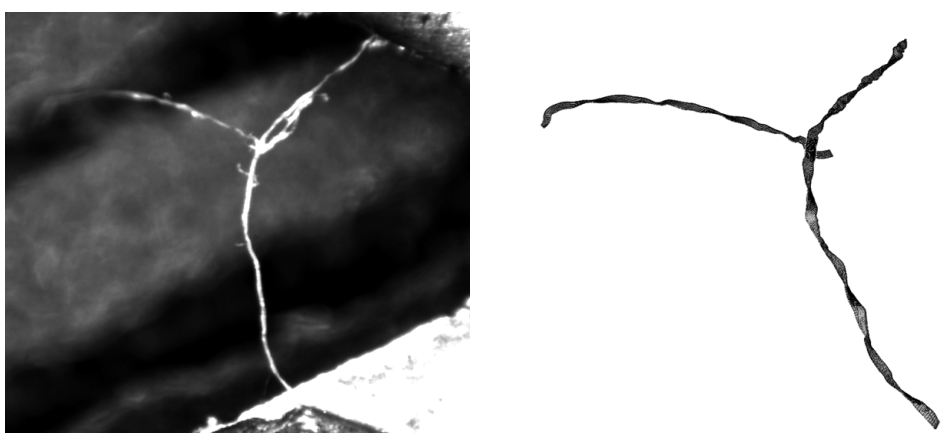

Figur 1: Mikroskopbild av ett typiskt fiberkors (vänster) och den modellerade strukturen (höger).

Kohesiva lagar för lims temperaturberoende

Tomas Walander
Materialmekanik, Högskolan i Skövde, epost: tomas.walander@his.se

Med lim kan hållfastheten på strukturer göras mer optimala. Detta fås främst genom att möjliggöra sammanfogning av lättvikts- och höghållfasta material, vilka normalt inte går att sammafoga med svetsning. Lims hållfasthetsegenskaper är dock kända för att vara temperaturberoende vilket behöver tas hänsyn till vid konstruktion av limmade strukturer. I konstruktionsskedet av en limmad struktur är det mera kostnadseffektivt att simulera strukturens hållfasthet än att prova den experimentellt. Detta medför att en simuleringsmodell som tar hänsyn till temperaturberoendet för lim är önskvärt.

Lims hållfasthetsegenskaper beskrivs med kohesiva lagar vilka kan mätas experimentellt. En kohesiva lag representeratar således det konstitutiva beteendet för ett limskikt. Deformationerna för ett limskikt sker huvudsakligen i två moder[1]. Dessa är mod I med fläkdeformation w och mod II med skjuvdeformationen v. I detta arbete studeras inflytandet av temperatur för två epoxilim. Experiment är utförda i båda moder för fem temperaturer inom temperaturspannet $-40 \leq T \leq 80$ °C. För varje enskilt experiments tas en kohesiv lag fram. Representativa experimentella resultat ges i Figur 1.

Tre parametrar i de kohesiva lagarna studeras i detalj. Dessa är den *elastiska styvheten*, *maximal spänning* samt *brottenergi*. Experimentella resultat visar att både den elastiska styvheten och den maximala spänningen minskar med en ökande temperatur för båda moder. För en ökande temperatur minskar brottenegin i mod II men ökar svagt i mod I. Genom att använda statistiska metoder kan dock brottenergin i mod I påvisas vara oberoende av temperaturen inom det utvärderade temperaturspannet.

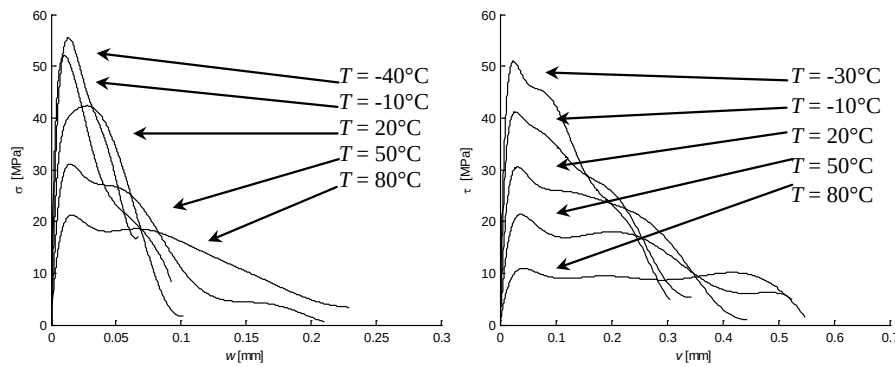

Figur 1: Representativa kohesiva lagar för ett 0,3 mm tjockt limskikt vid olika temperaturer och belastningsmoder[2]. Vänster: mod I. Höger: mod II.

[1] Klarbring, A. *Journal of Engineering Science*., **29**, 493 (1991)
[2] Walander, T. *Lic. no. 2013:08.*, Chalmers Tekniska Högskola, Göteborg, (2013)

Experimentell studie av tröskelvärde för limutmattning med kohesiv lag.

Alexander Eklind
Materialmekanik, Högskolan i Skövde, epost: alexander.eklind@his.se

För fordonsindustrin i Sverige är limning en fogningsmetod som är högaktuell. Limfogning öppnar möjligheten att blanda material som inte kan fogas med traditionella metoder, t.ex. punktsvets. Det är viktigt att bestämma limmets utmattningsegenskaper och speciellt tröskelvärde mot utmattning vid dimensionering av strukturella komponenter. Att utföra utmattningsexperiment på prototyp-konstruktioner är kostsamt och tidsödande. Att kunna prova limfogar i mindre och enklare provstavar är därför önskvärt. Det är intressant att utveckla analytiska metoder för att bestämma limmets tröskelvärd mot utmattning.

Limmets fläkegenskaper mäts med hjälp av experimentella metoder där energifrirörelse-hastigheten kan utvärderas med hjälp av Tamuzs metod. Med denna metod kan den kohesiva lagen tas fram för ett fläkprov utfört med Double Cantilever Beam provstav, DCB, se figur 1.

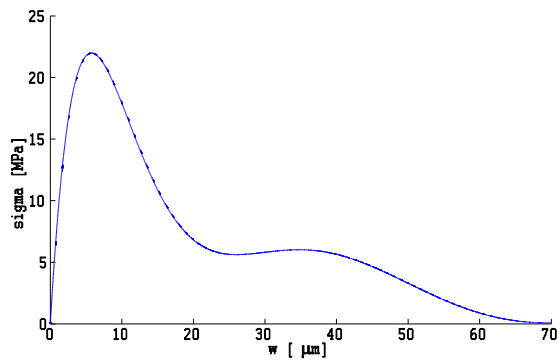

Figur 1. Kohesiv lag för limfog i fläkmod där *w* är separationen och sigma är spänningen vid sprickspetsen.

Arean under kurvan i figur 1 motsvarar brottenergin i fläkmod. För ett fläkprov startar spricka-propagering då brottenergin uppnås vid sprickspetsen. Tröskelvärdet för att sprickpropagering ska ske vid utmattning beräknas med Tamuzs metod samt med andra metoder så som ekvation 1

$$G = \frac{F^2}{2b}\frac{dc}{da} \qquad (1)$$

där *G* är energifrirörelsehastighet, *F* är fläkkraft, *b* är provstavsbredd, *C* är provstavens komplians och *a* är spricklängd. Utifrån den kohesiva lagen och vetskapen om tröskelvärdet, G_{th}, kan tröskelvärdet för separationen av limmet, w_{th}, uppskattas. Samma lim analyseras för olika separationer, *w*, i ett svepelektronmikroskop för att se när mikrosprickor uppkommer. Separationen, *w*, vid spricktendens i SEM jämförs med *w* från den kohesiva lagen. En dylik SEM-studie och en kohesiv lag bör ge en god uppskattning av det sökta tröskelvärdet G_{th}. Värt att notera är att utrustningen för att kunna utföra dessa test är standard hos svensk fordonsindustri idag.

Strömning i roterande maskiner I

torsdag 13/6 14:05-15:05

The effect of atmospheric boundary layer depth on wind turbine power production

Ali Al Sam[1], Robert Szasz[2], Johan Revstedt[3]
[1]PhD Student, email: Ali.Al_Sam@energy.lth.se
[2]Researcher, email: Robert-Zoltan.Szasz@energy.lth.se
[3]Professor, email: Johan.Revstedt@energy.lth.se

The strong growth of wind energy capacity worldwide is combined with an increase in wind turbine size. Within the last 20 years, the wind turbine size has increased from less than 20 m to more than 150 m. This exponential growth in wind turbine size is expected to continue in the feature and therefore it is important to understand the flow characteristics and wind turbine performance at such heights.

Although the Atmospheric Boundary layer (ABL) flows are mostly turbulent, they are similar in a dynamical sense and similarity laws can be used to represent the ABL complex dynamic processes. The Monin-Obukhov (MO) similarity theory is commonly used to describe the vertical wind velocity profile in horizontally homogeneous atmospheric surface layers, which accounts for the lowest part of ABL where the momentum and heat fluxes are assumed to be constant with height. The MO similarity theory implies that the change in mean velocity and temperature with height can be expressed by coordinate Z and that the statistical structure of the horizontally homogenous ABL is governed by only four parameters: Z; u_*; g/T_o and Q_o, where Z is the distance from the ground, u_* is the surface friction velocity, g/T_o is the buoyancy parameter and Q_o is the surface temperature flux.

Nevertheless, this similarity theory does not take into account the effect of ABL depth (Z_i) on the flow structures and the size of large eddies. Deardorff[1] has noticed the effect of ABL depth earlier and he scaled the convective ABL by the convective velocity and the ABL height Z_i while he scaled the shear ABL with the capping inversion base height (i.e. the ABL depth Z_i). Furthermore, McNaughton[2] showed that for very unstable conditions the peak of temperature spectrum depends on the mixed length scale $Z_i^{1/2}Z^{1/2}$.

In wind energy applications the MO similarity theory is usually used to predict the vertical wind speed profile by extrapolating wind speed measured at a certain height. Depending on two length scales: the wind turbine height and the ABL depth, the turbine might operate inside or outside the atmospheric surface layer at which the MO similarity theory is applicable.

The purpose of this study is to investigate the effect of ABL depth (Z_i) on the wind turbine power production by using Large Eddy Simulations of ABL over a wind turbine for different (Z_i/Z_{hub}) ratios.

[1] Deardorff, J. W., *J. Atmos. Sci.*, **29**, 91-115, (1972)
[2] McNaughton, K. G., *Nonlin. Process. Geophys.*, **14**, 257-271, (2007)

Experimental study of pressure fluctuations on a Kaplan turbine runner blade

Amiri, K.[1], Cervantes, M.[2], Mulu, B.[3],
[1]Luleå University of Technology, Division of Fluid and experimental mechanics, email: kaveh.amiri@ltu.se
[2]Luleå University of Technology, Division of Fluid and experimental mechanics, email: Michel.Cervantes@ltu.se
[3]Vattenfall Research and Development, email: berhanu.mulu@vattenfall.com

Investigation of the unsteady pressure distribution on the runner of reaction turbines is essential to have better understanding of the flow condition in such complex machines. The results can be used to evaluate the runner performance and investigate the flow condition in blade channel. They are also useful for evaluation of the water supply systems performance; guide vanes, stay vanes and spiral casing. Interaction between the rotor and stator can be quantified as well. The last one plays an important role in evaluating the lifespan and overhaul schedule of the rotating parts including runner and bearings. In low head turbines, propeller and Kaplan, there are a low number of blades without any support at the shroud. Hence, the blades and consequently other rotating parts of the turbine may experience significant deflection and vibration according to the periodic forces. Moreover, the numerical simulation of such a complicated flow is not still reliable. Thus, more experimental investigations are required to increase the knowledge about the physics and support numerical validation.

Unsteady pressure measurements on the suction side and pressure side of the blades of a Kaplan turbine model (Porjus U9) at several operating points were performed. Two adjacent blades were equipped with Kulite miniature Piezo-resistive pressure sensors in such a way that the pressure results in a blade-to-blade channel can be acquired. Phase averaging and frequency analysis methods are applied to the results. The results indicated the presence of a complex flow in the blade channel and high level of fluid structure interaction. They also indicated the high level of asymmetry in the spiral casing distributor and flow separation on some of the guide vanes. The separation on the guide vanes results in inappropriate flow angle of attack on the blades and consequently runner blades vibration. The phase resolved pressure data at Best Efficiency Point is presented in figure 1. The highest peak in the figures shows the blade vibration according to the flow asymmetry in the spiral casing lip-entrance region and the following oscillations are related to the blade vibration due to the guide vanes flow separation.

The strain gauge results on the shaft of Porjus U9 prototype are also acquired to clarify the flow structure interaction and compare the model and prototype results. The comparison showed that the blade vibration is transferred to the bearings through the shaft.

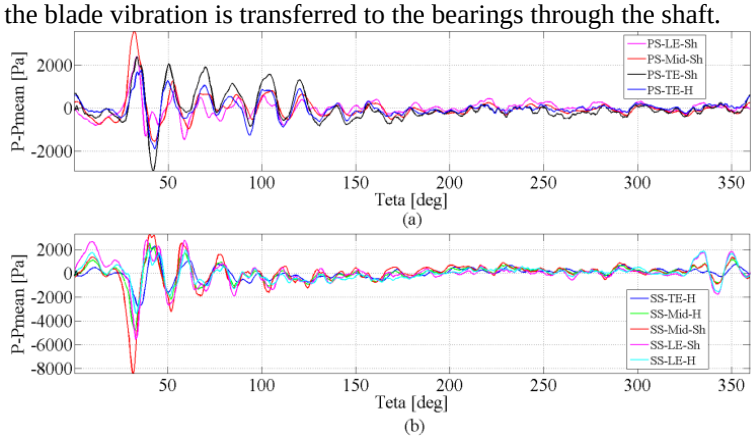

Figure 1: Phase averaged pressure results on the suction side and pressure side of the blades at BEP

Unsteady Turbulent Flow in Rotating Turbomachinery

Ardalan Javadi[1], Håkan Nilsson[2]
[1] Division of Fluid Dynamics, Chalmers University of Technology, Gothenburg: ardalan.javadi@chalmers.se
[2] Division of Fluid Dynamics, Chalmers University of Technology, Gothenburg: hani@chalmers.se

The application of computational fluid dynamics (CFD) in the understanding, design and optimizing of water turbines and pumps started about 30 years ago with the plausible role of Division of Fluid Dynamics, Chalmers University of Technology. In this context, the self-induced unsteadiness and pulsation at part load discharge is simulated with more advanced turbulence models (hybrid-LES) as a breakthrough using OpenFOAM C++ to accomplish two scenes. The hybrid-LES method is a combination of RANS in near-wall regions and LES in main stream which is more affordable than LES and more accurate than unsteady RANS. The studied test case is a swirl generator which is designed and experimented in Timisoara, Romania[1], see Figure 1.

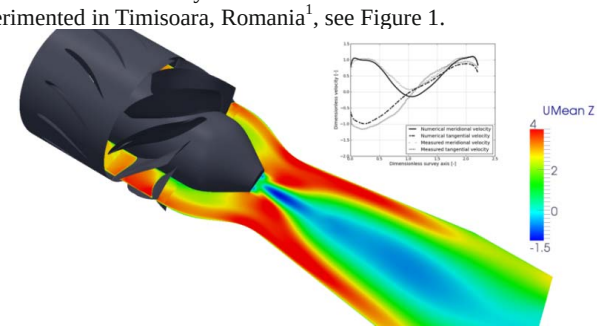

Figure 1. The swirl generator computational domain in concert with axial mean velocity, m/s.

The highly resolved LES and hybrid-LES of strongly swirling turbulent flows through an abrupt expansion of gas turbine combustor is investigated as well to shed more light on stagnation region and spiral vortex breakdown. The spurious suppression of the low-frequency, large scale precession of the vortex core is avoided using less diffusive methods. The results are compared with experimental measurement of Dellenbach[2], see Figure 2.

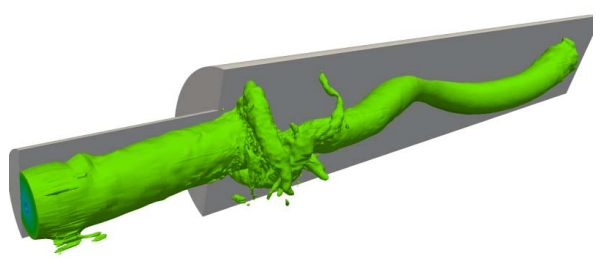

Figure 2. The Dellenbach sudden expansion computational domain in concert with pressure iso-surface -1.5 *Pa*.

The next step is full 3D simulation of Kaplan turbine which is less attended in the literature due to complexity of the geometry and the extravagancy of simulation. The unsteady RANS simulation of U9 Kaplan turbine located in Porjus, Sweden is our near future plan to dig deeper the flow features.

[1] Susan-Resiga, Muntean, Bosioc, Stuparu, Milos, Baya, Bernad and Anton, *Proceedings 2nd IAHR Transcations on Mechanics* **52(66)** Issue 6 203-16 (2007)
[2] Dellenback, Metzger and Neitzel *AIAA Journal*, **26**(6) 669-681 (1987)

Flerfasströmning II

torsdag 13/6 15:25-16:25

Large eddy simulation of unsteady turbulent flow in a semi-industrial size spray dryer

F. Innings[1] F. J. Jongsma[2] M. Olsson[2] F.
1 Tetra Pak Processing Systems, fredrik.innings@tetrapak.com
2 Tetra Pak CPS, alfred.jongsma@tetrapak.com
3 Tetra Pak Packaging Systems michale.olsson@tetrapak.com

Abstract This work is concerned with the numerical simulation of gas flow inside spray dryers, which is known to be highly transient. Experimental evidence presented in the literature to date is acquired either at a scale much smaller than industrial or at a limited number of locations in the system (e.g. the central axis). Alternatively, computational fluid dynamics (CFD) simulation, in particular methods based on the Reynoldsaveraged Navier-Stokes (RANS) equations, may provide the information of the complete flow field at industrial scales. However, RANS methods to some extent are hampered by the limitations of turbulence modelling. In this study, it has been investigated whether the current limitations of experiments and RANS CFD simulations can be omitted by the use of large eddy simulation (LES). The spray dryer studied was of semiindustrial size with a volume of 60m3. Via grid size and time step refinement studies, the minimum numerical requirements for obtaining converged time averaged velocity profiles could be identified. Spectral analysis and estimates of the Kolmogorov scales demonstrated that LES resolves scales well into the inertial subrange of turbulence scales. The LES calculation shows a complex precession of the jet. The jet moves around in the drying chamber seemingly with no reoccurring modes. Even with very long sampling times, no typical frequencies could be found. This work demonstrates the feasibility of LES for a spray dryer of semi-industrial scale and the ability of LES to predict large-scale motions. Future work will include the further validation of the LES via comparison with laser Doppler anemometry measurements and, subsequently, the comparison of RANS, unsteady RANS and LES simulations.

Ice accretion modeling based on LES and LPT

Robert Szasz[1], Laszlo Fuchs[1,2]
[1]Dept. Energy Sciences, LTH, email: robert-zoltan.szasz@energy.lth.se
[2]Linné Flow Center, KTH

Ice accretion is a major concern for wind turbines built in cold climate areas (Nordic and alpine regions) since the accreted ice deteriorates the efficiency of the turbine, might lead to failures due to the extra load and represents a safety risk due to the possibility of ice throws. Consequently, there is an intensive research to predict the occurrence of icing for given geographic areas. A lot of effort is put also in developing strategies to avoid icing, or to remove accreted ice layers. Much less effort is put in the understanding of how ice accretion occurs. Such understanding would help optimizing de- and anti-icing strategies.

There are experiments carried out in wind tunnels with controlled climatic conditions[1]. Numerical computations can complement such experiments by offering greater flexibility for parametric studies and scaling. Currently, most of the prediction methods are based on the Makkonen model[2].

Our goal is to develop a numerical tool to model ice deposition based on a combined Large Eddy Simulation (LES)-Lagrangian Particle Tracking (LPT) approach. The unsteady three-dimensional flow field is computed by solving the incompressible Navier Stokes equations on a cartesian equidistant grid. LES is used to account for turbulence. The solid surfaces are modeled using the Immersed Boundary Method. To model ice deposition, water droplets are released upstream and tracked using LPT. It is assumed that the droplets freeze instantaneously when they impact on the solid surfaces. As a second stage, the shape of the blade profile is remorphed to account for shape changes due to the accreted ice.

The proposed model is used to model ice accretion on a NACA 63415 airfoil. The set-up corresponds to the 'In-fog icing event 2' reported in [1]. The computational domain is shown in Figure 1. The droplets are released at the rectangular area denoted P1 in the figure, and, to save the computing efforts, all droplets passing P2 are removed from the computations since they are considered unable to collide with the surface. Figure 2 shows the distribution of the accreted ice, for better visibility logarithmic scale is used for coloring, the shape of the airfoil is changed proportional to the amount of accreted ice. One can observe that most ice accretes at the leading edge region, but small amount can be seen in the trailing edge region as well.

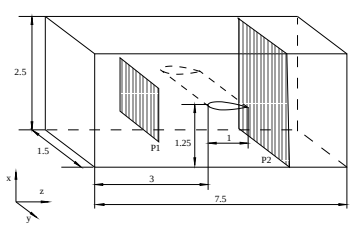

Figure 1: Computational domain

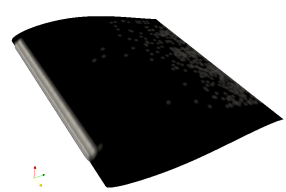

Figure 2: Accreted ice. Logarithmic color scale.

[1]Hochart et al., *Wind Energy*, **11**, 319-333, (2008)
[2]Makkonen, L., *Phil. Trans. Royal Soc.*, **358**, 1776, pp.2913-2939, (2000)

Simulering av en vätskestråles uppbrytning i stationär gas

Alexander Nygård[1], Lisa Prahl-Wittberg[2], Laszlo Fuchs[2]

[1]Linné FLOW Centre, KTH Mekanik, Stockholm, email: alexander@mech.kth.se
[2]Linné FLOW Centre, KTH Mekanik, Stockholm

Användning av förbränningsmotorer påverkar miljön. Därför sker en kontinuerlig utveckling för att minska dess utsläpp av skadliga föroreningar och partiklar. Koncentrationen av föroreningar som lämnar motorn påverkas till viss del av tillståndet i cylindern innan förbränning av bränslet sker. Det är därför önskvärt att kunna påverka hur fördelningen av drivmedel utvecklas i förbränningsrummet för olika driftfall. Ett sätt att förändra egenskaperna hos den resulterande blandningen är att sprida ut den totala bränslemängden under en cykel på flera pulser[1]. Snabbare blandning har observerats experimentellt för transient insprutning och detta är intressant eftersom den tid som finns tillgänglig för blandning i detta sammanhang är begränsad. Även en förenklad teoretisk betraktelse indikerar vikten av insprutningshastighetens tidsberoende för massflödet av omgivande gas som sugs in i en decelererande jet[2].

I syfte att studera uppbrytningsprocessen för fall liknande dieselinsprutning, simuleras intermittent insprutning av en jet i vätskefas i stationär gas. Simuleringarna bygger på en implicit LES-metod som löser upp de hastighetsskalorna som är relevanta för förloppet. För att utreda hur uppbrytningstakten och genererade flödesstrukturer förändras med injektionsschema jämförs simuleringar i vilka insprutning sker vid olika frekvens.

Som ett mått på uppbrytning används medelkrökningen κ. Denna är proportionell mot kvoten mellan vätskans ytarea A och volym V, i domänen. Resultaten indikerar att högre injektionsfrekvens kan tillämpas utan att κ förändras alltför mycket. För de fall där endast densitetskvoten mellan vätska och gas skiljer sig åt kan en högre initial uppbrytningstakt observeras när densitetskvoten ökas. I Figur 1 visas den relativa storleken av yta, volym och medelkrökning mellan två fall. Gasens densitet är densamma i dessa simuleringar och vätskefasens densitet är 20 gånger högre i fall 2. Staplarna i botten på figuren markerar när insprutning sker.

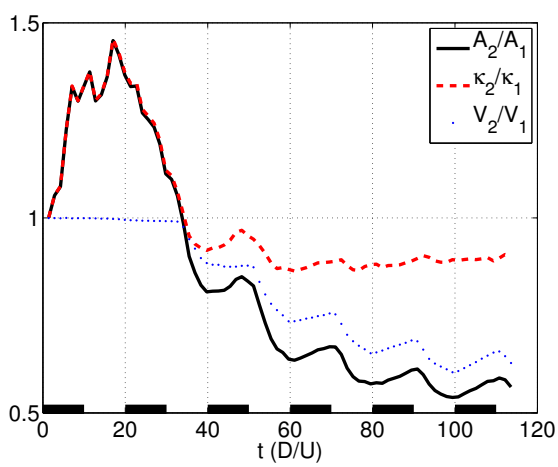

Figure 1: Påverkan av högre densitet hos vätskan på uppbrytningsförloppet

[1]M. Badami, F. Mallamo, F. Millo, E. E. Rossi, *Int. J. Engine Research*, **4**, No. 4, (2003)
[2]M.P. B. Musculus, *J. Fluid. Mech.*, **638**, pp. 117-140, (2009)

Dynamik I

torsdag 13/6 15:25-16:25

Dynamic higher order micropolar plate equations

Hossein Abadikhah[1], Peter D. Folkow[2]
[1]Division of Dynamics, Department of Applied Mechanics, Chalmers University of Technology 1, email: hossein.abadikhah@chalmers.se
[2]Division of Dynamics, Department of Applied Mechanics, Chalmers University of Technology 2, email: peter.folkow@chalmers.se

This work considers the analysis and derivation of dynamical equations on rectangular plates governed by micropolar continuum theory. The proposed method is based on a power series expansion of the displacement field and micro-rotation field in the thickness coordinate of the plate. This assumption results in sets of equations of motion together with consistent sets of boundary conditions. These derived equations are hyperbolic and can be constructed in systematic fashion to any order desired. Hence it is believed that these sets of equations are asymptotically correct. The construction of the equation is systematized by the introduction of recursion relations which relates higher order displacement and micro-rotation terms with the lower order terms. Furthermore the equations can be divided into two categories of motions, namely extensional and flexural motion.

Results are only obtained for the flexural motion of the plate using different truncation orders of the present theory, comparisons are performed with the plate theories developed by Eringen, Sargsyan and the exact theory for micropolar continuum. Numerical examples are presented for dispersion curves on an infinite plate for the three lowest flexural modes. The first eigenfrequency of three lowest modes for a simply supported plate are presented for different truncation orders, Eringen's, Sargsyan's plate theory and the exact theory. Furthermore the first eigenfrequency of the three lowest modes for the cases where two opposite boundaries are simply supported and the other two boundaries are either clamped or free are also studied with the present theory, Eringen's and Sargsyan's plate theories. Also various plots on mode shapes and stress distributions are compared with each theory for a infinite plate vibrating with a fix frequency.

Micropolar cloaking against Rayleigh waves

Alexey Khlopotin[1], Peter Olsson[2], Fredrik Larsson[3]

[1]PhD Student Chalmers University of Technology 1, email: alexey.khlopotin@chalmers.se
[2]Professor Chalmers University of Technology 2, email: peter.olsson@chalmers.se
[3]Professor Chalmers University of Technology 3, email: fredrik.larsson@chalmers.se

Transformation elastodynamics, the solid mechanical counterpart of transformation optics, is an approach to re-routing of mechanical, potentially harmful transient waves and vibrations, to protect structures or substructures from harm. A large-scale example would be to try to re-route seismic waves, whether from ground explosions or earthquakes, by arranging the properties of the material beneath and around some sensitive infrastructure so as to mimic the surrounding soil without any infrastructure. A less ambitious (and considerably more realistic) application would be to re-route elastic vibrations around the clamping points of panels in a vehicle, so as to minimize the noise from vibrating panels. Just as for transformation optics, the approach utilizes the concept of form-invariance of the equations of motion under diffeomorphisms to give recipes of how graded materials can mimic homogeneous and isotropic bodies, and cloak the presence of structures within the transformational cloak.

We have studied the use of several types of graded materials for cloaking, and in the present paper we describe how graded micropolar materials may be used to cloak against Rayleigh waves. We have implemented recipes for the graded properties of a micropolar cloak from transformation elastodynamics into a modified version of the Structural Mechanics module of COMSOL Multiphysics^{TM}. In numerical experiments we consider how a modeled, partially buried 'pipeline' may be protected from an incident transient Rayleigh wave by re-routing the wave under the pipeline.

Future work involve new and exotic material configurations, eg. fibre-reinforced material with pores and/or rotations. In the present paper we have studied cylindrical geometry of the cloak in 2D, this will be expanded to 3D together with diffierent cloak geometries, for example a plate geometry in 3D. The homogenization of the cloaking material will be made in futher studies.

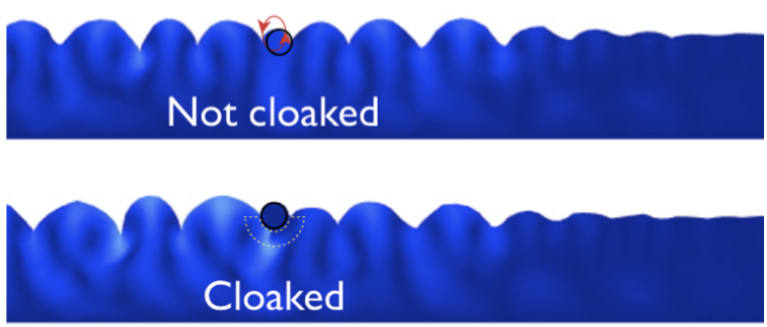

Figure 1: Rayleigh wave cloaking in COMSOL Multiphysics^{TM}: (a) Not cloaked configuration, (b) Micropolar cloak configuration

Experimental-Analytical Dynamic Substructuring

Mladen Gibanica[1], Anders T. Johansson[2]
[1]Chalmers University of Technology, email: gibanica@student.chalmers.se
[2]Chalmers University of Technology, email: anders.t.johansson@chalmers.se

In Dynamic Substructuring, Component Mode Synthesis (CMS) methods such as the Craig-Bampton method [1] are usually employed to couple analytical models. With the recently renewed interest in experimental-analytical substructuring, methods requiring less information become competitive. Frequency Response Based methods [1] have usually been used to overcome the CMS shortcomings; these suffer from numerical ill-conditioning and introduce difficulties in the system identification of the coupled systems, however. A state-space based synthesis method developed by Sjövall and Abrahamsson [2] has been proposed to circumvent difficulties which exist with both CMS and Frequency Response based methods.

For researchers to have a common test bed and be able to share data, the Society for Experimental Mechanics (SEM) Substructuring Focus Group have initiated a research project in experimental dynamic substructuring using the Ampair 600 W wind turbine as a test bed. [3] Previously, the blade-to-blade spread of said test bed has been quantified [4] and a Finite Element (FE) model of the blades has been calibrated. [5]

The next step in the research project is to couple the wind turbine parts by dynamic substructuring. The blades are coupled to analytical models of their mounting brackets using both experimental and analytical models of the blades. The coupled systems are validated by vibration measurements of the blade and bracket systems. Further, three blades are coupled to the wind turbine nacelle, where both experimental and analytical models of the blades are used with FE models of the nacelle and brackets. These couplings are also validated with respect to measurements of the assembled structure.

The state-space based substructuring method [2] is focused on in this work. A quantative and qualitative comparison with the widely used CMS and Frequency Response based methods [1] is performed. It has been found that the state-space method is numerically unstable for higher order models, and an evaluation of these problems is performed. The state-space synthesis procedure has also been translated to the general framework presented by de Klerk et al. [1]

To obtain models from vibration data an automated order estimation method developed by Yaghoubi and Abrahamsson [6] is used which is based on the state-space subspace system identification method. The input is an initial high order model from which the method compares realisations of the same model and builds statistics of which modes to keep.

[1]Klerk, D. de, Rixen, D. J., Voormeeren, S. N., *General Framework for Dynamic Substructuring: History, Review and Classification of Techniques*, AIAA Journal, Volume 46 (5), (2008), 1169-1181.

[2]Sjövall, P., Abrahamsson T., *Component system identification and state-space model synthesis*, Mechanical Systems and Signal Processing, Volume 21 (7), (2007), 2697-2714.

[3]Mayes, R., *An Introduction to the SEM Substructures Focus Group Test Bed - The Ampair 600 Wind Turbine*, Conference Proceedings of the Society for Experimental Mechanics Series. 30th IMAC, A Conference on Structural Dynamics, Jacksonville, (2012), 61-70.

[4]Gibanica, M., Johansson A. T., Rahrovani, S., Khorsand, M., Abrahamsson, T., *Spread in modal data obtained from wind turbine blade testing*, Conference Proceedings of the Society for Experimental Mechanics Series. 31th IMAC, A Conference on Structural Dynamics, Garden Grove, (2013).

[5]Johansson, A. T., Lindholm, C-J., Khorsand, M., Abrahamsson, T., *Modeling and calibration of small-scale wind turbine blade*, Conference Proceedings of the Society for Experimental Mechanics Series. 31th IMAC, A Conference on Structural Dynamics, Garden Grove, (2013).

[6]Yaghoubi, V., Abrahamsson, T., *Automated Modal Analysis Based on Frequency Response Function Estimates*, Conference Proceedings of the Society for Experimental Mechanics Series. 30th IMAC, A Conference on Structural Dynamics, Jacksonville, (2012), 9-18.

Konstitutiv modellering III

torsdag 13/6 15:25-16:25

A remark on homogenization and virtual testing of micro-heterogeneous materials

Robin Andersson[1], Fredrik Larsson[2], Kenneth Runesson[3]
[1]Applied Mechanics, Chalmers, email: robin.andersson@chalmers.se
[2]Applied Mechanics, Chalmers, email: fredrik.larsson@chalmers.se
[3]Applied Mechanics, Chalmers, email: kenneth.runeson@chalmers.se

The macroscopic mechanical properties of an engineering material depend on its physical structure on different subscales. A nowadays common approach to account for the subscale heterogeneities in an explicit fashion is to deploy constitutive models for the individual constituents and use the the tools of homogenization within a Representative Volume Element (RVE). For a random substructure, the effective (or macroscopic) properties are obtained in theory only when the RVE-size approaches infinity. To be specific, we target the macroscale strain energy density by assuming the existence of a pseudo-elastic strain energy for the subscale response, which pertains to a time-increment for a standard dissipative material.

An obvious challenge is that it is not possible to construct an infinitely large RVE. In practice, therefore, the aim is rather to establish computable upper and lower bounds on the macroscale strain energy by analyzing sufficiently many finite-sized realizations. Classical bounds obtained from Dirichlet and Neumann boundary conditions, respectively, on the RVE are extended to computable statistical bounds with the pertinent confidence intervals[1]. The strategy, coined "virtual testing", employs a sufficiently large number of realizations within a finite-sized Statistical Volume Element (SVE). As it turns out, the computation of the lower bound presents a particular difficulty, and the result presented here seems to be novel.

For the numerical assessment, we consider an "academic" composite with stiff circular inclusions embedded in a more compliant matrix material. Total deformation plasticity with linear hardening is assumed to be sufficently accurate for each subscale constituent. It is then shown how the statistically guaranteed upper and lower bounds are affected by the size of the SVE for a fixed macroscopic strain. In addition, the upper and lower bounds for a sequence of increasing strain levels, for a fixed SVE-size, are used as "data" for the calibration of a macroscopic elastic-plastic constitutive model.

[1]R. Andersson. "On homogenization and virtual testing of nonlinear composites". *Master's thesis, Applied Mechanics, Chalmers University of Technology* (2011)

Micromechanical model for back-calculation of stiffness contribution from cellulose nanoelements to the overall properties of composites

Gabriella Josefsson[1], Fredrik Berthold[2], E. Kristofer Gamstedt[1]
[1] Uppsala University, Box 534, SE-751 21 Uppsala, Sweden, gabriella.josefsson@angstrom.uu.se
[2] Innventia AB, New Materials & Composites, Box 5604, SE-114 86 Stockholm, Sweden

Presently, many composites are based on non-renewable materials. However, the focus on environmental friendly materials has increased the interest for renewable and biodegradable composites. This project investigates such biodegradable composites made of a matrix of polylactic acid (PLA) mixed with different kinds of nanoscale cellulose components. Nanocomposites based on nanofibrillated cellulose (NFC), i.e. fibrils with lateral dimensions in the ~10 nm scale, have remarkable properties as compared with micro composites based on wood fibres with a diameter in the ~ 10 µm scale.[1] However, a major drawback for further investigation is based on lack of knowledge about the properties of the cellulose fibril and their effective contribution to the properties of the composite. This study examines the contribution from different types of fibril to the overall elastic properties of composites. The material used as reinforcement here was nanofibrillated cellulose (NFC), nanowhiskers and microcrystalline cellulose (MCC). For comparison, pure PLA matrix material was also tested. The composites were manufactured by hot press moulding and the final composites were cylindrical plates, from which dog-bone shaped samples were cut with a water jet. The stress-strain curves were characterized with a conventional tensile machine. Careful scanning electron microscopy showed that the NFC and nanowhiskers tend to agglomerate during the processing and that the fibrils form films that lie unidirectional in the plane of the composite. The over-all Young's modulus of the samples was used as input data in a mechanical model for back-calculation of the Young's modulus of the reinforcement fibrils. The used model was based on Mori-Tanaka assumption, three dimensional laminate theory and Hashin's micromechanical models for composite spheres assemblage. [2-4] An axial Young's modulus of around 40 was determined for all the reinforcing fibrils. The back-calculated axial elastic properties of the fibrils are roughly the same as predicted values from nano-structural characterization and theoretical estimates of crystalline and amorphous cellulose.[5] Literature values from direct mechanical testing of NFC are also in the same order of magnitude. It is suggested that the simplified approach may be used to rank different qualities of cellulose nanofibrils with regard to their stiffening contribution to the composite material.

[1] M. Henriksson, L. Berglund, P. Isaksson, T. Lindström and T. Nishino, *Biomacromolecules*, **9**, 1579-1585, 2008
[2] T. Mori, K. Tanaka, *Acta Metallurgica*, **21**, 571-574, 1973
[3] T. Joffre, E. L. G. Wernersson, A. Miettinen, C. L. Luengo Hendriks, E. K. Gamstedt, *Composites Science and Technology*, **74**, 52-59, 2013
[4] Z. Hashin, *Journal of Applied Mechanics*, **43**, 543-550, 1979
[5] G. Josefsson, B. S. Tanem, Y. Li, P. E. Vullum, E. K. Gamstedt, *Cellulose*, **20**, 761-770, 2013

Strömning i roterande maskiner II

torsdag 13/6 15:25-16:25

LES Prediction of Near Surge condition in a Centrifugal Compressor

Jyothish Kumar V[1], Bernhard Semlitsch[2], Mihai Mihaescu[3], Laszlo Fuchs[4]
[1]Post doc, Department of Mechanics and CCGEx, KTH Royal Institute of Technology, Sweden, Stockholm, 100 44, email: jyothish@mech.kth.se
[2]PhD student, *Linné FLOW Center* - Department of Mechanics, KTH Royal Institute of Technology, Sweden, Stockholm, 100 44, email: bernhard@mech.kth.se
[3]Docent, Department of Mechanics and CCGEx, KTH Royal Institute of Technology, Sweden, Stockholm, 100 44, email: mihai@mech.kth.se
[4]Professor, Department of Mechanics and CCGEx, KTH Royal Institute of Technology, Sweden, Stockholm, 100 44, email: lf@mech.kth.se

The research work aims at understanding the flow phenomena during the extreme operable conditions (near surge) of a centrifugal compressor. It is necessary to understand the flow structure details during the off-design operation of a centrifugal compressor namely the rotating stall and the surge condition. The compressor is always subjected to work within certain limit of the mass flow condition particularly the operation at peak efficiency is very important as it is very close to the surge line. The study of the flow structures during such low mass flow condition is necessary to find out methods that improve the stability or the flow operating regime of the compressor. In this study large-scale structures of the flow field are resolved using Implicit Large Eddy Simulation, which is a compromise in terms of accuracy between the two extremes of the turbulent methodologies namely the RANS and DNS method. Compressor taken for this simulation is a ported shroud compressor with vaneless diffuser, volute and exit pipe. Full 360° of the compressor geometry is taken for the simulation, which is different from the usual approach of considering a section of the blade passage. The transient sliding mesh technique is used for the mesh motion for an accurate prediction of the interaction between the impeller and the stationary diffuser.

From the analysis it is seen that the FFT of the data from the numerical probe in the diffuser reveals the presence of rotating stall. In the frequency spectrum (Fig. 1) a peak is observed at a frequency (550 Hz) of about half of the rotating frequency of the rotor and could be due to the rotating stall. Similar peak is observed at different locations within the diffuser region. Also, the study is further carried out with low mass flow condition at the compressor inlet with an objective to understand the flow details during the surge condition. Instantaneous velocity field of the flow structures during near surge and surge condition are shown in Fig. 2a and 2b. It shows that a high velocity region exist in the diffuser at 3'O clock position. At some instance of the flow field there occurs a low velocity region in the diffuser that results in stronger pressure gradient, which directs the flow towards the wheel inlet. So, the flow through the compressor can no longer be maintained and results in momentary flow reversal. Performance parameters (pressure ratio and efficiency) from the numerical values (near surge condition) are compared with the experimental data from Gutmark et al. in the Gas Dynamics and Propulsion Laboratory at the University of Cincinnati and are found to be in good agreement.

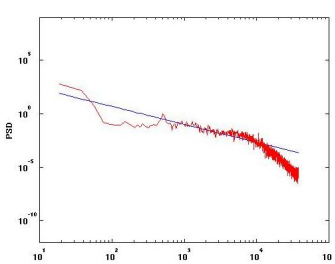

Figure 1: Frequency spectrum inside the diffuser at 12'O clock position

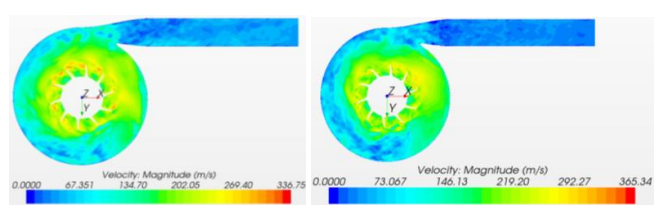

(a) (b)

Figure 2: Instantaneous Velocity Magnitude (a) Near surge condition (b) Surge Condition

Numerical investigation of different gaps in Couette rheometer

Naser Hamedi[1], Johan Revstedt[2], Fredrik Innings[3], Eva Tornberg[4]
[1]Lund University, email: naser.hamedi@energy.lth.se
[2] Lund University, email: johan.revstedt@energy.lth.se
[3]Tetrapak Processing System, email: Fredrik.innings@tetrapak.com
[4] Lund University, email: eva.tornberg@food.lth.se

The Couette rheometer is used to measure the rheological properties of Newtonian and non-Newtonian fluids. In this type of rheometer the fluid is placed between two concentric cylinders. The outer cylinder (the cup) is stationary and the inner one (the bob) is rotated. Normally, one strives to have a narrow gap between bob and cup so that the velocity distribution may be assumed to be linear. However, in certain applications one must use a wider gap. In this work, we focus on studying the effects of gap width on the flow in the rheometer and, hence, the measurement of the rheological properties. Simulation of three dimensional flow fields in the Couette rheometer for both Newtonian and non-Newtonian liquids are performed. Two gap sizes, small gap (1mm) and wide gap (7 mm), were used in the simulations. The results are compared to rheometer data with and without corrections for the gap width.

Carboxymethyl cellulose solution of 1% was selected as the studied fluid and the rheological behavior was estimated by power law fluid defined by equation (1). The fluid showed a shear thinning behavior in a limited range of shear rates.

$$\tau = 2.3\dot{\gamma}^{0.6} \qquad (1)$$

All rheological measurements were performed on a controlled shear stress rheometer (Kinux® rotational rheometer) at controlled temperature of 20°C.

Having a narrow gap, the wall slip has small effect on the shear flow and velocity profile is linear. Figure (1) shows the velocity profile along the wide gap for a Newtonian fluid which is obtained by CFD simulations. The deviation from ideal velocity profile is clearly showed in the figure. Moreover, there are some other error sources in the rheometer which belongs to the end effects and secondary flow effect and this study tries to formulate them.

In addition, the power law fluid was studied and the results were compared with the experimental outcomes for different gap sizes.

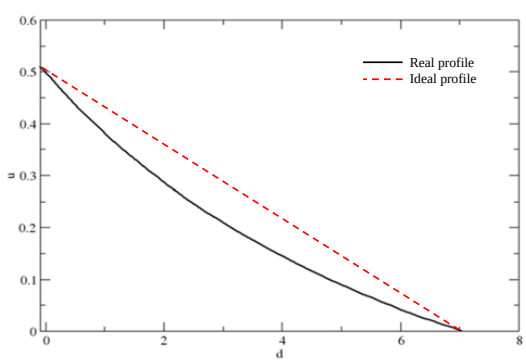

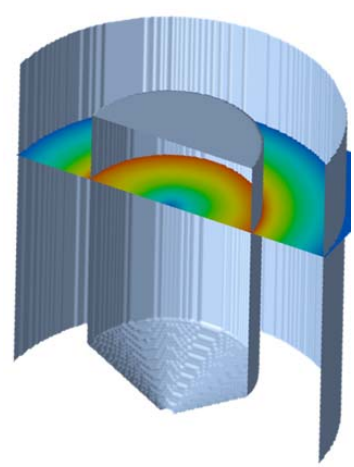

Figure 1: Velocity distribution in the wide gap rheometer for Newtonian fluid (a) velocity profile curve compared to the ideal profile (b) Contour of velocity profile in the middle sectional plane

Fluid mechanics of rotor stator mixers

Andreas Lindahl[1], Fredrik Innings[2], Hans Henrik[3]
[1]Tetra Pak Processing System - Master student, email: Andreas.Lindahl@tetrapak.com
[2] Tetra Pak Processing System, Research & Technology, email: Fredrik.Innings@tetrapak.com
[3]Tetra Pak Scanima, email: HansHenrik.Mortensen@tetrapak.com

Inline rotor-stator mixer are used in various different process industries; food, chemical and pharmaceutical to mention some. One of the uses for rotor-stator mixer is to perform liquid-liquid homogenization. The small gap between the rotor tip and surrounding stator in combination of high rotational speeds yields high magnitudes of what is considered as break-up forces. The flow inside the mixer is highly turbulent and extremely complex. There exist today a limited number of papers explaining the flow and turbulence fields inside the mixer. With the continuous increase of computational power comes the possibility of performing full scale CFD-simulation useful in understanding the flow field and mixing effects in rotor-stator mixers. A workflow consisting of verified methodology custom for inline mixer, reviewing the steps from a CAD-model to steady-state of a CFD-simulation would effectively decrease the time needed compared to if one start from naught every time.

In development of the workflow the steps in the methodology is tested on an existing inline mixer. This has allowed experimental measurements to serve as verification of result given from the simulations. When developing the methodology different mesh strategies, grid sizes and ways to model the rotors movement has been tested.

The final workflow consists of two methodologies in where a RANS model is used to model the turbulence. One methodology is aimed to obtain the mixers pump curve. The other methodology is developed in purpose to model the local flow variables i.e. model the flow field inside the mixer. Experimental measurements and grid convergence studies has been used in verifying the workflow. In Figure 1 pump curves from simulation and measurements are plotted together.

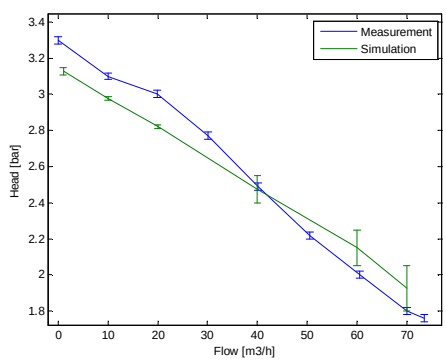

Figure 1: Pump curve for a mixer from simulation and experimental measurements.

Experimentella metoder IV

fredag 14/6 09:50-10:50

Experimental and Numerical fracture of cracks emanating from different types of flaws in thin polymer films

Nasir Mehmood[1,2], Eskil Andreasson [1, 2], Tan Mao[2], Sharon Kao-Walter [2,3]
[1]Tetra Pak Packaging Solutions, SE 221 86, Lund, Sweden *1,email:NasirX.Mehmood@tetrapak.com*
[2]Dept. of Mech. Eng. School of Eng., Blekinge Institute of Technology, SE 371 79, Karlskrona, Sweden
[3]Faculty of Mech. & El. Eng., Shanghai Second Polytechnic University, 201209, Shanghai, China

Abstract: Fracture mechanical Mode I tensile testing has been performed on an oriented polyproplyne film used in packaging industry. Physical Tensile testing for the continuum material has been performed to observe the material strength and to extract continuum material properties for numerical analysis. Fracture mechanical testing of different shaped notches is performed to observe the failure initiation in the material. A brittle-like failure was shown in the polypropylene film while the low density polyethylene presented a highly ductile behavior. A finite element method (FEM) strategy has been successfully developed to perform numerical analysis of polymer films. The developed FEM model gives an accurate and approximate method to compare and analyze the experimental and numerical results. The obtained results have shown a very fine similarity under theoretical, experimental and numerical analysis. Depending on crack geometry different shape crack effects showed the transferability of localized stresses at different points around the crack. Fracture surface and fracture process is analyzed using scanning electron microscope (SEM). Brittle failure with small deformation and presence of small voids and their coalescence has also been shown in SEM micrographs for LDPE material. The methods discussed will help classify different groups of materials and can be used as a predictive tool for the crack initiation and crack propagation path in packaging material, especially thin polymer films.

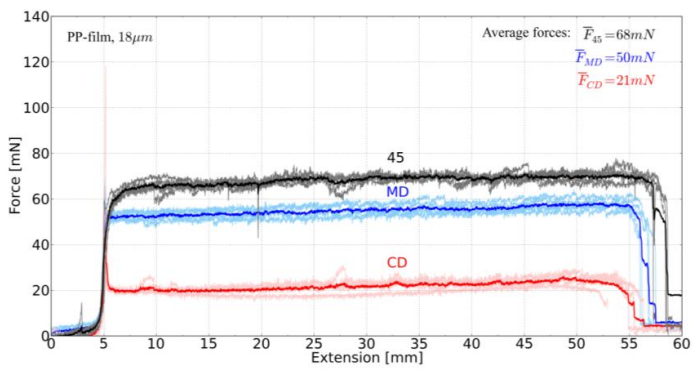

Figure 1. Trouser tear test in material direction 45°, MD and CD for PP-film, force vs. extension. Bold lines represent mean curves for each material direction.

Thermally-activated delayed failure in heterogeneous solids: An experimental model system

Stefan B. Lindström[1], Joris Sprakel[2]
[1]Mechanics, IEI, Linköping University, email: stefan.lindstroem@gmail.com
[2]Laboratory of Physical Chemistry and Colloid Science, Wageningen University.

Many pervasive construction materials, including wood, paper, plastics and concrete, exhibit creep when subjected to stresses below the yield stress. This can lead to catastrophic failure at prolonged, moderate loads. Remarkably, the creep response of these dissimilar materials shares at least two important features: First, the average time-to-failure decreases exponentially with the applied stress. This suggests that a stress-enhanced, thermally-activated process governs the creep. Secondly, the variability of the time-to-failure between samples is huge, which is usually attributed to their stochastic microstructures.

Owing to the strong molecular bonds between the constituents of typical construction materials, they creep slowly, and the time-to-failure under typical loading conditions can be very long, which is experimentally challenging. Therefore, we consider an experimental model system for studying the thermally-activated, delayed failure. Weakly attractive colloidal particles in suspension form a sample-spanning network with the low-frequency mechanical response of an elastic solid. This material is a statistically homogeneous, hierarchically structured solid, with two distinct length-scales: that of the particles and that of the filaments. The interaction potential between the particles is controlled in this system, so that the thermally-activated remodeling of the material operates on experimental time-scales.[1]

The creep response of the colloidal gel is investigated in simple shear, using a stress-controlled rheometer. For each constant shear stress σ, the shear strain γ is measured as a function of time. After an initial elastic deformation, the material deforms slowly at an essentially constant rate. After a time-delay τ, the material fails abruptly (Fig 1b). This delay time decreases exponentially with the applied stress (Fig 1c, squares). Moreover, if the gel is made anisotropic by applying a high rate pre-shear γ_{pre}, the delay time is reduced, and two regimes appear with different exponential factors (Fig 1c).

It is hypothesized that the initial creep is governed by a distributed, stochastic failure process, which preserves the statistical homogeneity of the sample. This slow process is followed by avalanching critical crack growth and failure. The time-to-failure is dominated by the initial process, which can be model using mean-field theory, by virtue of the assumed statistical homogeneity.[2] In this model, the stress-enhanced dissociation dynamics of individual particle bonds are related to the stochastic fracture of strands, which, in turn, are govern the delay time of the macroscopic failure.

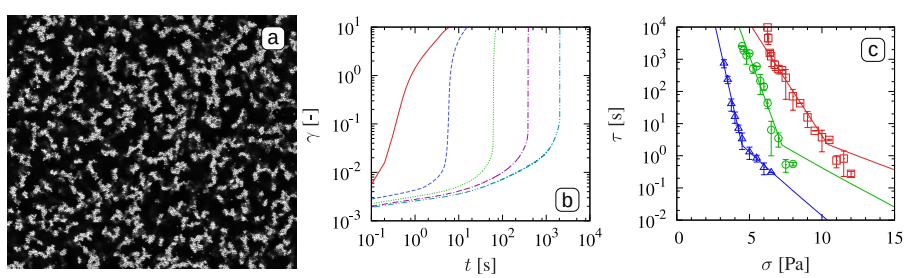

Figure 1: (a) Confocal micrograph of colloidal gel, with 12 vol%, 1.1 μm spherical particles; courtesy of T. Kodger. (b) Shear strain as function of time at a constant stress $\sigma = \{12; 10; 8; 7; 6.5\}$ Pa. (c) Delay time as a function of applied stress after a pre-shear $\gamma_{\text{pre}} = 0.0$ (squares), $\gamma_{\text{pre}} = 0.2$ (circles) and $\gamma_{\text{pre}} = 1.2$ (triangles). The lines represents the fitted model.

[1]Sprakel et al., *Phys. Rev. Lett.*, **106**, 248303, (2011)
[2]Lindström et al., *Soft Matter*, **8**, 3657, (2012)

Experimentell metod för stabila dragprov för tråd

Anders Biel[1], Michael Persson[1]
[1] Högskolan i Skövde, Box 408, 541 28 Skövde, email: anders.biel@his.se

Dragprov för tråd är ofta instabila. När tråden mjuknar frigörs elastisk lagrad energi och förloppet blir instabilt. Vanligtvis är det svårt att fånga den mjukande delen av materialbeteendet.

För lim finns en stabil experimentell metod[1,2] som använder en fläkprovstav, se Figur 1a. Metoden ger limskiktets hela spännings-deformationssamband. Under experimentet mäts kraft F, rotation av lastangreppspunkten, θ samt fläkdeformationen vid limskiktets början, w. Med vissa modifieringar är det möjligt att använda samma metod för trådexperiment. En motsvarighet till limskiktet skapas genom att med konstant delning linda balkarna med tråd, se Figur 1b. Runda stänger minskar spänningskoncentrationerna i tråden, se tvärsnittet i Figur 1c. För att metoden ska fungera krävs att tråden inte glider på balkarna. Tråden kan t.ex. fästas mot balkarna med lim. Idealt ska bara sträckan mellan x_1 och x_2 vara fri.

Ett experiment har utförts med ståltråd (diameter 0,7 mm) vilken är lindad runt två rundstänger (diameter på 20 mm), se Figur 2. Avståndet mellan varje trådvarv är 1,4 mm. I experimentet mäts kraften, F med dragprovningsmaskinens inbyggda lastcell, rotationen, θ via ett optiskt mätsystem och förlängningen av tråden, w med två LVDT-givare. De experimentella resultaten visar att tråden har en sträckgräns på 220 MPa. Detta stämmer väl överens med tidigare utförda experiment i enaxlig dragning.

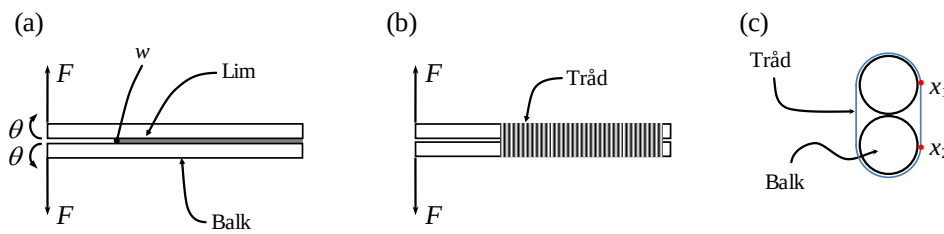

Figur 1: Provstav med lim (a), provstav med lindad tråd (b) och tvärsnitt med tråd (c).

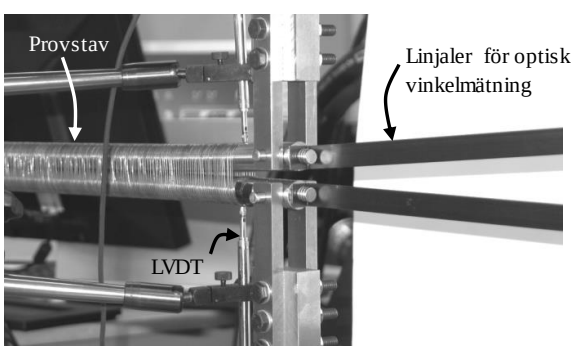

Figur 2: Experiment med ståltråd.

[1] Sørensen, B.F. *Acta. Mat.*, **50**, 1053, (2002)
[2] Andersson, T. and Stigh, U. *Int J Solid Struct.*, **41**, 413, (2004)

Dynamik II

fredag 14/6 09:50-10:50

The granite rock fragmentation in percussive drilling

M. Saadati[1,2], P.L. Larsson[1], K. Weddfelt[2]
[1]Royal Institute of Technology (KTH), Stockholm, Sweden (msaadati@kth.se and plla@kth.se)
[2]Atlas Copco, Örebro, Sweden

The percussive drilling method has been used for decades in the mining industry. A sound understanding of the rock fragmentation mechanism at impact helps to increase the efficiency of the drilling process. A lot of attempts have been made to numerically model the rock fracture in this situation, but due to the very complex behavior of rock material from one side, and the complicated dynamic interaction of bit-rock from another side, there is still a lack of a comprehensive model that covers the whole process.

The aim of this study is to numerically model the fracture system in percussive drilling. Due to the complex behavior of rock material, a continuum approach is employed. The KST (Krieg, Swenson and Taylor)[1] plasticity model is coupled with the DFH (Denoual, Forquin and Hild)[2] anisotropic damage model. The radius of the yield surface is a quadratic function of the mean pressure in principal stress space. The DFH damage model consists of a probabilistic approach to deal with the dynamic fragmentation process of brittle material due to the impact loading.

Granite material is investigated in this work and the experiments are performed to characterize the material behavior. Quasi-static compression and tension, three point bending and also spalling tests are performed in order to calibrate the KST and DFH model parameters for granite. Also the Edge-On Impact test is performed to investigate the fracture pattern in granite due to the impact of a projectile. A quantitative information on the location and evolution of damage can be obtained from the later experiment.

The equation of motion is discretized using the FE approach and the explicit time integration method is employed. Abaqus FE software is used in this study and the problem is modeled in 3D. The percussive drilling process is simplified so that one spherical button is taken and only the first impact is simulated. The stress wave in the drill rod is transferred to the rock material and the bit-rock interaction is modeled using contact mechanics. The area beneath the indenter, with high value of confining pressure, is exposed to inelastic deformation mainly due to compressive stresses. In the area far from the indenter, different types of tensile cracks including radial and side cracks are captured where the latest is considered as the most responsible for the material removal in the percussive drilling process (see Figure 1).

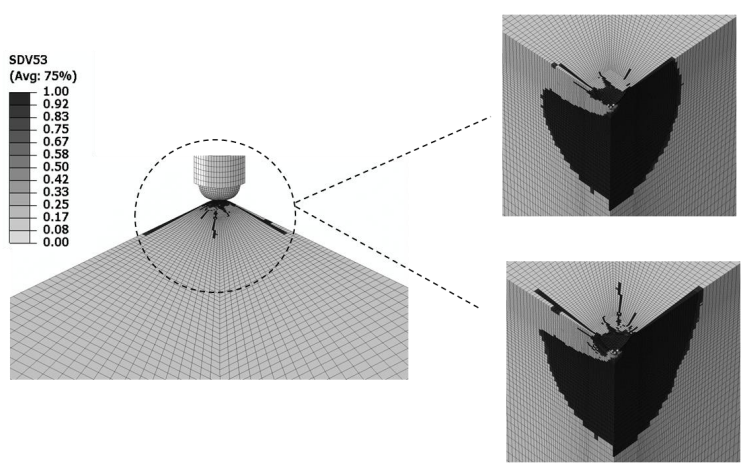

Figure 1: Damage variable from quarter-symmetry model of one button in percussive drilling with 400000 elements at the end of loading (a) and at the end of un-loading (b).

[1] Swenson D V, Taylor L M, A Finite Element Model for The Analysis of Tailored Pulse Simulation of Boreholes, *International Journal for Numerical and Analytical Methods in Geomechanics* 1983;7:469-484.
[2] Forquin P, Hild F, A Probabilistic Damage Model of the Dynamic Fragmentation Process in Brittle Materials, *Advances in Applied Mechanics* 2010;44:1-72.

Comparison of contact dynamics in bladed Jeffcott rotors

Florian Thiery, Jan-Olov Aidanpää
Luleå University of Technology
Division of Mechanics of Solid Materials
emails: florian.thiery@ltu.se , joa@ltu.se

Contacts in rotordynamics are mainly described as rubbing cylinders between rotors and stators. However, blade contacts can also appear in typical machines such as hydropower rotors or aircraft rotors, which can lead to catastrophes due to the high nonlinearity of the system.

Three models based on a Jeffcott (midspan) rotor are developed to study the effect of different parameters. The first model with three blades (see Figure 1a) describes the contact between a blade and the fixed stator with the non-linear beam deformation theory. Contacts only occur due to an initial eccentricity y_0 of the shaft. The tangential friction force is described with Coulomb friction, and the axial and tangential stiffness of the beam is fitted with a polynomial of the force as function of the displacement. The second model has the same general characteristics, excepted that a radial restoring force from a non-fixed stator is applied to the rotor with rigid blades. The third model has the same properties as the second one, excepted that the rotor is discretized by finite elements and an external force induced by mass unbalance is included.

The first model shows that all types of motion can appear in this type of non-smooth impact systems. From bifurcation diagrams, chaotic motions could be seen at integer frequencies of 1/3 with alternation of periodic motions over the whole frequency range. This model has the advantage of giving insight of the contact forces, but simulations are more time-consuming. The second model gives similar results in terms of bifurcations diagrams, but it lacks the information about forces in the system. However, the simplicity of the model allows us to perform a two-dimensional parametric study by calculating the Maximum Lyapunov Exponent, which identifies chaotic regions (in black) from periodic regions (in white) in Figure 1b. The 2-dimensional Lyapunov graph is a great tool to predict the dynamics of nonlinear systems. Moreover, it was shown that damping has a stabilizing effect, while the initial misalignment value influences differently the results over certain ranges. The finite element model still gives the same characteristic regions with misalignment only. The addition of a small unbalance force to the system affects slightly the dynamic behaviour under a threshold value. To conclude, each model give similarities in the results and has advantages and drawbacks that should be taken in consideration depending on which type of study is performed.

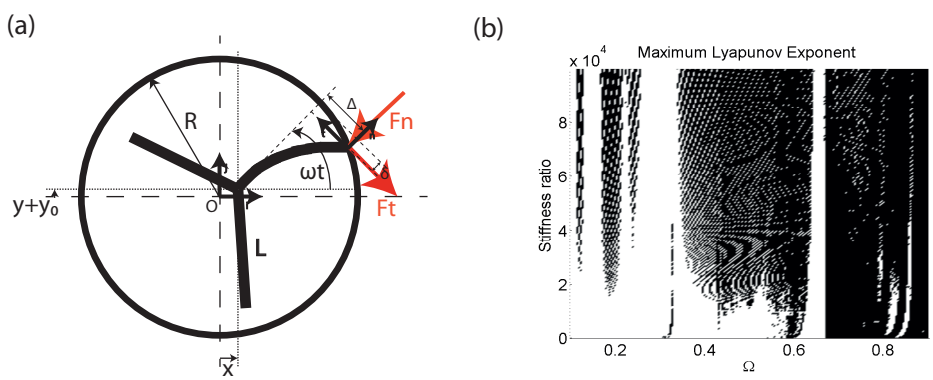

Figure 1: (a) Model of a bladed Jeffcott rotor (b) Maximum Lyapunov Exponent for the simplified bladed Jeffcott rotor model as function of the stator-to-rotor stiffness ratio and normalized rotating speed

Wavelet transform of torsional vibrations of a Kaplan turbine

Ida Jansson[1] and Jan-Olov Aidanpää[2]
[1]Division of Fluid Mechanics, email: Ida.Jansson@ltu.se
[2]Division of Mechanics of Solid Materials, email: Jan-Olov.Aidanpaa@ltu.se
Department of Engineering Sciences and Mathematics, Luleå University of Technology

In conventional hydropower, the power that drives the water's cycle on earth is transformed to electrical power on the grid by means of a rotating shaft. With the release of power it always follows a risk of undesired vibrations and pressure pulsations that not only reduce the efficiency but also put the health of the machine at stake. The power companies struggle to benefit from selling regulation power without loosing the gain in terms of increased maintenance cost and reduced life length of the machine. It is hence in the plant owner's interest to make estimates of the increased stress levels a machine experience during a start-up and closure of the machine. This work discusses the unsteady loads a Kaplan turbine experiences during a normal start-up of the machine based on strain gage measurements of the torsion and axial strain of the rotating axle. We visualize the time variations of signals as a distribution of energy intensity in the time-frequency plane by applying a complex Morlet wavelet transform. Before the angle of the runner blades is adjusted so the runner functions properly, both the torsion and axial strain of the shaft reveal broadbanded noise in the time-frequency plane. The axial strain and torsion of the shaft function as mechanical filters of the unsteady load acting on the runner. The impulse response of the filters corresponds to by free damped mechanical vibrations. The time-frequency plane of the torsion signal reveals a region with bursts of concentration of energy intensity close to the eigenfrequency of the twisting motion of the shaft. This concentration of energy is also visible in the time-frequency plane of the signal of the straining motion of the shaft. This is most likely forced axial vibrations. The twisting motion of the shaft implies that the speed of the hydrofoils oscillates and so will the hydraulic load that has a component in the axial direction. The same kind of reasoning also applies to a heaving motion. If the hydrofoils move in the axial direction the angle of attack must change and so the lift and drag force acting on the hydrofoil. If those bursts of energy intensity in the time-freqency planes are free damped torsional vibrations excited by random noise in the turbine, we can conclude that most of them do not survive longer than a second. When the turbine approaches its region of design operation, less random noise is present and the intensified region close to the torsional eigenfrequency disappears. The damping could most probably be attributed to the viscous damping of the water. The wavelet transform of the axial strain reveals frequencies as multiplies of the rotatational frequency of the shaft with the highest intensity being twice the rotational frequency. The intensity of the frequencies that depend on the shaft speed does not seem to change when the broad-banded noise disappears. speed-dependent frequencies In conclusion, this work shows how time-frequency analysis of strain gage measurements can be used as a tool to reveal the stress levels a machine experience during regulation.

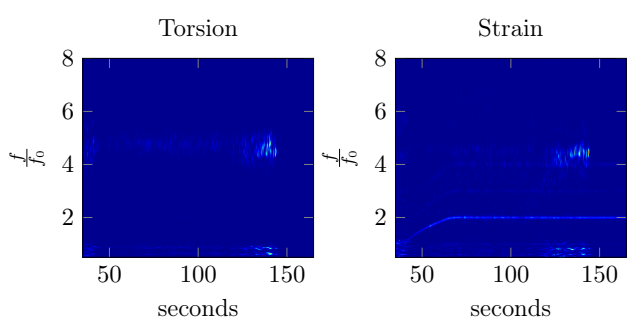

Figur 1: Time-frequency analysis of a shaft with nominal speed $f_0 = 10$ Hz.

Förbränning I

fredag 14/6 09:50-10:50

Large eddy simulations and dynamic mode decomposition of flame/flow interaction in a lean premixed low swirl stabilized flame

Henning Carlsson[1], Christian Carlsson[1], Laszlo Fuchs[1], Xue-Song Bai[1]
[1]Division of Fluid Mechanics, Lund University 22100 Lund, email: henning.carlsson@energy.lth.se

Swirl stabilized combustion in stationary gas turbines has become a popular to meet the more stringent legislation towards pollutants. Flame temperature control through lean premixed fuel/air mixtures can give ultra low NO_x emissions and still sustain a high efficiency; however, the unstable nature of swirl stabilized premixed flames will cause sensitivity to helical structures and processing vortex core (PVC), which can cause noise and structural damage[1].

Towards the understanding of such sensitivity, numerical studies are performed on the effect of flame/flow interaction at large and medium scales and its impact on flame stabilization in a lean premixed low swirl stabilized methane/air flame. The numerical simulations are based on a large eddy simulation (LES) approach with a two-scalar flamelet model with mixture fraction and level-set G-function to account respectively for stratification and flame front tracking. Distinctive frequencies associated with the flame stabilization process are identified from point data of LES in the outer and inner shear layers of the burner induced flow field. To understand the spatial structures related to the observed frequencies, dynamic mode decomposition[2] (DMD) analysis is performed.

Based on the analyses of LES data, frequency specific coherent flow structures are extracted along with associated flame structures. Real and imaginary parts of two combined flow/flame DMD modes are shown in Figure 1. The inner shear layer generated vorticity is linked to recurring frequency specific coherent structures of both flow and flame and thereby is a contribution to the flame stabilization in the outer regions of the flow quantified.

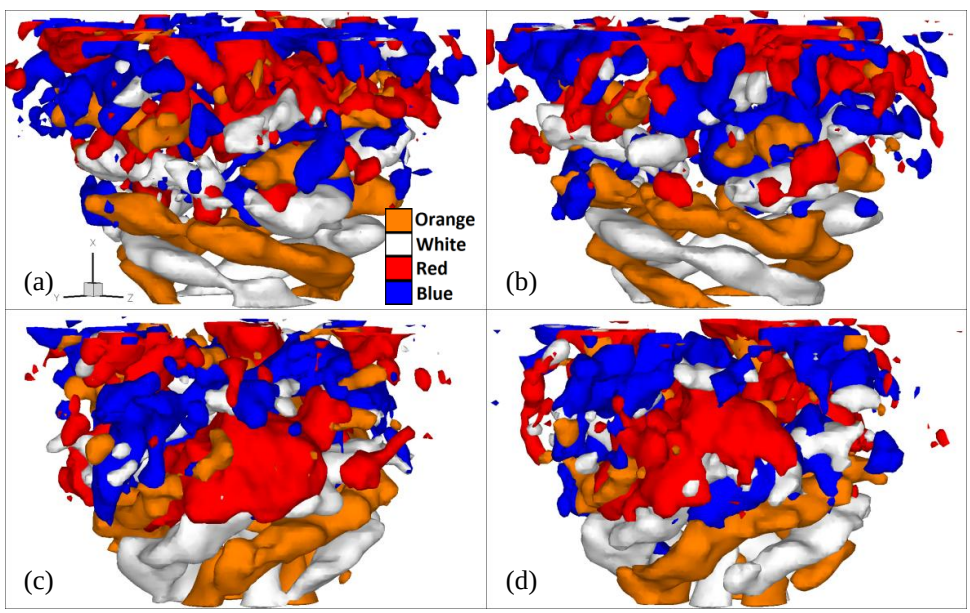

Figure 1: Real (a) and imaginary (b) parts of a DMD mode of frequency f = 210 Hz and real (c) and imaginary (d) parts of a DMD mode of frequency f = 175 Hz. Orange and white isocontours denotes positive and negative values of radial velocity components, respectively, and red and blue isocontours corresponds to positive and negative values of flame coordinate, respectively.

[1] Gupta, Lilley and Syred, *Swirl Flows*, Abacus Press, 1984
[2] Schmid, *J. Fluid Mech.* **656**, 5-28, (2010)

Comprehensive study on combustion of single biomass particle

Hesameddin Fatehi[1], Xue-Song Bai[1]
[1] Division of Fluid Mechanics, Lund University, Sweden, hesaeddin.fatehi@energy.lth.se

As a sustainable and renewable source of energy, biomass has a great potential in generating heat and power while reducing greenhouse gases. Utilization of biomass energy can be done in different systems, among which combustion is one of the most common approaches of utilization of biomass. Understanding the processes taking place during thermochemical conversion of biomass is important for modeling biomass combustion systems. Using coarser biomass particles in such reactors is preferred due to economical and practical reasons such as; lower energy cost for feeding and more favorable in terms of transportation and storage. On the other hand, the bigger the particle is the more important the intra particle heat and mass transfer become. To have a better understanding and efficient design of biomass reactors suitable for large particle, numerical simulation of single particle combustion is a valuable tool which can provide valuable insight of the reactor design.

When the fresh wet biomass particle is exposed to hot environment, drying will take place after the temperature of the fuel particle reaches 100°C. Thereafter, pyrolysis takes place. This process is usually an endothermic process which depending on temperature, heating rate, the composition of fuel, particle size and moisture content, can produce different pyrolysis products. The volatiles produced from particle pyrolysis can further react depending on the amount of oxygen or other gasification agents available and the residence time of the gases in the reactor. Char combustion and gasification is a surface reaction process that typically cannot start before the completion of pyrolysis due to the gas flow out of particle that prevents oxygen from reaching the char surface. All these processes along with the particle shrinkage is presented in Figure 1.

A comprehensive study of combustion of single particle of biomass is conducted. Various sub-processes involved in thermochemical conversion of biomass are described and mathematical modeling of these processes is presented. Biomass sources are usually high in moisture content. Different drying models were evaluated to find the simplest model which is able to predict the drying behavior of biomass. The comprehensive model was validated compared to different experimental data. This model can act as a bench mark for development of simplified models which are more suitable for CFD simulations of real combustors.

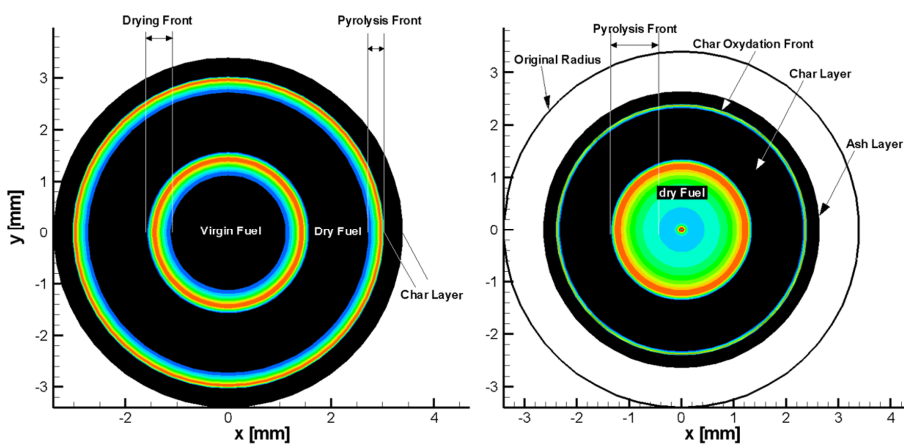

Figure 1: 2-D representation of particle; overlapping different process rate at two different times during particle burn out

Flame Modelling with Finite Rate Chemistry and Implicit Large Eddy Simulations

Erdzan Hodzic[1], Emma Alenius[1], Christophe Duwig[1], Robert-Zoltán Szász[1], Laszlo Fuchs[1]
[1]Division of Fluid Mechanics, Department of Energy Sciences, email: Erdzan.Hodzic@energy.lth.se

In order to reduce the emissions from industrial combustors they are operated under fuel lean premixed conditions, near the limit of flame extinction. Despite 60 years of research, simulations of turbulent flames under these conditions are still a considerable challenge. The reason is that they consist of a multi-scale non-linear problem, due to the interaction between turbulent structures and chemical reactions.

Several different combustion models exist, but they are partially valid in different combustion regimes, and with different flow modelling approaches. Here we focus on finite rate chemistry models. In these models a system of reaction equations, based on the Arrhenius expression, is solved to get the heat release, as well as the production and consumption of different species. However, the complexity of this can be varied, by using only one or up to hundreds of reactions.

With the aim of studying flame dynamics, the flow modelling approach used is large eddy simulations (LES). The idea with LES is to explicitly simulate large-scale energetic structures in the flow, while small scales are modelled. Combustion takes place at relatively small scales, and hence traditionally a model is added to take into account that the combustion is not properly resolved. However, as the available computational power increases, it is possible to resolve more and more of the combustion process adequately. Thus, under certain conditions it is today possible to avoid using an extra model for the combustion in LES, a method referred to as implicit LES (ILES). Not having to use a model reduces the total computational cost while, compared to other models, a more restrictive assumption on validity of the approach is adopted.

ILES for combustion is valid when the mixing of species and temperature can be considered perfect within one grid cell. With an adequate grid resolution this can be achieved in the so called distributed combustion regime, where the chemical time-scale is larger than the time-scale of the smallest resolved turbulent scales. This happens in very lean flames, close to lean blow off, with intense turbulent fluctuations, since the former decreases the chemical time-scale and the latter increases the turbulent time-scales.

The described approach is exemplified with the bluff-body stabilized flame and a partially premixed swirl stabilized flame illustrated in Fig. 1 which will be presented at the conference.

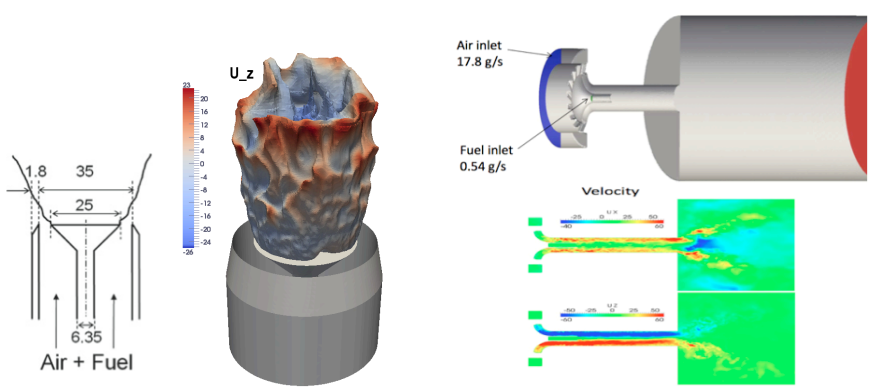

Figure 1: To the left is a cross-section of the burner [mm] and an iso-surface of temperature at 1500K, coloured by axial velocity. To the right, a partially premixed swirl stabilized flame showing the geometry on top and velocity field underneath.

Konstitutiv modellering IV

fredag 14/6 11:10-12:10

On the modeling of grain size-dependent hardening in polycrystalline metals

Magnus Ekh[1], Swantje Bargmann[1,2,3]
[1]Division of Material and Computational Mechanics, Department of Applied Mechanics, Chalmers University of Technology, email: magnus.ekh@chalmers.se
[2]Institute of Continuum Mechanics and Material Mechanics, Hamburg University of Technology, email: swantje.bargmann@tu-harburg.de
[3]Institute of Materials Research, Materials Mechanics, Helmholtz-Zentrum Geesthacht

It is well-known that the macroscopic behavior of a polycrystalline material is influenced by the size and morphology of the grains, the volume fraction of different phases, and the subgrain processes, for example. The size effect in metals is known as the Hall-Petch effect and is one of the important unresolved issues in computational material modeling. Standard crystal plasticity models cannot predict size dependent effects. Models including plastic strain gradients have been introduced in order to overcome this drawback[1]. This contribution discusses the computational modeling of size dependence using microstructure models for polycrystals.

The purpose of this work is to discuss issues on the formulation and numerics of gradient crystal plasticity[2][3]. The microstructure is taken into account when modeling macroscopic stress-strain response. This is done within the context of computational mesoscale analysis of a Representative Volume Element (RVE). The grain interaction within the RVE is resolved using finite elements. The formulation results in a boundary value problem with the displacements and the gradient hardening (internal) variables in the slip system being the unknowns, i.e. the degrees of freedom. The system of equations is highly coupled. More specifically, a domain decomposition is applied where each grain constitutes a subdomain. Particular issues that will be addressed are grain boundary conditions[4] and thermomechanical coupling[5] . Numerical examples for polycrystals are presented.

[1]Gurtin, *J. Mech. Phys. Solids*, **52**, 2545, (2004)
[2]Ekh et al, *Int. J. Num. Meth. Eng.* **72**, 197, (2007)
[3]Bargmann et al, *Phil. Magazine*, **90**, 1263, (2010)
[4]Ekh et al, *Acta Mechanica*, **218**, 103, (2011)
[5]Bargmann and Ekh, *Int. J. Solids Struct.*, **50**, 899 (2013)

Modeling of recrystallization

Håkan Hallberg
Division of Solid Mechanics, Lund University, Sweden, email: hakan.hallberg@solid.lth.se

The macroscopic behavior of metallic materials is to a large extent controlled by the size and shape of the grains that constitute the material microstructure. The grain structure will influence macroscopic material properties such as strength and ductility. Being able to predict and control the morphology of this microstructure during materials processing allows the development of tailored material properties, optimized products and more efficient production processes. Understanding and manipulating the material microstructure are key components in the production of functionally graded materials. Grain size control is also of primary interest in the development of high strength steels, being materials of importance for example in the automotive and aircraft industries where a well-chosen compromise between strength and weight is of great importance.

Recrystallization is the main mechanism, controlling the evolution of grain microstructures. This process is generally defined as the formation of a new grain structure in a plastically deformed material. The recrystallization occurs through the formation and migration of high-angle boundaries. Boundary migration, and hence also recrystallization, is driven by reduction of the stored cold work-energy and minimization of grain boundary surface energy.

Recognizing that grain refinement through recrystallization can be achieved by exposing the material to severe plastic deformation (SPD), several processes such as equal channel angular pressing (ECAP) and asymmetric rolling (ASR) have been devised. In order to optimize such processes and to gain further insight into the mechanics of recrystallization, physically motivated and computationally efficient simulation models are vital. Simulations can be used to predict the microstructure evolution, e.g. in terms of grain size, influence of second-phase particles and relative grain misorientation, during plastic deformation and also to indicate suitable settings of process parameters such as deformation magnitude, deformation rate and processing temperature.

The existence and importance of recrystallization as a metallurgical process has been recognized for many years and simulation models of the process continue to evolve and new techniques continuously emerge. The present contribution gives a summary of the research related to recrystallization modeling, conducted at the Division of Solid Mechanics at Lund University. This ongoing work involves continuum-scale, internal variable, models of SPD processes such as ECAP and ASR as well as mesoscale models of grain structure evolution based on cellular automata, Monte Carlo Potts models and level set formulations. The formulation of level set models of recrystallization will be given special attention.

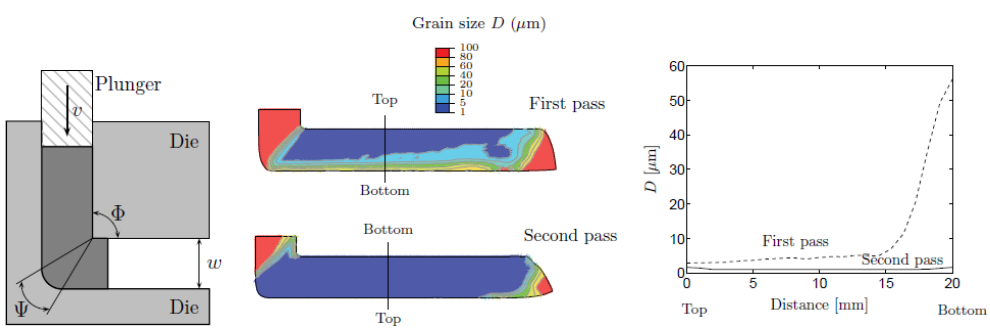

Figure 1: *Left*: Schematic illustration of an ECAP setup. *Right*: Distribution of grain size in the processed specimen after one and two passes through the die, respectively.

Unstable Formation of Hydride Precipitates

Wureguli Reheman[1], Per Ståhle[2]
[1]Div. of Solid Mechanics, Lund Institute of Technology, wureguli.reheman@solid.lth.se
[2]Div. of Solid Mechanics, Lund Institute of Technology, per.stahle@solid.lth.se

Hydrogen embrittlement has been a core study of the research concerning formation of hydride in metals. Hydrogen migrates through the metal lattice to regions of high tensile hydrostatic stress. When the hydrogen concentration in the matrix exceeds a terminal solid solubility, it starts to form a hydride. In the metals the precipitation of small and local amounts of hydrides strongly affect the local mechanical properties and the over all integrity of the entire structure.

The objective of the present investigation is understand the shape of the hydride as it forms at the tip of a crack. The hydrogen is known to accumulate at the crack tip where the hydrostatic stress is larger than in the rest of the body. This process is supposed to be slow compared with the growth of the hydride that is assumed to take place in a quasi static manner. The swelling of the hydride will affect the distribution of the hydrostatic stress. In this pilot study a finite element study is performed in which time is incremented. The time increments are such that only one element integration point transforms to a hydride in each time increment. The result is that for each unit that transforms, the hydrostatic stress in the surrounding material decrease and this creates an on-off situation even if the element size is chosen to be very small.

To understand this better an analytical study of the stability of the hydride matrix interface is performed. The analysis utilizes a superposition that put the interface boundary value problem into one for a free surface. The Cerruti solution is then used to compute the perturbed stress field in the body with a wavy surface. It is shown that the flat interface is unstable and that perturbations will grow. The growth rate is faster for shorter wavelengths which imply that an initially flat interface will break up in smaller and smaller fragments.

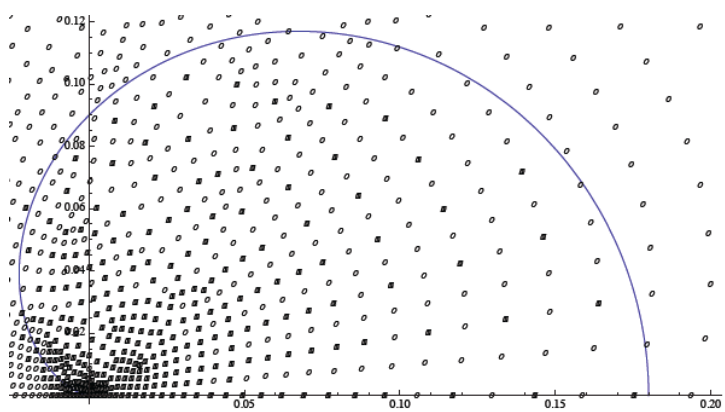

Figure 1: Distribution of hydride around crack tip with expansion coefficient is two.

Numeriska metoder III

fredag 13/6 11:10-12:10

Numerical modeling and analysis of dynamic crack propagation in rubber

Elsiddig Elmukashfi[1,a], Martin Kroon[1,b]

[1]Department of Solid Mechanics, Royal Institute of Technology (KTH), Stockholm
[a] elsiddig@kth.se, [b]martin@hallf.kth.se

Elastomers are important engineering materials that have contributed to the different technical developments and applications since the 19th century. The study of crack growth mechanics for elastomers is of great importance to produce reliable products and therefore costly failures can be prevented. On the other hand, it is fundamental in some applications such as adhesion technology, elastomers wear, etc.

In the present work, dynamic crack propagation in rubber is investigated. Both theoretical and computational frameworks are presented. In the theoretical framework, a propagating crack in an infinite body is studied wherein the fracture separation process is presumed to be described by a cohesive zone model and the bulk behavior is assumed to be determined by viscoelasticity theory. Hence, the microstructural failure mechanisms and the bulk deformations are directly related. The region around the crack tip vicinity is then investigated using the viscoelasticity theory revealing that a viscous dissipation might take place. In the computational framework, a nonlinear finite element analysis using cohesive zone modeling approach is used. The problem of a suddenly initiated crack at the center of stretched sheet is studied under plane stress conditions. The continuum is assumed to be characterized by finite-viscoelasticity theory and the fracture separation process is modeled using a cohesive zone model. Rate-independent and rate-dependent cohesive laws are applied using such that the later accounts for the viscous dissipation at the crack tip vicinity. A Kelvin-Voigt element is used to describe the cohesive behavior. The spring represents the rate-independent behavior and is described by a bilinear law and the dashpot with a constant viscosity is adopted to model the rate dependency. A nonlinear finite element analysis using a mixed explicit-implicit integration is applied. The computational framework is able to model and predict the different contributions to the fracture energy, i.e. surface energy, viscoelastic dissipation (in the bulk surrounding the crack tip and at vicinity of the crack tip) and inertia effects.

The numerical model is able to predict the dynamic crack growth and a steadily propagating crack is resulted. In order to study the fracture process, the steady crack propagation velocity is evaluated and compared with experimental data for different combinations of separation work per unit area, strength and viscosity of the cohesive zone. The estimated total work of fracture shows an excellent agreement with the effective fracture energy reported in the literature. The results show that the surface energy, strength and viscosity vary with the crack speed. The contribution from viscoelastic dissipation in the bulk material to the total work of fracture is found to be negligible. Further, an additional dissipation takes place in the bulk material surrounding the crack tip and it might be related to the cavitation and crystallization processes. Moreover, the fracture-related processes, i.e. creation of new surfaces, cavitation and crystallization; contribute to the total work of fracture in a contradictory manner.

Thermo-mechanical analysis of crack propagation in amorphous polymers

Martin Kroon[1]
[1]Kungliga tekniska högskolan, Stockholm, email: martinkr@kth.se

Polymers constitute an important class of engineering materials, and the fracture mechanics properties of polymers are of great interest in such applications as tires, seals, and packages. Just like in metals, dissipative processes in polymers play a significant role for the fracture toughness of the material. Over the last decades, the theoretical understanding of the fracture processes in metals has increased significantly. In comparison, the theoretical study of fracture in polymers is clearly less developed.

The present work consists in a computational study, where the dissipation at a crack tip, propagating under steady-state conditions in an amorphous polymer, is analysed. Dissipation at different crack speeds and different loading conditions is considered. The viscosity of polymers is strongly temperature-dependent, and a full analysis of the problem at hand therefore requires a coupled thermo-mechanical analysis.

Hence, two sets of equations need to be solved simultaneously, i.e. the equations of equilibrium and the equations of heat transfer, where both sets of equations depend on the displacement field and the temperature field. The WLF (Williams, Landel, Ferry) relation for the time-temperature equivalence of polymers is adopted for modelling the influence of temperature on the viscosity of the material. Weak forms of the two sets of equations are derived, and the coupled problem is solved by use of the finite element method. The outcome of the analysis consists for example in the displacement, stress, and temperature fields, and also the associated values of the *J*-integral.

A non-affine micro-sphere formulation for electroactive polymers

Sara Thylander[1], Andreas Menzel[1,2], Matti Ristinmaa[1]
[1]Lund University, Div. of Solid Mechanics, email: sara.thylander@solid.lth.se
[2]TU Dortmund, Inst. of Mechanics

With the capability to convert electrical energy into mechanical energy together with low cost and weight make electroactive polymers (EAP) a suitable candidate for new and more advanced applications every day. Along with increased industrial applications follows the need for reliable simulation techniques. Advanced modelling of EAP and predictive simulation methods constitutes an active area of interdisciplinary research. In this work, an electromechanical framework for the modelling and simulation of EAP is established which enables the use of micro-mechanically based models of the polymer chains. The statistics-based one-dimensional chain models is extended to the three-dimensional continuum level by means of a so-called micro-sphere.

A previously established micro-sphere formulation[1] is further extended to include non-affine kinematics, constraints on the movements of the chains in the polymer network and a new form of the purely electric part of the free energy function to account for saturation effects in the polarisation.

To show that the chosen form of energy function together with the extended electromechanically coupled micro-sphere framework captures the essential behaviour of non-linear electroelasticity, a numerical example of homogeneous deformation is discussed. Related simulation results are shown in Figure 1.

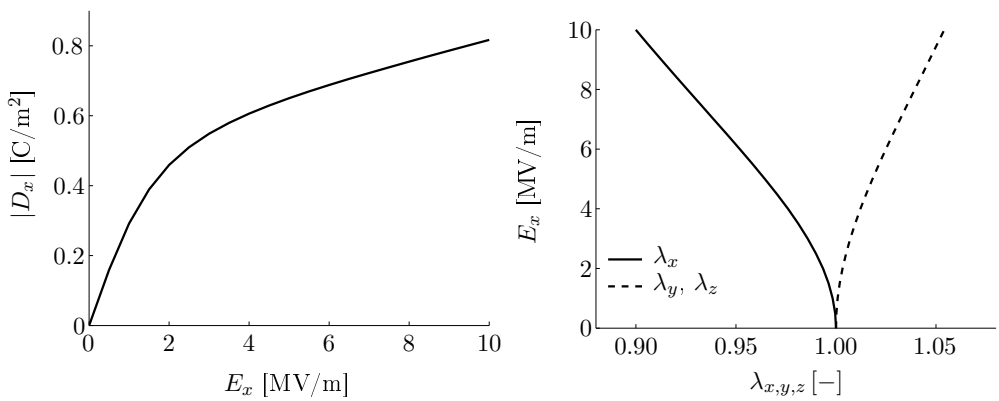

Figure 1: Homogeneous deformation under tension: (left) longitudinal electric field E_x plotted vs. absolute value of longitudinal electric displacement D_x and (rigth) longitudinal electric field E_x plotted vs. longitudinal stretch λ_x and transverse stretches λ_y and λ_z.

[1]Thylander, Menzel and Ristinmaa, *Smart Mater. Struct.*, **21**, 094008, (2012)

Förbränning II

fredag 14/6 11:10-12:10

The Effect of Aluminium Particle Combustion on the Afterburning during a TNT Blast

Ekaterina Fedina[1]
[1]Defence & Security Systems and Technology, Swedish Defence Research Agency – FOI, SE–147 25 Tumba, Stockholm, Sweden, email: ekaterina.fedina@foi.se

The latest trend in explosives technology is the addition of metals, e.g. aluminium particles, to the explosive charges, which is intended to increase the performance in terms of an increase of the amount of energy released during the explosion. When reactive particles are added to explosions, the detonation products heat up the particles and subsequently ignite them. Once the particles reach the ignition temperature, they start to burn and thereby reacting with the detonation products. Performance evaluation of an explosive compound requires assessment of the afterburning properties of the explosive charge and thus this study focuses on the effect that the inclusion of solid aluminium particles to a TNT charge has on the afterburning of the detonation products. The presented work evaluates the flow, afterburning and mixing resulting from simulated pure TNT and TNT/Aluminium charge explosions at 0.5 m height of blast. The simulations are conducted using Large Eddy Simulation (LES) with a Partially Stirred Reactor (PaSR) combustion model. The two–phase afterburning model contains a two–way coupling between the solid and gas phases, including interaction terms for mass, momentum and energy, together with TNT and aluminium reduced kinetic mechanisms and particle–particle collisions. The preliminary simulation results indicate that the presence of particles causes additional Rayleigh–Taylor instabilities, thus further enhancing the mixing and afterburning. The total heat release is also increased due to exothermic aluminium–oxygen reactions.

On Auto-Ignition in Heavy Duty Diesel engines, a Large Eddy Simulation Study

Rickard Solsjö[1], Mehdi Jangi[1], Öivind Andersson[2], Xue-Song Bai[1]

[1]Division of Fluid Mechanics, Lund University, Rickard.Solsjo@energy.lth.se
[1]Division of Internal Combustion Engines, Lund University

Auto-ignition of fuel jets occur at the most beneficial condition and is a combination of mixture composition, mixture temperature and residence time. In combustion test rigs, e.g. constant volume chambers, conditions similar to engine environments are manufactured to perform parametric inquires on single fuel sprays. In internal combustion engines however, there are complex flow patterns that may alter the natural behavior of a reacting jet. Such flow patterns may be spray-induced turbulence from the additional sprays, the swirling motion generated by the intake valves and wake induced turbulence on the leeward side of the jets.

In this study, a heavy-duty optical diesel engine operating at 20% load with a swirl number of 1 is simulated using Large Eddy Simulations (LES) to investigate the effect of local conditions on auto-ignition. The swirling motion is accounted for by a solid body rotation. The numerical calculations are performed using OpenFOAM libraries and an efficient combustion model, the Chemistry Coordinate Mapping method, together with a kinetic chemistry-reducing algorithm allows for an extensive kinetic mechanism generally to computationally costly for LES. The injector setup consist of four holes, three of which has an inter-jet angle of 45° and one with 135° spacing from the last hole, see Figure 1.

The four jets all have the same boundary conditions and initial conditions, such as fuel injection-rates, fuel temperature, fuel density, ambient density and temperature etc., however results indicate a longer ignition delay for the right most jet of the three jets in the narrow angle configuration, also seen in Figure 1. This delay of formation of high temperature zones in the downstream position may be due to various reasons, for instance; initial entrainment of cold air due to cooling effects from the evaporating jets in the vicinity of the the nozzle retarding the chemical processes, the deficit of oxidizers in the downstream position due to the presence of the other jets, or the turbulence flow structures generated on the leeward side of the adjacent jet. The reasons will be scrutinized by analysis of mass-flow rates, time-averaged mixture composition and temperature as well as ambient flow patterns at different locations of the jet.

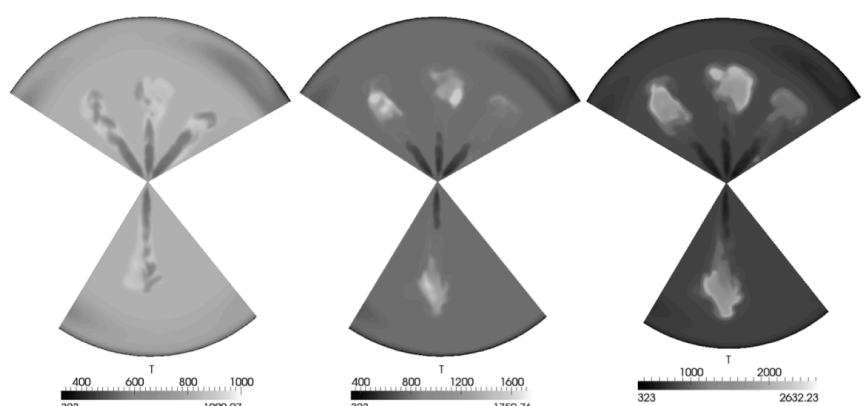

Figure 1. Temperature fields at three instances; at 2 CAD bTDC (left), 1.7 CAD bTDC (middle) and 1.3 CAD bTDC (right). The nozzle configuration consists of three jets with an inter-jet angle of 45° and a single jet with 135° spacing from the last jet of the three narrow angle jets.

Large Eddy Simulations of the flow in the exhaust port of a Diesel engine

Yue Wang[1], Mihai Mihaescu[2], Laszlo Fuchs[3]
[1]CCGEx, Department of Mechanics, Royal Institute of Technology (KTH), Stockholm, Sweden, email: yue@mech.kth.se
[2]CCGEx, Linné Flow Center, Department of Mechanics, Royal Institute of Technology (KTH), Stockholm, Sweden, email: mihai@mech.kth.se
[3]CCGEx, Linné Flow Center, Department of Mechanics, Royal Institute of Technology (KTH), Stockholm, Sweden, email: lf@mech.kth.se

In general, in a Diesel engine approximately 30 to 40% of the total energy available after combustion is lost in the exhaust gases. Some of it can be partially recuperated using a turbocharger. The efficiency of the impeller in the turbocharger's turbine is highly depended on the exhaust flow characteristics (e.g. uniformity, turbulence levels, pulsed versus continuous etc.). Due to the complex geometry and the in-cylinder conditions, the hot flow exhausting the cylinder through the exhaust port is highly three-dimensional, displaying secondary flow motion, stagnation regions, flow separation, and a high interaction with the manifold in the region of the port, as depicted in Figures 1a and 1b.

In one-dimensional simulations, the exhaust port is represented by experimentally measured discharge coefficients. The measurements are performed at fixed valve lifts and for a low pressure-drop. With these values, the total pressure loss is estimated for an arbitrary valve motion. However, higher pressure-drops may occur when the flow chokes. Hence, this procedure might lead to notably high errors when the flow rushes through the gap of the port at small valve lifts.

With advanced 3D unsteady flow approaches this process can be predicted more accurately assuming that the initial / boundary conditions and the grid resolution are adequate. Thus, the dynamics of the complex flow field have been simulated by Large Eddy Simulation (LES) approach, using a compressible finite volume code. A grid sensitivity study and a comparison of the computational results to available experimental data obtained for fixed valve lifts have been performed for verification and validation purposes. During a realistic exhaust stroke, the valves and the piston move. Cycle to cycle simulations from exhaust valve opening to exhaust valve closing have been performed. The characterization of the flow-structures and of their impact on the homogeneity of the flow-field and the losses in an exhaust port were assessed.

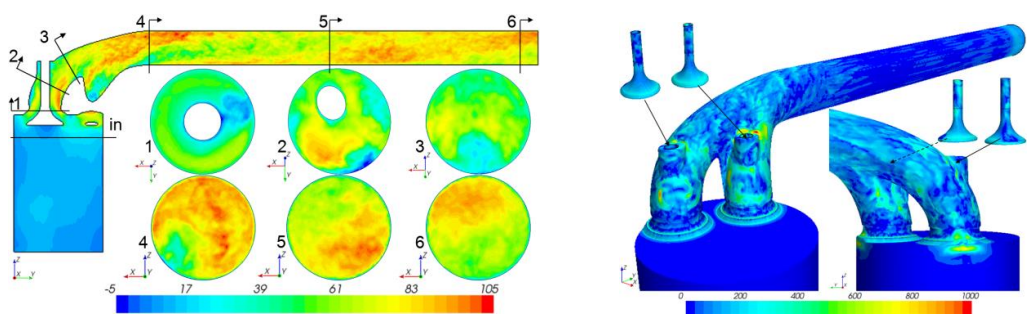

(a) (b)

Figure 1: (a) Velocity distribution during the outtake of the exhaust gases. (b) Wall shear stresses illustrating the manifold regions with a high interaction between the flow and the walls.

Föredragshållare